

UNIVERSITY OF CAPE TOWN

FACULTY OF ENGINEERING AND THE BUILT ENVIRONMENT

Department of Civil Engineering



**Investigating the Performance Requirements for Proprietary
Concrete Repair Materials with respect to Durability and Cracking
Resistance**

Prepared by: Brian Vukindu

Supervisor: Professor Hans Beushausen

Co-Supervisor: Dr. Philemon Arito

Date of Submission: April 2020

The copyright of this thesis vests in the author. No quotation from it or information derived from it is to be published without full acknowledgement of the source. The thesis is to be used for private study or non-commercial research purposes only.

Published by the University of Cape Town (UCT) in terms of the non-exclusive license granted to UCT by the author.

Plagiarism declaration

1. I know that plagiarism is wrong. Plagiarism is to use another's work and pretend that it is one's own.
2. I have used the Harvard convention for citation and referencing. Each contribution to, and quotation in, this thesis from the work(s) of other people has been attributed and has been cited and referenced.
3. This master's thesis is my own work.
4. I have not allowed, and will not allow, anyone to copy my work with the intention of passing it off as his or her own work.

Student Number: VKNBRI001

Surname: Vukindu

Date: 27th April 2020

Signature:

Signed by candidate

Dissertation submitted to the Department of Civil Engineering, University of Cape Town in partial fulfilment of the requirements for the degree of Master of Science in Civil Engineering.

Acknowledgements

I would like to thank and acknowledge the following persons, institutions, and companies who made significant contributions towards the completion of this dissertation.

1. The supervisor, Professor Hans Beushausen, for his invaluable guidance, encouragement, and continual academic and technical assistance throughout the duration of this dissertation.
2. The co-supervisor Dr. Philemon Abuti Arito for his guidance, encouragement and support.
3. The Directors of the Concrete Materials and Structural Integrity Research Unit (CoMSIRU), Emeritus Professor Mark Alexander and Professor Pilate Moyo, for providing useful suggestions and constructive criticism.
4. The following institutions; Sika (SA) Pty Ltd, BASF Construction Chemicals South Africa (Pty) Ltd, StonCor Africa and a.b.e. Construction Chemicals Pty Ltd, which provided the materials used in this research.
5. Mr Nooredien Hassen, the Civil Engineering Concrete Laboratory Manager, University of Cape Town for his assistance with the experiments carried out in the laboratory.
6. Mr Tahir Mukaddam, Senior Technical Officer, Department of Civil Engineering, University of Cape Town.
7. The Civil Engineering Concrete Laboratory staff; Mr Chris Caesar, Mr Charles May, Mr Leonard Adams and Mr Elvino Witbooi, for assisting in the laboratory with experimental work when needed.

Abstract

The premature deterioration of recently constructed concrete structures leads to the need for remedial measures to reinstate their safety and/or serviceability. Bonded concrete overlays (BCOs) are the most widely used concrete repair technique. The premature failure of these overlays, often manifested by cracking and/or debonding, is common despite their widespread use. There are many repair standards, codes and technical guidelines for BCOs. The performance requirements for BCOs stated in these standards vary. This makes the specification of repair materials difficult. This problem is further compounded by the existence of many proprietary concrete repair materials. The objective of this study was to investigate the performance requirements for proprietary repair mortars on cracking resistance and durability with respect to EN 1504-3:2005. This was achieved through an investigation of the mechanical, durability and transport properties of proprietary repair mortars in the hardened state.

The mechanical properties that were tested comprised: compressive strength, tensile strength, elastic modulus, tensile relaxation, restrained shrinkage cracking and drying shrinkage. Durability index tests of OPI, CCI WSI were also done. Twelve proprietary repair mortars were tested in the laboratory. Their chemical and physical characteristics based on the afore-mentioned material properties were determined. The mortars under investigation exhibited significant differences in their physical properties and chemical composition. A review of the existing performance criteria, as stipulated in EN 1504-3:2005, was also conducted to determine if the repair mortars under investigation conform to the requirements of this code.

From the test results it has been noted that the tested proprietary repair materials achieved the compressive strengths as stated by the standard EN 1503-4:2005. 11 of the tested repair materials were categorised as “structural” with only mix P2 being a “non-structural” repair mortar. These results also confirmed the specifications/categorisation from the manufacturers. Mixes PS, PFS, SA, S1, S2, G1, PF1, G2, P1, PF2 and A were categorised as high strength mortars to be used for structural repairs. Mix P2, having a low compressive strength is to be used as a cosmetic repair mortar. Furthermore, it was observed that a high compressive and tensile strength of the overlay does not necessarily translate into a high bond strength. The proprietary repair mortars exhibited low permeability. A review of the EN 1504-3:2005 showed that this code does not specify important

crack-determining material parameters such as elastic modulus, tensile relaxation and shrinkage despite the critical role they play in the cracking performance of repair mortars.

Further research into the microstructural properties of the proprietary repair materials is recommended to give additional insights into the causes of their different physical properties. This should be combined with on-site observation and testing to identify any potentially problematic macro-scale issues associated with repair mortars, particularly in relation to moisture transmission and retention. Understanding these factors amongst others, are essential to prevent damage to repaired structures by the use of incompatible repair materials.

Table of contents

Plagiarism declaration.....	i
Acknowledgements.....	ii
Abstract.....	iii
List of figures.....	ix
List of tables.....	xii
Abbreviations.....	xiv
Symbols.....	xvi
1. Introduction.....	1
1.1 Background.....	1
1.2 Problem statement.....	2
1.3 Research objectives.....	4
1.4 Scope of study.....	4
1.5 Research significance.....	4
1.6 Thesis layout.....	5
2. Literature review.....	6
2.1 Bonded concrete overlays.....	6
2.1.1 Introduction.....	6
2.1.2 Bonded overlay repair method.....	6
2.2 Failure of concrete repairs.....	14
2.2.1 Introduction.....	14
2.2.2 Debonding.....	16
2.2.3 Cracking.....	18
2.2.4 Factors influencing shrinkage cracking of overlays.....	18
2.3 Compatibility of repair materials with substrate.....	28
2.3.1 Introduction.....	28
2.3.2 Shrinkage.....	29

2.3.3	Elastic modulus	30
2.3.4	Thermal compatibility	31
2.3.5	Creep and tensile relaxation	32
2.4	Performance requirements for BCOs	34
2.4.1	EN 1504	34
2.4.2	Other standards	41
2.5	Closure	44
3.	Experimental methodology	46
3.1	Introduction	46
3.2	Testing philosophy and experimental approach	46
3.3	Test equipment	47
3.4	Test materials – proprietary repair mortars	48
3.5	Specimen preparation	51
3.5.1	Mix design	51
3.5.2	Casting and curing	52
3.6	Material characterisation	52
3.6.1	Grading	53
3.6.2	Energy Dispersive Spectrometry (EDS)	53
3.7	Tests	54
3.7.1	Compressive strength	54
3.7.2	Tensile strength	55
3.7.3	Tensile relaxation	57
3.7.4	Elastic modulus	57
3.7.5	Drying shrinkage	58
3.7.6	Restrained shrinkage cracking	59
3.7.7	Bond strength	61
3.7.8	Durability indexes	63
3.8	Closure	63
4.	Results and discussion	65
4.1	Introduction	65

4.2	Material characterization	65
4.2.1	Product description	65
4.2.2	Sieve analysis.....	66
4.2.3	Energy Dispersive Spectrometry (EDS)	67
4.3	Compressive strength.....	70
4.4	Tensile strength.....	73
4.5	Elastic modulus.....	76
4.6	Tensile relaxation.....	77
4.7	Drying shrinkage.....	79
4.8	Restrained shrinkage cracking	81
4.8.1	Age at cracking	82
4.8.2	Crack widths	83
4.8.3	Interrelationships between material parameters and age at cracking.....	84
4.9	Bond strength.....	89
4.9.1	Effect of mix type	91
4.9.2	Failure modes.....	92
4.10	Durability indexes.....	95
4.10.1	Oxygen Permeability Index (OPI)	95
4.10.2	Water Sorptivity Index (WSI).....	96
4.10.3	Chloride Conductivity Index (CCI)	98
4.11	Closure	99
5.	Conclusions and recommendations.....	103
5.1	Introduction.....	103
5.2	Effect of time-dependent material properties on crack resistance and durability.....	104
5.2.1	Compressive strength.....	104
5.2.2	Tensile strength.....	104
5.2.3	Elastic modulus.....	105
5.2.4	Tensile relaxation.....	105
5.2.5	Drying shrinkage.....	105
5.2.6	Restrained shrinkage cracking	105

5.2.7	Bond strength	106
5.3	Durability and permeability performance of proprietary repair mortars	106
5.4	Recommendations for further research	107
6.	References	108
Appendix A: Testing procedure		120
A.1	Sieve analysis	120
A.2	Compressive strength	120
A.3	Elastic modulus	121
A.4	Drying shrinkage	122
A.5	Restrained shrinkage	123
A.6	Durability indexes	124
A.6.1	Oxygen Permeability Index (OPI)	124
A.6.2	Water Sorptivity Index (WSI)	124
A.6.3	Chloride Conductivity Index (CCI)	125
A.7	Tensile relaxation	125
Appendix B: Detailed test results		126
B.1	Compressive strength	126
B.2	Tensile strength	130
B.3	Elastic modulus	132
B.4	Drying shrinkage	134
B.5	Bond strength test	136
B.6	Restrained shrinkage	138
B.7	Durability tests	140
B.7.1	Oxygen Permeability Index (OPI)	140
B.7.2	Water Sorptivity Index	143
B.7.3	Chloride Conductivity Index	145
B.8	Tensile relaxation	147
B.9	Sieve analysis	149
B.10	Energy Dispersive Spectrometry Tests (EDS)	155

List of figures

Figure 2-1: Factors affecting bond between concrete substrate and repair material – adopted from (Courard et al., 2014).....	7
Figure 2-2: Material selection process for concrete repair - adopted from (ICRI, 2003).....	11
Figure 2-3: Idealized model of a surface repair system - adopted from (Emmons & Vaysburd, 1995).....	15
Figure 2-4: Cracking and edge lifting of a bonded overlay exposed to shrinkage – adopted from (Carlswärd, 2006).	16
Figure 2-5 : Debonding of mechanical origin - adopted from (Turatsinze et al., 2005).....	17
Figure 2-6: Cracking, curling and debonding - adopted from (Turatsinze et al., 2005).....	17
Figure 2-7: Effect of aggregate concentration on shrinkage of concrete – adopted from (Alexander & Mindess, 2005).....	20
Figure 2-8: The effect of water-cement ratio on drying shrinkage or creep – adopted from (Mehta & Monteiro, 2006).	21
Figure 2-9: Influence of water content on (a) 28-day elastic modulus, and (b) age at cracking of ring test specimens – adopted from (Dittmer, 2013).	21
Figure 2-10: Effect of w/b ratio on shrinkage of cement pastes – adopted from Haller P 1940 as cited in (Alexander & Beushausen, 2009).	23
Figure 2-11: Age of visible cracking as a function of fibre volume – adopted from (Shah & Weiss, 2006).	25
Figure 2-12: Influence of fibre type and volume on average crack width – adopted from (Grzybowski & Shah, 1990).	26
Figure 2-13: Relation between shrinkage and time for concretes stored in different relative humidities – adopted from (Troxell et al., 1958).....	28
Figure 2-14: Three forms of elastic modulus - adopted from (Alexander & Beushausen, 2009).	30
Figure 2-15: Thermal expansion of concrete having different aggregate types and contents - adopted from (Browne, 1972).....	31
Figure 2-16: Characteristics of creep: time-dependent increase in strain under constant stress - adopted from (Alexander & Beushausen, 2009).....	32

Figure 2-17: Characteristics of relaxation: time-dependent decrease in stress under constant imposed strain - adopted from (Alexander & Beushausen, 2009).....	33
Figure 3-1: Sieve Analysis.....	53
Figure 3-2: X-ray analysis of the repair mortar.	54
Figure 3-3: Amsler compression testing machine.	55
Figure 3-4: (a) Notched dog-bone specimen dimensions and (b) notch detail – adopted from (Beushausen & Bester, 2016).	56
Figure 3-5: Zwick Roell Z020 Universal Testing Machine (UTM).	56
Figure 3-6: Instron; elastic modulus under compression testing machine.....	58
Figure 3-7: Strain extensometer on two strain targets measuring the shrinkage.	59
Figure 3-8: Ring Test Apparatus and test specimen dimensions - Adopted from ASTM, C1581/C1581M).	60
Figure 3-9: Ring mould preparation.	60
Figure 3-10: Ring specimen showing crack width measurement and hand microscope.	61
Figure 3-11: (a) Overlay casting (b) Cored specimen dimensions after shortening.	62
Figure 3-12:(a) Pull off test set up (b) Aluminium disks glued to the shortened cored samples..	63
Figure 4-1: Photomicrographs for the proprietary repair mortars.	68
Figure 4-2: Compressive strength results.	70
Figure 4-3: Compressive strength development of the repair mortars	72
Figure 4-4: Acceptable hour glass shear failure shape of the repair mortar cubes.	73
Figure 4-5: Tensile strength results.....	74
Figure 4-6: Failure mode within the prismatic section.	74
Figure 4-7: Failure below the tapered section within the gripping jaws.....	75
Figure 4-8: Elastic modulus for 7 and 28-day cured specimens.....	76
Figure 4-9: Tensile relaxation results for 7 and 28-day cured specimens.	78
Figure 4-10: Scatter plot for drying shrinkage.....	80
Figure 4-11: 60 day drying shrinkage test results.....	81
Figure 4-12: Average age at cracking test results for the repair mortars.....	82
Figure 4-13: Average crack widths at 14 days after appearance of the first crack.	83
Figure 4-14: Average age at cracking vs. 28-day compressive strength.	85
Figure 4-15: Average age at cracking vs. 28-day tensile strength.....	86

Figure 4-16: Average age at cracking vs. 28-day elastic modulus.	87
Figure 4-17: Average age at cracking vs. drying shrinkage.	88
Figure 4-18: Average age at cracking vs. tensile strength.	89
Figure 4-19: 7 and 28-day pull off test results.....	90
Figure 4-20: Typical failure at the interface for the pull off test.	93
Figure 4-21: OPI test results.	96
Figure 4-22: WSI test results	98
Figure 4-23: CCI test results.....	99
Figure B.1: Mix PS sieve analysis.	149
Figure B.2: Mix PFS sieve analysis.....	149
Figure B.3: Mix SA sieve analysis.	150
Figure B.4: Mix S1 sieve analysis.	150
Figure B.5: Mix S2 sieve analysis.	151
Figure B.6: Mix G1 sieve analysis.....	151
Figure B.7: Mix PF1 sieve analysis.	152
Figure B.8: Mix G2 sieve analysis.....	152
Figure B.9: Mix P1 sieve analysis.	153
Figure B.10: Mix PF2 sieve analysis.	153
Figure B.11: Mix P2 sieve analysis.	154
Figure B.12: Mix A sieve analysis.....	154

List of tables

Table 2-1: Methods of Concrete removal – adopted from (Bissonnette et al., 2013).....	8
Table 2-2: Composition of concrete repair system - adopted from (Baldwin & King, 2003).....	12
Table 2-3: European standards related to concrete repair products and systems - adopted from (Arito, 2018; Tilly & Jacobs, 2007).....	35
Table 2-4: Performance characteristics for structural and non-structural repair products for all intended uses and certain intended uses - adopted from EN 1504-3:2005.	36
Table 2-5: Performance requirements for repair products - adopted from EN 1504-3:2005.	37
Table 2-6: Concrete durability classification based on the UCT DI prediction tests – adopted from (Gillmer, 2012).	41
Table 2-7: Contents of the design and execution manual from Japan – adopted from (Bissonnette et al., 2013).	43
Table 3-1: Mix proportions and mix property for the commercial repair mortars.	48
Table 3-2: Mix Property description as per the product data sheets.	49
Table 3-3: Property test methods for the proprietary repair mortars	51
Table 3-4: Amount of water used, w/b ratio and the mixing time.	52
Table 4-1: Classification of the repair mortars based on the product datasheets.....	66
Table 4-2: Cumulative % retained and passing the 0.075 µm sieve.	66
Table 4-3: Analysed spectrum showing the elemental composition of proprietary repair mortars under investigation.....	67
Table 4-4: Bond strength quantification - adopted from (Sprinkel & Ozyildirim, 2000).....	91
Table 4-5: 7 and 28-day cohesive failure location.....	94
Table 4-6: Porosity results for the repair mortars	97
Table B.1: 3-day compressive strength results	127
Table B.2: 7-day compressive strength test results.....	128
Table B.3: 28-day compressive strength test results.....	129
Table B.4: 7-day direct tensile strength test results	130
Table B.5: 28-day direct tensile strength test results	131
Table B.6: 7-day elastic modulus test results.....	132
Table B.7: 28-day elastic modulus test results.....	133

Table B.8: Drying shrinkage test results	134
Table B.9: 7 day pull off bond strength test results	136
Table B.10: 28- day pull off bond strength test results.....	137
Table B.11: Age at cracking for the restrained shrinkage test results	138
Table B.12: 14-day crack widths and crack area for the ring specimens	139
Table B.13: 7-day OPI test results	141
Table B.14: 28-day OPI test results	142
Table B.15: 7-day WSI test results	143
Table B.16: 28-day WSI test results	144
Table B.17: 7-day CCI test results.....	145
Table B.18: 28-day CCI test results	146
Table B.19: 7-day Tensile Relaxation	147
Table B.20: 28-day Tensile Relaxation	148
Table B.21: Analysed spectrum showing the element composition of the repair mortars	155

Abbreviations

ACPA	American Concrete Pavement Association
BCO	Bonded Concrete Overlays
CEN	The European Committee for Standardization
CoV	Coefficient of Variation.
CTE	Coefficient of Thermal Expansion
CSH	Calcium Silicate Hydrate
CSF	Condensed Silica Fume
DI	Durability Indexes
EDS	Energy- Dispersive Spectrometry
EVA	Ethylene Vinyl Acetate
EN	European Standards
FA	Fly Ash
GGBS	Ground Granulated Blast Furnace Slag
HAC	High Alumina Cement
h	Hour
ITZ	Interfacial Transition Zone
l	Litre
MK	Metakaolin
NaCl	Sodium Chloride
OPC	Ordinary Portland Cement
OPI	Oxygen Permeability Index
PC	Portland Cement
PFA	Pulverised Fly Ash
PRM	Patch Repair Mortar
RHPC	Rapid Hardening Portland Cement
SEM	Scanning Electron Microscope
SRA	Shrinkage Reducing Admixtures
SRPC	Suphate Resisting Portland Cement
SF	Silica Fume

TICC	Thermal Incompatibility of Concrete Components
UTM	Universal Testing Machine
US	United States
WSI	Water Sorptivity Index
w/b	Water to binder ratio
EU	European Union
REHABCON	Strategy for Maintenance and Rehabilitation in Concrete Structures

Symbols

E_t	Tensile modulus of elasticity
ϵ	Strain
ϵ_{FSS}	Free shrinkage strain of the overlay
f_t	Tensile strength
μ	Degree of restraint
ψ	Tensile relaxation factor
σ	Stress
σ_t	Restrained shrinkage stress
f_v	Tensile bond
v_u	Bond demand shear stress
v_m	Bond stress determined
ϕ	Reduction factor
C_u	Coefficient of uniformity
C_c	Coefficient of curvature

1. Introduction

1.1 Background

Concrete has been and is still the material of choice in most construction projects. Tilly and Jacobs (2007) report that structural concrete has been in use since the late 1800s with most of these ancient structures being in operation for more than 100 years. Recent concrete structures, however, appear to perform worse than their earlier counterparts. They are characterised by premature deterioration which leads to the need for remedial measures to reinstate their safety and/or serviceability (Alexander & Beushausen, 2009). Baldwin & King (2003) report that the principle objective of investing in the repair of structures is to restore their performance during their service life. The premature failure of repairs and lack of certainty in the durability and performance of some repaired concrete structures is a worldwide problem (Matthews, 2007).

The cost of protection, repair and maintenance of aging infrastructure and deteriorating concrete structures is high. It is estimated that maintenance repair work consumes 50% of the European construction budget. This figure is likely to increase as the current infrastructure ages (Tilly & Jacobs, 2007). In the US, the annual cost to owners for repair, protection, and strengthening of concrete structures is estimated between \$18 to \$21 billion (Emmons & Sordyl, 2006). Moreover, the costs resulting from poorly designed or executed repairs are often higher than those associated with the actual repair of deteriorating concrete structures. Achieving durable concrete repairs is further crucial to the sustainability of concrete structures.

Concrete repair methods include bonded concrete overlays (BCOs), surface protection systems and coatings, corrosion inhibitors, electrochemical techniques, and cathodic protection. BCOs are widely used for repair and rehabilitation of concrete members. When used on a relatively small surface area, the BCOs are typically referred to as patch repairs (Alexander & Beushausen, 2009). BCO repair process involves casting a new layer of concrete in the form of an overlay, on an existing substrate. The premature failure of these overlays is common, often manifested by cracking and/or debonding.

The fresh overlay tends to contract more than the already matured substrate due to the thermal and hygral gradients; consequently, leading to differential shrinkage between the two composites. The differential shrinkage causes tensile stresses to be set up in the overlay whilst the substrate is

subjected to compression. The tensile stresses lead to cracks and/or debonding of the overlay when they exceed its inherent tensile strength/capacity (Beushausen & Bester, 2016; Bissonnette et al., 1999; Masuku et al., 2009). Cracking may be prevented if the tensile stress due to restrained shrinkage is maintained at a level that is below the tensile strength of the overlay. Debonding can be prevented by ensuring a high bond strength between the overlay and substrate through proper substrate preparation and cleaning, overlay compaction, and curing.

Despite the significant advancement in the understanding of various chemical and physical phenomena responsible for failure of bonded concrete overlays, repair failure analysis shows that repair materials are underperforming (Tilly & Jacobs, 2007). The existing standards and specifications for the design of bonded concrete overlays are generally deficient in scope and detail and it is left to the engineer to specify appropriate materials and application procedures (Alexander & Beushausen, 2009). More research is therefore needed to determine the exact performance requirements for repair mortars to mitigate cracking and debonding in BCOs.

1.2 Problem statement

There are many repair standards, codes and technical guidelines for BCOs. The performance requirements for BCOs stated in these standards vary. This makes the specification of repair materials difficult. Mangat & O’Flaherty (2000) report that most existing repair standards and design guidelines for BCOs specifications are based on limited quantitative knowledge of the structural interaction between the overlay and the concrete substrate during the service life of a structure. They limit the “design” aspect of BCOs to very crude requirements or recommendations of limit values, usually strengths, to achieve or not to exceed (Bissonnette et al., 2013). Their emphasis is on short term properties such as strength (compressive, tensile, bond) and early age shrinkage and do not consider the mismatch in bond properties - such as elastic modulus, shrinkage and creep - on long-term in-service performance of the repair.

The selection of proprietary repair materials for reinstating a deteriorated concrete structure continues to be done on a relatively ad hoc basis. This has led to an overreliance on the experience and knowledge of specialist contractors for the design of BCOs (Mangat & O’Flaherty 2000). This problem is further compounded by the existence of many proprietary concrete repair materials. Currently each manufacturer of these proprietary products develops their own material data sheets

with properties (strength, durability, unit weight, etc.), but they do not always use the same tests to determine the material properties of their various products (Harrell, et al., 2017). This makes it difficult to compare the products.

The repair industry mainly specifies appropriate repair techniques and product requirements for concrete repair products by the European Standards, EN 1504-3. This study focuses on this code. There also exists USA recommendations from the American Concrete Pavement Association (ACPA), Japanese requirements published by The Japan Highway Research Foundation and Swedish requirements by The Swedish National Road Administration. These codes and technical guidelines specify different performance requirements. Regarding tensile bond strength for instance, EN 1504-3:2005 recommends a tensile bond strength of ≥ 2.0 MPa (Class R4), while ACPA states that, for a durable bonded overlay, it is sufficient to achieve a 0.7 MPa tensile strength of the bond. The required tensile bond strength according to the Swedish practice is 1.0 MPa (Bissonnette et al., 2013).

According to the EN 1504-3:2005, the following are the material properties that a repair mortar ought to possess: compressive strength, limited chloride ion content, adhesive bond, restrained shrinkage/expansion, durability – carbonation resistance and thermal conductivity, elastic modulus, skid resistance, coefficient of thermal expansion and capillary absorption (water permeability). It specifies material properties such as skid resistance and compressive strength, yet they do not have a direct correlation with durability and crack resistance in repair mortars. Material properties such as elastic modulus, thermal and hygral deformations creep and tensile relaxation which are more relevant to the performance should therefore be specified. Arito (2018) reports that a careful analysis of EN 1504-3:2005 shows that strict compliance to its performance specifications does not necessarily result in crack-free repair mortars.

There is, therefore, a need to identify and specify the material properties that directly contribute to the durability and crack resistance of repair mortars. A critical review of the existing performance criteria, EN 1504-3:2005, should be conducted with a view to provide a platform for the development of performance requirements for repair mortars which can be used for project specification and quality control in industry.

1.3 Research objectives

The overarching objective of this research is to investigate the performance requirements for proprietary repair mortars on cracking resistance and durability with respect to the EN 1504-3:2005. This study further sought to realise the following sub-objectives.

- a) To investigate the mechanical properties of proprietary repair mortars in their hardened state.
- b) To investigate the durability and transport properties of the proprietary repair mortars.

1.4 Scope of study

This study was be limited to:

- a) Locally available proprietary repair mortars in the South African concrete repair industry.
- b) EN 1504-3:2005, SANS 5863:2006a, BS 1881: Part 121:1983, ASTM C1581/C1581M and ASTM C1583/C1583M – 13 as the reference codes and technical guidelines.
- c) The number of repair mortars tested in the experiments was limited to twelve. This was due to the large number of tests and the extensive amount of time required for the full range of tests that needs to be conducted on each mix.
- d) The mix design used was as specified in the product data sheets by the repair mortar manufacturers.

1.5 Research significance

This study will:

- a) Provide a platform for the development of performance requirements on cracking resistance and durability for proprietary repair mortars that could be used in the industry for project specifications and quality control.
- b) Contribute to the body of knowledge on the proprietary repair mortars that comply with the performance requirements stated in EN 1504-3:2005 reference code.

1.6 Thesis layout

This study comprises five chapters, a list of references and appendixes A & B. Chapter 1 contains an introduction to the background information about this study. The problem statement, research objectives, scope of study and research significance are subsequently presented. Chapter 2 presents a detailed review of relevant literature on BCOs. This chapter specifically discusses BCOs, their uses, characteristics and application techniques. The causes of failure on concrete overlays and the compatibility of repair materials with substrate are presented. The chapter ends with discussions on the performance requirements for BCOs and the repair standards, codes and technical guidance that exist. Chapter 3 presents the experimental methodology applied in this study. The testing philosophy & experimental approach, test equipment, test materials, test methods and standards used are presented. A discussion of the results from the experimental work is presented in Chapter 4. Chapter 5 summarises the conclusions arrived at during the study and recommendations for further research. A list of literature that was reviewed in this study is then presented. Finally, appendixes containing the testing procedures and methods and the test results are presented.

2. Literature review

2.1 Bonded concrete overlays

2.1.1 Introduction

BCOs are widely used for repair and rehabilitation of concrete members. It involves casting a new layer of concrete on an existing substrate. Overlays extend the service life of deteriorating structures by providing a protective and visually appealing layer to the damaged substrate or by increasing the structural strength and stiffness of the concrete section. Bissonnette et al. (2013) further report that concrete overlays are used to;

- a) Match the horizontal profile of an adjacent slab or element;
- b) Replace the deteriorated or contaminated concrete and reinstating the protection of the structure (especially its reinforcement);
- c) Provide a more durable wearing surface;
- d) Improve the bonding characteristics of the surface for pavements or bridge decks;
- e) Restore architectural features such as colour or texture.

The premature failure of BCOs is common, often manifested by cracking and/or debonding. Poor workmanship and differential shrinkage between the substrate and the overlay are the main causes of failure (Alexander & Beushausen, 2009). Other possible causes of failure include: poor surface preparation, choice and application of overlay materials, curing procedures, time-dependent material properties and environmental influences.

2.1.2 Bonded overlay repair method

Deterioration of concrete is a common problem observed in concrete structures. The need for repair and protection of these structures has therefore grown considerably in recent years. For durable repairs, it is necessary to have a better understanding of their performance in practice. Some of the performance data required include: types and causes of the original deterioration, types of repair carried out, success or failure of the repair, mode of failure, cause of failure and lastly the life of the repair (Tilly & Jacobs, 2007).

Various design and construction factors have to be considered to ensure sufficient bond strength and crack resistance of BCOs (Beushausen & Bester, 2016). The bond strength is influenced by

the substrate surface preparation characteristics while the crack resistance is influenced by the overlay material properties which include tensile strength, shrinkage, elastic modulus, creep and relaxation.

2.1.2.1 Substrate preparation

A good quality bond between the overlay and concrete substrate depends on many factors. These can be divided into three main groups, namely: substrate characteristics, overlay characteristics and environmental conditions (Courard et al., 2014). An overview of these factors is shown in Figure 2-1.

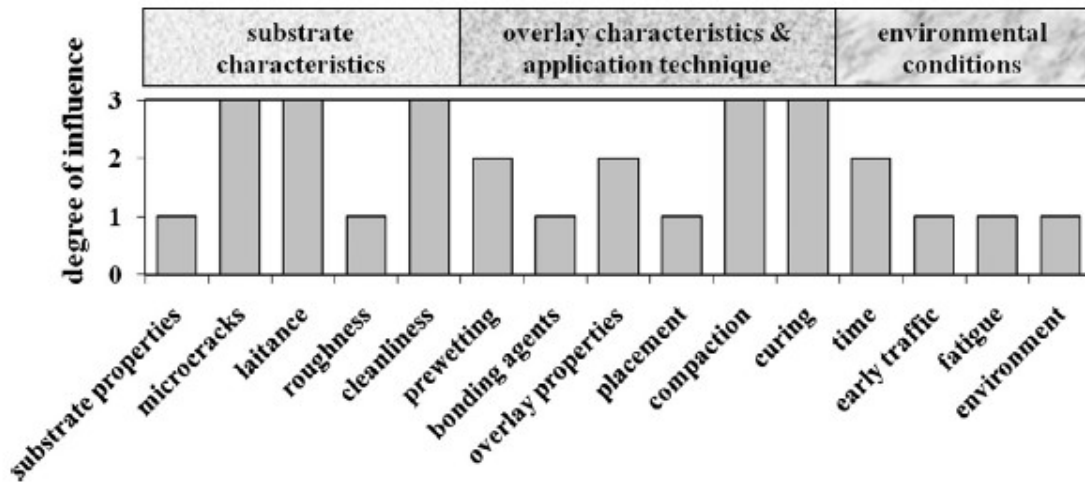


Figure 2-1: Factors affecting bond between concrete substrate and repair material – adopted from (Courard et al., 2014).

To achieve a good and durable repair, surface preparation and cleaning of the concrete substrate are the most crucial steps. The poor quality and deteriorated substrate concrete must be removed. No matter how good the repair material is or how thorough its application, a poorly prepared substrate surface will always constitute the weak link in the system. Surface preparation leads to the creation of a good, sound interface with adequate texture. It involves two main processes: substrate surface removal and substrate surface cleaning. Surface removal involves the taking away of parts of the substrate concrete and previously applied coatings, whereas cleaning refers to the removal of loose particles and contaminants (Holl & O'Connor, 1997).

There are several methods of substrate surface removal. These methods affect the surface and the properties of the uppermost layer of the remaining concrete significantly. Some methods leave a rough and sound surface that promotes a good bond, while others introduce micro-cracks to the remaining concrete (Bissonnette et al., 2013). Common concrete substrate preparation methods include mechanical surface removal techniques such as jackhammering, scarification and hydro-demolition. These are very efficient in removing poor concrete. They are, however, likely to cause microcracking of the substrate if not well operated. Microcracks result in zones of weakness that are prone to bond failure (Beushausen & Bester, 2016). Other less detrimental techniques are sandblasting and low-pressure water jetting (Courard et al., 2014). A summary of common substrate preparation methods is presented in Table 2-1.

Table 2-1: Methods of Concrete removal – adopted from (Bissonnette et al., 2013).

Substrate concrete removal method	Principal behaviour	Concrete removal capability Action depth (mm)	Notable advantages	Notable disadvantages
Sandblasting	Blasting with sands	No	No microcracking	Not selective, leaves considerable sand
Scrabbling	Pneumatically driven bits impact the surface	Little (6)	No microcracking, no dust	Not selective
Shot-blasting	Blasting with steel balls	Little (12)	No microcracking, no dust	Not selective
Grinding	Grinding with rotating lamella	Little (12)	Removes uneven parts	Dust development, not selective

Table 2-1: Methods of Concrete removal – adopted from (Bissonnette et al., 2013) - cont'd.

Substrate concrete removal method	Principal behaviour	Concrete removal capability Action depth (mm)	Notable advantages	Notable disadvantages
Flame-cleaning	Thermal lance	No	Effective against pollutants and painting, useful in industrial and nuclear facilities	The reinforcement may be damaged, smoke and gas development, safety considerations limit use, not selective
Milling (Scarifying)	Longitudinal tracks introduced by rotating metal lamellas	Yes (75)	Suitable for large volume work, good bond if followed by water flushing.	Microcracking is likely, reinforcement may be damaged, dust development, noisy, not selective
Pneumatic (jack hammers (chipping), hand-held or boom mounted)	Compressed air operated chipping	Yes	Simple and flexible use, large ones are effective.	Microcracking, damages reinforcement, poor working environment, slow production rate, not selective
Explosive blasting	Controlled blasting using small, densely spaced blasting charges	Yes	Effective for large removal volumes	Difficult to limit to solely damaged concrete, safety and environmental regulations limit use, not selective
Water-jetting (hydro-demolition)	High pressure water jet from a unit with a movable nozzle	Yes	Effective especially on horizontal surfaces), selective, does not damage reinforcement or concrete, improved working environment	Water handling, removal in frost degrees, costs for establishment.

Silfwerbrand & Petersson (1993) report that field tests have shown that good bond strength can be achieved if mechanical removal, which in many cases is necessary to remove deteriorated concrete to sufficient depth, is followed by high-pressure water-jetting. The boundaries of repair patches should be cut straight and normal to free surfaces to avoid feather edges that may result in localised patch repair failure and unsightly appearance.

Bond strength is also affected by the substrate moisture condition. A dry substrate will suck water from the fresh overlay material, which may result in a weak interfacial layer and low bond strength while a wet surface tends to dilute the repair material at the interface and increases the w/b ratio, hence leading to low material strength, increased shrinkage and low bond strength (Alexander & Beushausen, 2009). It is recommended that the substrate should be saturated but surface dry as the water in the pores prevents the interlocking effect.

Bonding agents may be used to improve the bond strength for certain materials, especially stiff repair mortars that cannot properly fill open pores and cavities. They, however, cannot compensate for bad substrate surface preparation and may act as a bond breaker when used inappropriately (Pigeon & Saucier, 1992; Beushausen & Bester, 2016b). Repair mortars should be applied before the hardening of the bonding agent.

2.1.2.2 Overlay characteristics and application technique

There exists many variables and systems in repair materials that strongly influence the bond strength and durability. They include the technique or form of repairs, material composition, method of application, fresh properties and hardened properties (Baldwin & King, 2003). The specification of the repair materials should only be done after the properties that best satisfy overall project objectives are identified and prioritised. ICRI (2003) reports that the selection of appropriate materials for surface repairs is a complex process that must be guided by the following criteria: constructability, serviceability, aesthetics, and an understanding of the users' concept and the engineering requirements. It is often observed that more than one material or systems of materials will satisfy the above requirements. The final selection is usually based on the relationship between cost, performance, health and safety and the environment (Baldwin & King, 2003; ICRI, 2003). Figure 2-2 shows the process of selecting repair materials.

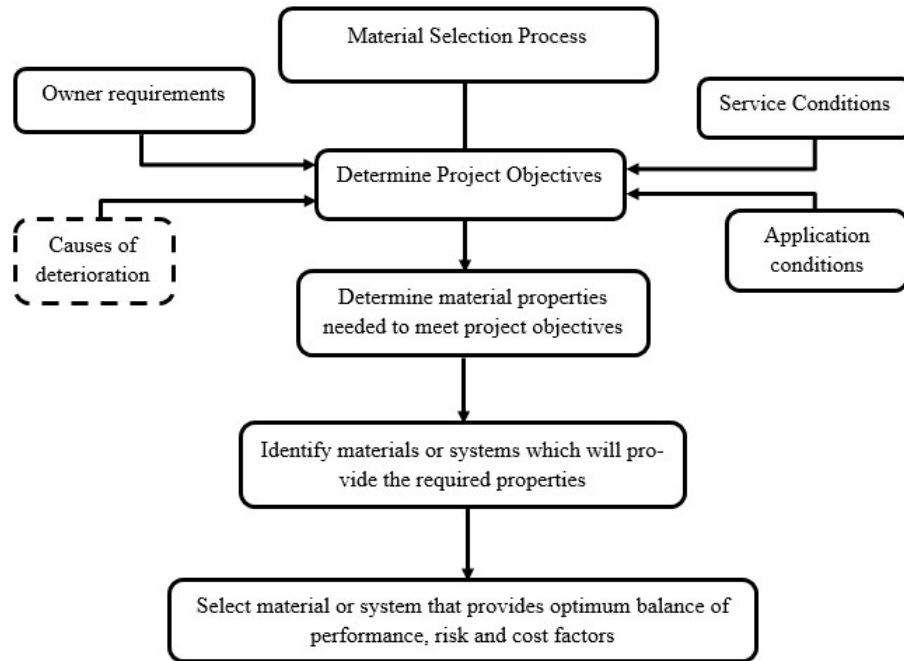


Figure 2-2: Material selection process for concrete repair - adopted from (ICRI, 2003).

For early-age bond strength development and bond durability, the properties of the repair material in its fresh state are important. The workability and compaction of a freshly-placed overlay will influence its ability to fill open cavities and voids on the substrate concrete surface and determine the effective contact area between the two composites (Alexander & Beushausen, 2009). Capillary suction in the substrate is further enhanced by a relatively fluid overlay which would consequently improve its physical anchorage in substrate surface pores and cavities.

Bond strength development between a well-prepared substrate and the overlay under ideal curing conditions is mainly influenced by the mechanical strength development of the overlay. The important material properties influencing stress development include elastic modulus, shrinkage, and the coefficient of thermal expansion. Overlays are supposed to have as little shrinkage as possible and a coefficient of thermal expansion similar to that of the substrate. High compressive strength or elastic modulus values are not required in non-structural applications. Overlays with high strength and high stiffness are generally outperformed by overlays with low strength, which, due to a lower stiffness, have much better crack resistance.

The hardened material properties required for bonded overlays comprise: load-bearing properties (compressive strength, elastic modulus, abrasion resistance, etc.), aesthetics (colour to match

existing concrete), durability (permeability, absorption, and diffusion characteristics), and dimensional stability (shrinkage, thermal deformations) (Beushausen & Alexander, 2005). Substrates and overlays subjected to load-induced deformations need to possess similar thermal deformation characteristics, similar elastic properties and low overlay creep. Shrinkage characteristics of a patch repair are the most critical. The application of surface coatings and thorough curing prevents the extensive development of shrinkage cracks. Shrinkage characteristics for conventional concrete can be better controlled compared to proprietary repair mortars and thus offer better performance on large repair areas. Repair mortars are recommended for areas of up to approximately 1 m² (Draft report, Bahrain: The Concrete Society Bahrain and the Bahrain Society of Engineers, 2000)

Many materials are used for bonded concrete overlays. Common repair mortars contain sand, cement, polymers, fibres and resins. A summary of the generic types of concrete repair materials is shown in Table 2-2.

Table 2-2: Composition of concrete repair system - adopted from (Baldwin & King, 2003).

Component or type of system	Type of material
Cement-only systems	OPC, SRPC, RHPC, White Portland HAC Magnesium Phosphate Others (regulated set, alkali activated, gypsum-based cements) Supplementary cementing materials (PFA, GGBS, SF, MK)
Polymer-modified cementitious systems:	Synthetic rubbers, e.g. styrene butadiene rubber Acrylic and modified acrylic latexes Polyvinyl acetate latexes (homo-polymers, co-polymers, terpolymers) Epoxy emulsions
Resin repair materials	Epoxy resins Polyester resins Acrylic resins
Fibres	Glass Steel wire (mild, stainless, hooked, crimped etc.) Polypropylene (polypropylene or homopolymer resin). Monofilament, fibrillated Acrylic (monomers and monomer blends etc.)

Repair mortars with cementitious-only binders provide acceptable protection to existing concrete structures with the set properties being influenced by the cement content and w/b ratio (Beushausen & Bester, 2016; Baldwin & King, 2003). The addition of polymers enhances the performance or application parameters of repair mortars. The benefits of polymer concrete include rapid set, reduced shrinkage, chemical resistance, abrasion resistance, high bond strength, and good workability. These advantages are also provided by materials with epoxy binders which rely on their very low intrinsic permeability to prevent ongoing deterioration (Baldwin & King, 2003). Arito (2018), Bode & Dimmig-Osburg (2011), and Pierard et al. (2006), however, report that the incorporation of polymers results to an increase in shrinkage. Some researchers have also reported mixed results where the incorporation of polymers in mortars caused either an increase or decrease in shrinkage (Miller, 2005; Ohama, 1995; Rixom & Mailvaganam, 1999).

The method of application of bonded overlays is one way of classifying the repair method. Various application methods exist with each being suitable for different repair applications. The most common forms are manual (by hand or trowel), placing in formwork, and spraying (Baldwin & King, 2003). The selection of the appropriate application method is crucial for a successful repair since failure of the application method will result in a poorly performing repair irrespective of the quality of the repair material. A summary of the methods is presented in the subsequent subsections.

Hand placement techniques

Hand placement techniques include the hand or trowel methods of application. It involves the repair material being mixed in a trowelable, non-flowing consistency. The repair material is pressed onto the substrate pore structure to develop good contact, without the formation of voids (Beushausen & Bester, 2016). The repair material usually sticks in place before subsequent layers are added. Good bond is achieved through roughening the subsequent layers. This method is applicable for small surface restoration repairs on vertical and overhead locations when reinforcing steel is absent.

Flowable

Repairs using flowable materials on prepared substrate surfaces involve the construction of formwork around the area to receive the material. A flowing repair material is then poured into the shutter through a funnel and a pipe. It is one of the most commonly used method of repair of vertical (columns, walls and slab edges), and in some cases, overhead locations (slab soffits). It is the best method in the presence of congested reinforcement, complex or inaccessible substrate and provides benefits in the volume of repair that can be effected at a single time (Baldwin & King, 2003). Curing is usually done on the exposed surface of the flowable repair material after the removal of the formwork. The formwork affords some degree of additional curing protection in the first days after casting.

Sprayed concrete

This form of concrete repair is composed of a cementitious binder, aggregates, water and additives that are formulated to be projected, or sprayed, from a nozzle and to form a cohesive, durable material upon impact with the target substrate. They are most ideal for large repair volumes e.g. large surface areas of repair. The challenge of using this repair method include sloughing off of the concrete or mortar due to excessively thick layer placement and the formation of voids behind reinforcement (Beushausen & Bester, 2016). To counter this problem Fujiwara et al. (2016) developed a high thixotropic material without using polymers which in spray tests was able to spray a wall surface to about 140 – 150 mm thickness, and a ceiling surface to about 60 mm thickness.

Flood grouting

This is a rare form of repair that involves pouring a highly fluid grout through a pre-placed single sized aggregate (Baldwin & King, 2003). The fluid then sets and binds the aggregate to form a solid material. This form of repair can only be used for horizontal surfaces.

2.2 Failure of concrete repairs

2.2.1 Introduction

The objective of a concrete repair is to produce a durable repaired structure with a limited and predictable degree of change without deterioration or distress throughout its intended life and

purpose. Emmons & Vaysburd (1995a) defines a repair system as a three-phase composite system consisting of the existing substrate, the repair material (overlay) and the transition zone.

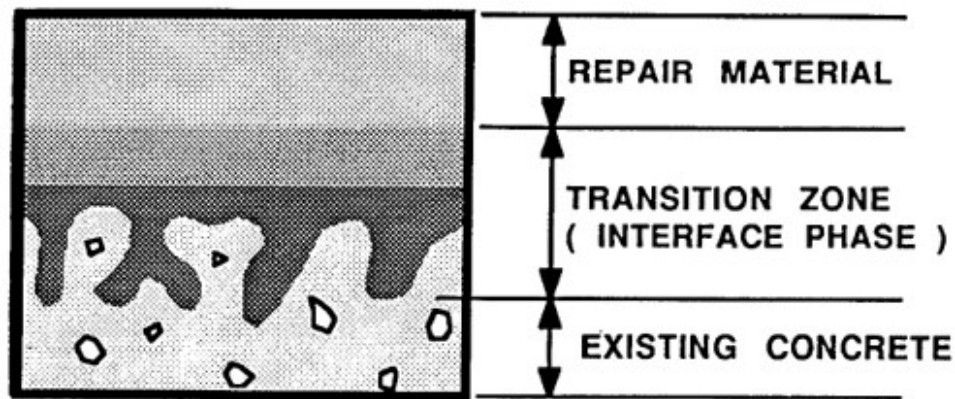


Figure 2-3: Idealized model of a surface repair system - adopted from (Emmons & Vaysburd, 1995)

Durability problems in repair materials are manifested as spalling, cracking, delamination, scaling and loss of strength. Many of these factors are interrelated thereby making it difficult or impossible to identify any single underlying problem (Emmons & Vaysburd, 1995).

Cracking and delamination are perceived to result from differences in deformation between the overlay and substrate. These differences originate from shrinkage and/ or temperature variations, settlements or external loads and chemical reactions (Carlsward, 2006). Shrinkage in the newly cast overlay causes normal tensile stresses to develop as the contracting movement, to some extent, is restrained by the substrate. If these stresses reach the tensile strength of the overlay material, cracks will start to propagate through the overlay. The stress field near the free edges introduced by restrained shrinkage tends to lift the edge vertically (curling/ edge lifting) as shown in Figure 2-4.

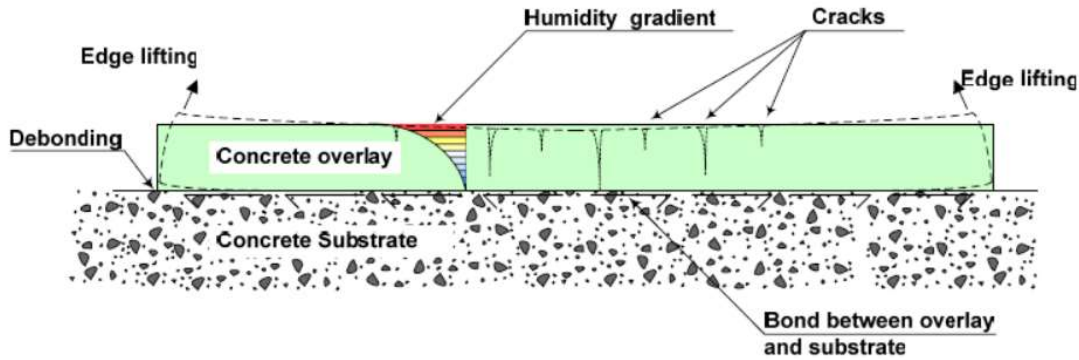


Figure 2-4: Cracking and edge lifting of a bonded overlay exposed to shrinkage – adopted from (Carlswård, 2006).

Differential shrinkage is generally considered to have the most critical influence on the long-term performance of composite members (Beushausen & Alexander, 2006; Carlswård, 2006). While the mechanisms of shrinkage in concrete members are well known, the effect of differential shrinkage on the performance of bonded overlays have, however, not been fully explained. Beushausen & Alexander (2006), report that this is mainly due to the large number of influences on differential shrinkage stresses, which are difficult to assess independently. They include time-dependent material characteristics, environmental conditions, structural properties of the system, and the effects of workmanship.

2.2.2 Debonding

Debonding is the separation of the overlay from its substrate. It leads to local delamination and/or spalling (Amba et al., 2010; Beushausen & Alexander, 2006; Beushausen & Bester, 2016a). It is related to cracking as it is commonly initiated at the overlay boundaries such as free edges, joints and cracks.

2.2.2.1 Causes of debonding

Debonding occurs due to the shear and the tensile stresses induced by the differential deformation between the overlay and the substrate. The tensile debonding stress is the result of the combined effects of bending of the structure and cracking of the overlay; and the peeling force induced by the shear effects along the interface (Granju, 2001). The former designated as of mechanical origin

and schematically presented in Figure 2-5 is a consequence of the flexural straining of the structure by the applied loads, especially by live loads.

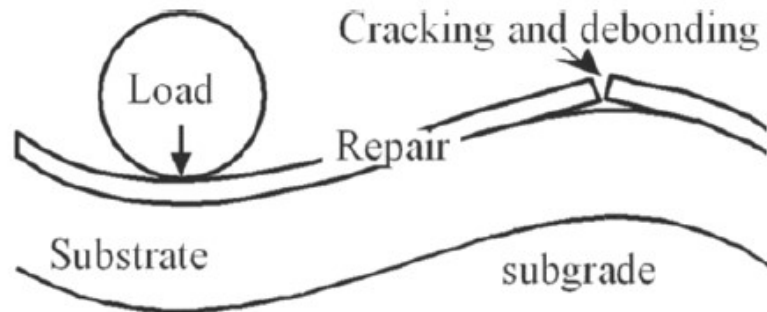


Figure 2-5 : Debonding of mechanical origin - adopted from (Turatsinze et al., 2005).

Debonding is possible due to the crack and the tendency of the overlay not to follow the curvature of the substrate. The latter described as the debonding of length change origin, illustrated by Figure 2-6, results from the effects of different length changes of the overlay and substrate due to restrained shrinkage. Curling due to thermal or shrinkage gradients aggravates these effects (Granju, 2001; Turatsinze et al., 2005).

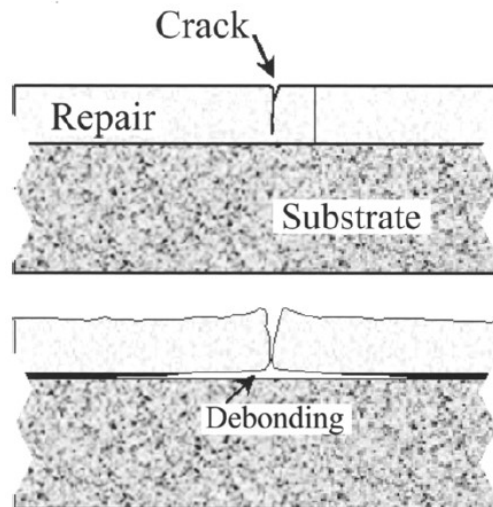


Figure 2-6: Cracking, curling and debonding - adopted from (Turatsinze et al., 2005).

2.2.2.2 Factors influencing debonding

The factors that affect bond strength include: substrate surface preparation and cleanliness, overlay compaction, curing, mechanical properties (fresh and hardened properties) and the moisture

condition of the substrate (Bissonnette et al., 2013). These factors have been discussed in detail in Section 2.1.2.1.

2.2.3 Cracking

Bonded concrete overlays crack due to the tensile stresses induced by restrained shrinkage deformations as explained in Section 2.2.1. Beushausen & Alexander (2006), report that restrained shrinkage cracking is difficult to control compared to debonding because it is related to the interaction between the time-dependent overlay material properties such as shrinkage, tensile strength, elastic modulus and tensile relaxation.

When the free shrinkage (ϵ_{FSS}) of the overlay is restrained to a certain degree (μ) by the substrate, tensile stresses (σ_t) are developed. The tensile stresses induced by the restrained shrinkage of the overlay are proportional to the stiffness (elastic modulus) (E_t) of the overlay, with stiffer (higher elastic modulus) overlays inducing greater tensile stresses. Part of the tensile stresses are however alleviated by tensile relaxation (ψ) - which is a stress relieving viscoelastic property of the overlay. Therefore, the magnitude of tensile stresses induced by restrained shrinkage is given by:

$$\sigma_t = \mu \times \epsilon_{FSS} \times E_t \times \psi \dots\dots\dots (2.1)$$

where σ_t = restrained shrinkage stress within the overlay at time t, μ is the degree of restraint, ϵ_{FSS} is the free shrinkage strain of the overlay, E_t is the elastic modulus of the overlay in tension and ψ is the tensile relaxation factor (Beushausen & Bester, 2016a). If the resulting tensile stresses after tensile relaxation are less than or equal to the inherent tensile strength (f_t) of the overlay, then the overlay will not crack. However, should the resulting tensile stresses after tensile relaxation be greater than the tensile strength of the overlay, then the overlay will crack. Restrained shrinkage cracking failure criterion is therefore;

$$Susceptibility\ to\ cracking = \begin{cases} \text{if } \sigma_t \leq f_t, \text{ uncracked} \\ \text{if } \sigma_t > f_t, \text{ cracked} \end{cases} \dots\dots\dots (2.2)$$

2.2.4 Factors influencing shrinkage cracking of overlays

Some of the factors influencing restrained shrinkage cracking include: fineness and composition of cement, aggregate type and content, water and paste content, w/b ratio, cement extenders,

admixtures, fibres, member geometry, environmental conditions and curing. These factors are discussed in the subsequent subsections.

2.2.4.1 Fineness and composition of cement

Cement composition affects restrained shrinkage cracking albeit to a small extent. There exists an optimum sulphate content for minimum shrinkage to occur, this content being the same as for minimum creep (Alexander & Beushausen, 2009; Powers, 1959).

The cement fineness influences restrained shrinkage cracking due to its influence on drying shrinkage. Mehta & Monteiro (2006) and Neville (2011) however report that this influence is limited to cement pastes and mortars as there is negligible effect on concretes made with normal or lightweight aggregates. The fineness of cement affects the drying shrinkage through the pore structure and the degree of hydration. A finer pore structure results in an increase in the radius of curvature of the menisci that form within the pores upon drying which leads to greater surface tension. This leads to an increase in drying shrinkage (Mehta & Monteiro, 2006; Tazawa et al., 1995; Uys, 1983). Fine cement particles hydrate completely however coarse cement particles only partially hydrate and thus become dense bodies encased by gel. These partially hydrated particles provide restraint to shrinkage, similar to that of aggregates, which results in decreased shrinkage (Beushausen & Bester, 2016a). Mehta (1997) has pointed out that for durability considerations, finer cements may not always be preferable to coarser ones. Furthermore, Bentz & Haeeker (1999) argue that in high-performance concretes with relatively low w/b ratios, coarser cements may offer equivalent long-term performance to finer cements, resulting in energy savings due to a reduction in grinding time.

2.2.4.2 Aggregate type and content

Aggregates have two effects on paste shrinkage, namely: dilution and restraint. Dilution is where the shrinkage of the concrete will decrease with increasing aggregate concentration. This depends on the standard water requirement of the aggregates and the w/b ratio which together, influences the paste and aggregate content. The restraint effect, which is due to the stiffness of the aggregate, restrains the paste movement as long as the aggregate is stiffer than the paste (Alexander & Mindess, 2005). An increase in aggregate content results in decreased shrinkage as shown in

Figure 2-7. Aggregates, being dimensionally stable, provide restraint because they do not undergo volume changes due to the changing moisture conditions. The volume, size, grading, texture and stiffness of an aggregate determines the magnitude of restraint it provides. Well-graded aggregates with a large maximum size have a low void space and, consequently, require a relatively small amount of paste, resulting in decreased shrinkage (Mindess et al., 2003).

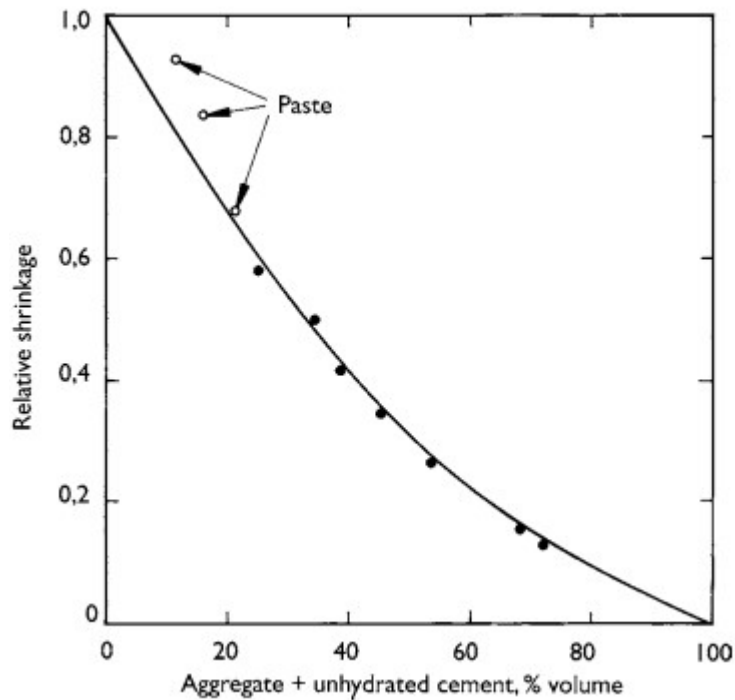


Figure 2-7: Effect of aggregate concentration on shrinkage of concrete – adopted from (Alexander & Mindess, 2005)

2.2.4.3 Water and paste content

For a given cement content, with increasing w/b ratio, both the drying shrinkage and creep are known to increase. This is due to the decrease in the strength and an increase in the permeability of the system (Mehta & Monteiro, 2006). Since the shrinkage of concrete occurs in the paste phase of concrete, an increase in paste content will result in a higher magnitude of shrinkage as a larger portion of the concrete will undergo shrinkage. This is illustrated in Figure 2-8.

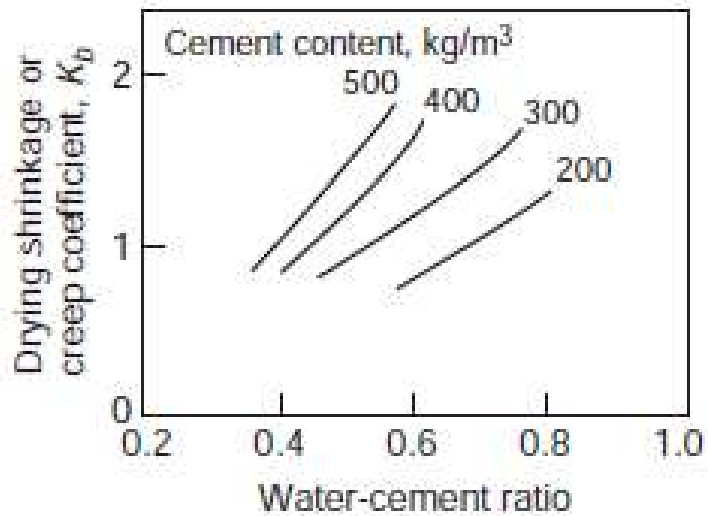


Figure 2-8: The effect of water-cement ratio on drying shrinkage or creep – adopted from (Mehta & Monteiro, 2006).

Since the elastic modulus of the cement paste of normal strength concrete is generally less stiff than that of the aggregate phase, an increase in paste content results in a cement paste with a lower stiffness and thus reduced elastic modulus of the concrete mix as shown in Figure 2-9a. Increase in paste content has a net result of a decrease in crack resistance as shown in Figure 2-9b (Beushausen & Bester, 2016b; Dittmer, 2013).

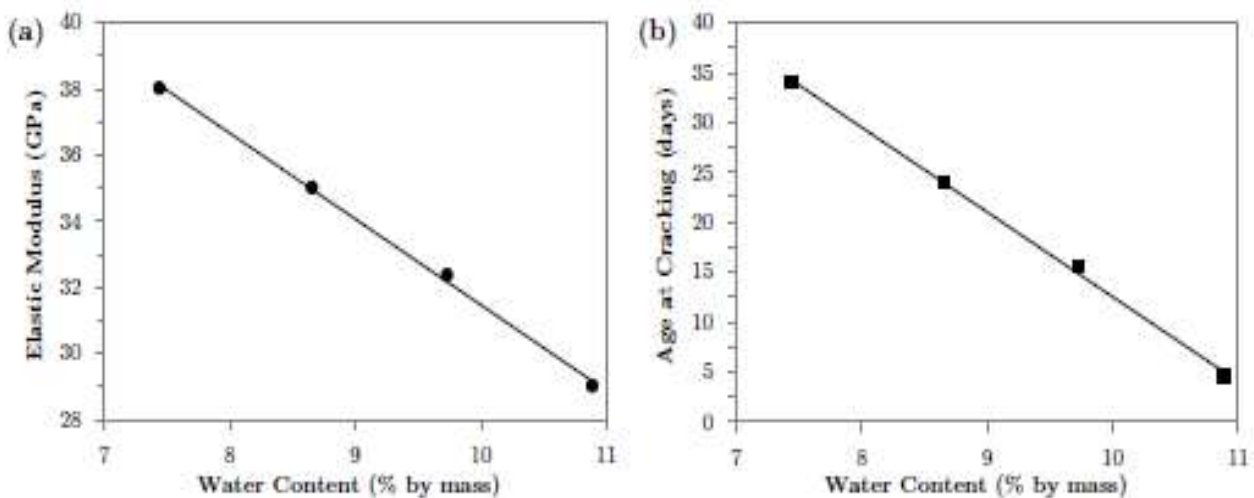


Figure 2-9: Influence of water content on (a) 28-day elastic modulus, and (b) age at cracking of ring test specimens – adopted from (Dittmer, 2013).

2.2.4.4 W/b Ratio

The w/b ratio significantly influences the structure of the hardened cement paste and has been reported as one of the most important factors affecting shrinkage cracking (Banthia and Gupta, 2009; Bentz et al., 2008; Rixom & Mailvaganam, 1999). The lower the w/b ratio and the greater the degree of hydration, the more will be the volume of hydration products (gel) formed, and the greater will be the ratio of gel pore to capillary pore volume. Alexander & Beushausen (2009) report that water is held in the paste at different bonding energies, the interlayer and gel pore water being very much more tightly held than the free capillary water. Consequently, as the paste dries it loses capillary water first, then adsorbed and gel-pore water, and finally interlayer water. The removal of free water in the capillaries leads to small shrinkages, while the removal of tightly bound water causes a larger component of shrinkage as forces of contraction come into play.

The effect of w/b ratio on shrinkage of cement pastes is shown in Figure 2-10. The lower the w/b the lower the ultimate shrinkage. Shrinkage is similar for all pastes since only capillary water is being lost as the early stages of drying represent the removal of free water. Although high w/b ratio pastes lose more water than the low w/b ratio pastes, their shrinkages are not very different. Once the free water has been lost, gel water begins to be removed, and the paste is subjected to contraction forces. The stronger pastes which have a lower w/b ratio will also be stiffer and will experience less contraction strain than the weaker pastes, even though they will contain a greater gel volume. Lower w/b ratio pastes (and concretes) are also more impermeable, hindering the free movement of moisture from the paste microstructure (Alexander & Beushausen, 2009). Uys (1983) reports that an increase in the w/b ratio increases the potential for shrinkage. Some studies however have shown that an increase in w/b ratio delays cracking. Banthia and Gupta (2009) report that an increase in the w/b decreases the total amount of heat evolved, increases the evaporation rate and delays the occurrence of first crack. They further reported that mixes with higher w/b generally have a higher rate of crack development. A lower w/b leads to lower crack areas and smaller crack widths.

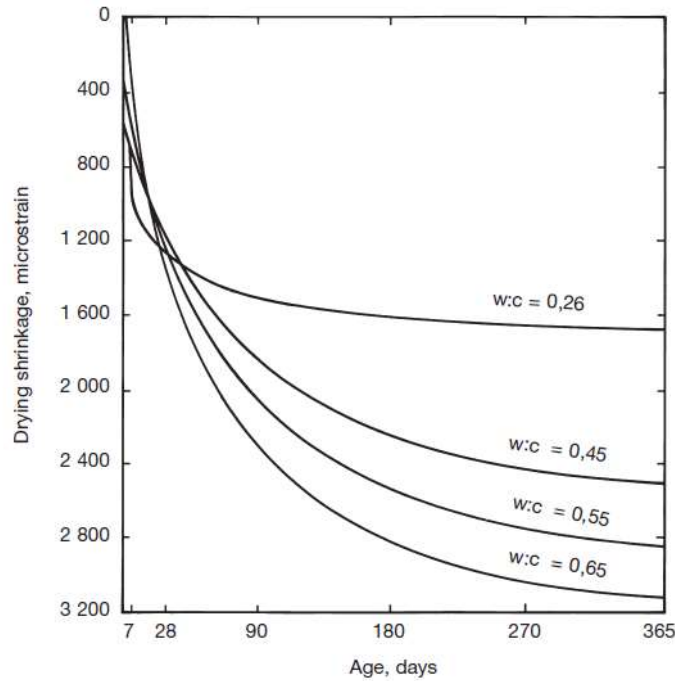


Figure 2-10: Effect of w/b ratio on shrinkage of cement pastes – adopted from Haller P 1940 as cited in (Alexander & Beushausen, 2009).

2.2.4.5 Cement extenders

Fly ash (FA), ground granulated blastfurnace slag (GGBS) and condensed silica fume (CSF) affect restrained shrinkage cracking. Their influence varies from the type and amount of extender used. Alexander (1994) reports that the incorporation of GGBS in Portland cement concretes at normal replacement levels (50%) has the effect of causing a possible increase of 20% in shrinkage at early ages in small exposed laboratory specimens. The effect is however reversed at later stages with the shrinkage strains being reduced in sealed specimens at all ages. Shrinkage characteristics of concrete made with GGBS measured by Jaufeerally (2003) showed that in higher strength concrete, with w/b ratio of 0.5 and below, the use of GGBS resulted in slightly lower drying shrinkage of 10 - 15% less compared to OPC concrete. There was no significant difference in drying shrinkage observed between OPC and GGBS on lower strength concrete with w/b ratio of 0.6 and above.

Grieve (1991) showed that for similar exposure conditions, concrete made with Matla FA had similar drying shrinkage as OPC mixes at comparable compressive strengths over a range of FA

contents up to 30%. Minor influence of Lethabo FA on concrete shrinkage was reported by Mukheibir (1990). Mehta & Monteiro (2006) and Neville (2011) state that GGBS and FA generally tend to increase shrinkage due to the pore refinement that they cause which leads to increased shrinkage stresses within the pores on drying. A finer pore structure results in an increase in the radius of curvature of the menisci that form within the pores upon drying which leads to greater surface tension. This leads to an increase in drying shrinkage as stated in Section 2.2.4.1.

Several authors have indicated that CSF has little influence on concrete shrinkage, at least up to 10% by mass of cement (Carette & Malhotra, 1983; Johansen, 1981; Sellevold et al., 1987). This is due to that fact that CSF has the effect of densifying the microstructure of concrete and thus reducing the rate of moisture loss from concrete. Shrinkage therefore takes place at a slower rate in CSF concretes, although the final shrinkage will be similar to other comparable concrete mixes (Fidjestol and Lewis, 1998; Neville, 2011).

2.2.4.6 Admixtures

Admixtures have variable effects on shrinkage. Their effect depends on the type of admixture and cement and the exposure conditions. Super-plasticising admixtures when added to concrete reduce either the permeability of the concrete by maintaining the same water content but reducing the w/b ratio or increase the workability of concrete whilst maintaining the same water content and w/b ratio. When they are used to decrease the water content while maintaining the same w/b ratio results in lower paste content thus causing a delay in the age at which concrete cracks.

SRAs reduce the rate of magnitude of shrinkage of concrete. This is through the reduction of surface tension of water in the capillary pores of concrete (Bentz, 2005; Kosmatka and Wilson, 2003; Radlinska, et, al.2007). This reduction results in reduced capillary stresses in the capillary pores and thus reduces autogenous and drying shrinkage strain. SRAs reduce plastic shrinkage by modifying the shape of the drying profile created with the mortar or concrete which leads to a concurrent reduction in the rate of evaporation (Bentz, 2005).

Accelerating admixtures are used to accelerate the early strength development of concrete although they may also coincidentally accelerate the setting of concrete. At high temperatures, accelerators

may result in a high rate of development of heat of hydration and in shrinkage cracking (Neville, 2011). Retarding admixtures tend to increase the plastic shrinkage because the duration of plastic stage is extended but drying shrinkage is not affected. Water reducing admixtures are used to reduce the water content of the mix, usually by 5 or 10%, sometimes (in concretes of very high workability) up to 15%. Their use allows the reduction in the w/b ratio while retaining the desired workability or, alternatively, improves its workability at a given w/b ratio. Neville (2011) states that Lignosulfonate-based water-reducing admixtures increase shrinkage, but other water reducing admixtures have been shown not to affect shrinkage.

2.2.4.7 Fibres

Fibres aid in controlling restrained shrinkage cracking by increasing the age at which visible cracking is observed and reducing total crack area, maximum crack width and the number of cracks (Banthia, & Gupta, 2006; Bissonnette & Pigeon, 1995; Carlswärd, 2006; Shah & Weiss, 2006). This is illustrated in Figure 2-11. The age of visible cracking is slightly delayed by the inclusion of randomly distributed steel fibres presumably due to the ability of the fibres to arrest cracking before the crack propagates across the specimen unstably (Shah & Weiss, 2006).

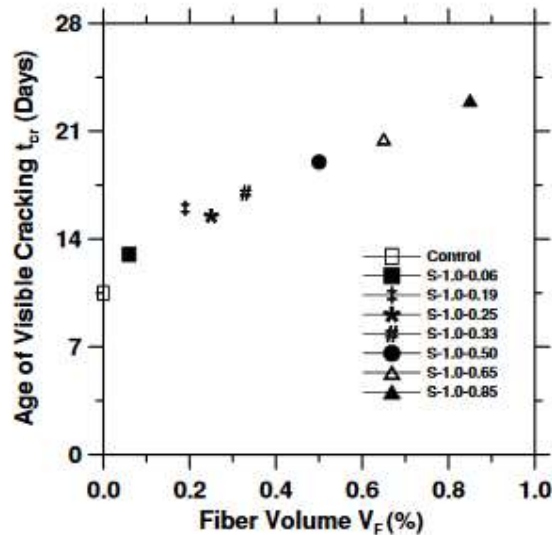


Figure 2-11: Age of visible cracking as a function of fibre volume – adopted from (Shah & Weiss, 2006).

The fibre type, volume, length, diameter, modulus, and spatial distribution influence restrained shrinkage cracking. An increase in fibre volume increases the age at which visible cracking is observed and decreases the average crack width. Steel fibres generally have a maximum efficiency at about 0.5% by volume whilst larger volumes of polypropylene fibres are required to obtain a similar crack area reduction. This is shown in Figure 2-12. Longer, finer fibres having smaller diameter are more effective than shorter, coarser fibres with larger diameter. This is due to the fact that they have a higher chance of bridging a crack and a larger surface area (for a given volume of fibres) over which the fibres can bond with the cement matrix, thus more transfer of tensile stress to the fibre (Grzybowski & Shah, 1990).

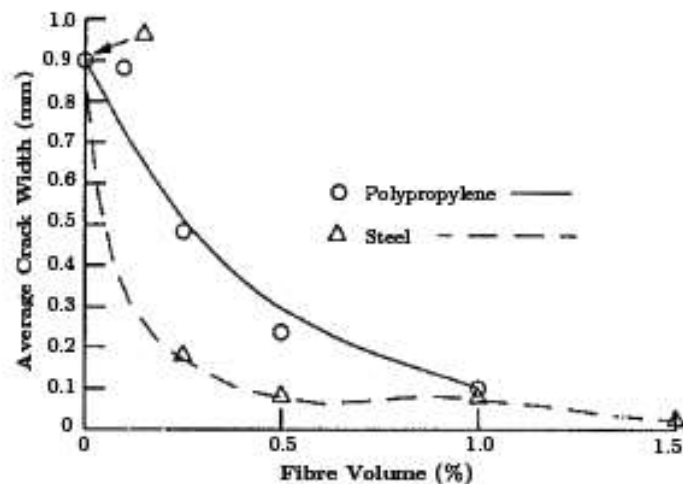


Figure 2-12: Influence of fibre type and volume on average crack width – adopted from (Grzybowski & Shah, 1990).

Shah & Weiss, (2006) report that material properties such as elastic modulus and splitting tensile strength are not heavily influenced by fibre addition and similarly free shrinkage in mortar and concrete is generally not influenced by fibre addition. Alexander & Beushausen (2009) and Dawood and Ramli (2011) report that the addition of fibre reinforcement in overlays enhances their crack resistance and bond durability, compressive strength, modulus of elasticity, flexural strength, toughness and strain capacity. The Concrete-Society (2003) reports that fibres reduce the risk of plastic shrinkage cracks due to an increase in the tensile strain capacity by a factor of 2 or 3. Filho et al. (2005) report that a high volume of vegetable fibres increases drying shrinkage, attributing the increase in drying shrinkage to the increase in the porosity of the cement matrix.

2.2.4.8 Member geometry

The member size and shape also influence the rate of moisture loss from the concrete consequently the rate and magnitude of drying shrinkage. This is because the drying of concrete takes place from the exposed surfaces. This generates a hygral gradient within the specimen, with associated restrained strains and internal strain gradients. Thus, although potential drying shrinkage is, at least conceptually, an intrinsic property of a concrete, actual observed shrinkage will depend upon member geometry and dimensions (Alexander & Beushausen, 2009).

Weiss (2002) reports that early age cracking behaviour of a cementitious system is geometry dependent. Thicker concrete sections are more resistant to cracking compared to thinner sections. Alexander & Beushausen (2009) report that large sections are less affected by carbonation and have longer effective curing times, consequently reducing the carbonation shrinkage component. The observed shrinkage decreases with an increase in member size, and is a function of the volume:surface area ratio of the member. The increased drying shrinkage of higher volume:surface area members, in addition to decreasing the age at cracking, also increases the crack area (Laurence et al., 2000). The influence of the member geometry on restrained shrinkage cracking is, however, less pronounced for concretes with lower w/b ratios. This is due to their low porosity and consequently slower rate of drying (Bissonnette et al., 1999).

2.2.4.9 Environmental Conditions and Curing

Environmental conditions have a marked influence on the moisture content within and movement of moisture out of the pores of concrete. This affects the drying shrinkage, tensile strength, elastic modulus and tensile relaxation material properties of concrete (Beushausen & Bester, 2016a). The concrete's environment comprises the type and extent of curing and the subsequent drying conditions, i.e. the ambient relative humidity and temperature (Alexander & Beushausen, 2009).

While moist curing delays the onset of shrinkage, the effect of curing on shrinkage of normal strength concrete is small. Alexander & Beushausen (2009) report that prolonged moist curing of greater than one month seems to somewhat reduce shrinkage of concrete, suggesting that this is one reason why the shrinkage of large structural members in which effective curing time is increased by slow drying is less than that of small members. Powers (1959), however, noted an

opposite effect for pastes presumably since the gel volume is increasing at the expense of unhydrated cement grains which restrain shrinkage.

The relative humidity of the environment directly affects the drying shrinkage. This is shown in Figure 2-13. Low relative humidities result in high shrinkage. This is due to the fact that concrete tends to achieve hygral equilibrium with the environment. Beushausen & Bester (2016a) and Neville (2011) report that neither wind nor forced convection affects the rate or magnitude of drying shrinkage. This is because the moisture movement in concrete is so low that only a negligible amount of evaporation is possible. The effect of temperature and wind, however, have a large influence on the rate at which bleed water evaporates from the surface of concrete and consequently increases the susceptibility of plastic shrinkage at early ages before the concrete has hardened.

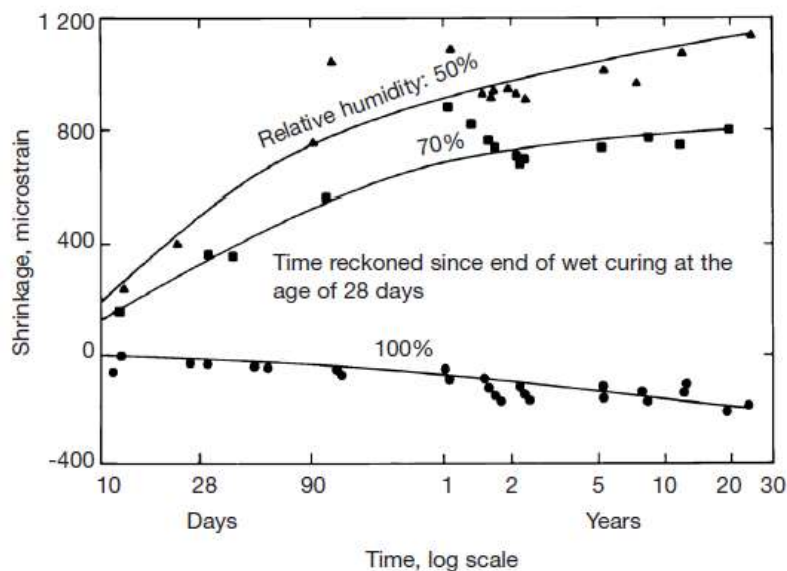


Figure 2-13: Relation between shrinkage and time for concretes stored in different relative humidities – adopted from (Troxell et al., 1958).

2.3 Compatibility of repair materials with substrate

2.3.1 Introduction

Compatibility is the balance of physical, chemical, and electrochemical properties and dimensions between the repair phase and the existing substrate phase of a repair system. This balance ensures

that the system withstands all anticipated stresses induced by volume changes, chemical, and electrochemical effects without distress and deterioration over its design service life (Emmons & Vaysburd, 1995). Dimensional compatibility is one of the most critical components of BCOs. The material properties that influence dimensional compatibility include shrinkage, modulus of elasticity, creep, thermal expansion, tensile strength and tensile relaxation. These factors are discussed briefly in Sections 2.3.2 to 2.3.5.

The service life of patch repairs depends on the correct choice and use of repair materials. Restrained shrinkage of patch repair materials, the restraint being provided through bond to the existing concrete substrate is a major factor which significantly increases the complexity of repair projects compared to new projects as discussed in Section 2.2.3. Many different proprietary brands are available with new materials being developed continually. The precise formulation of these materials varies from one manufacturer to another. Emmons & Vaysburd (1995) report that differences in properties will always exist between repair materials and the substrate concrete. It is therefore impossible to match all properties of the substrate material on an ancient structure, because at the time of repair, a large percentage of the ultimate shrinkage has already taken place.

The dimensional compatibility between the repair materials and the substrate is one of the greatest challenges facing the successful performance of repair materials. The use of materials that are identical with the substrate when subjected to loads, temperature and moisture changes is unlikely (Emmons & Vaysburd, 1995). The requirement for durable repairs is that the selected repair materials must have properties that are compatible with the substrate to a degree such that the stresses induced at the interface and in the overlay will not exceed the tensile strength of the overlay.

2.3.2 Shrinkage

The shrinkage of concrete is that portion of the time-dependent strain which would occur without the imposition of stress from external loads (Beushausen & Bester, 2016; Uys, 1983). It occurs during the fresh and hardened states of concrete due to the movement of moisture within or out of the concrete. It comprises of the following types of shrinkage, namely plastic, chemical, autogenous, drying, and carbonation shrinkage. Plastic and drying shrinkage which are both due to moisture diffusion are the two main contributors to the total shrinkage of repair mortars

(Alexander & Beushausen, 2009). Additional details regarding shrinkage can be found in Section 2.2.

2.3.3 Elastic modulus

Elastic modulus is the ratio of uniaxial stress to the resultant axial strain. It represents the material stiffness of the concrete to an imposed stress. The stress-strain relationship of concrete does not obey Hooke's law, this is due to the non-linear stress strain responses of the paste and ITZ, and to microcracking in the matrix. The initial portion of the curve where the stress represents approximately 30 to 40% of the ultimate strength may be regarded as linear. The elastic modulus (slope of the linear portion) within this range is referred to as the initial tangent modulus. Two other forms of elastic modulus may be considered, namely the tangent modulus, represented by the slope of the tangent to the curve at particular stress, and the secant modulus represented by the slope of the line connecting the origin to the point on the curve corresponding to the stress selected (Neville, 2011). This is illustrated in Figure 2-14.

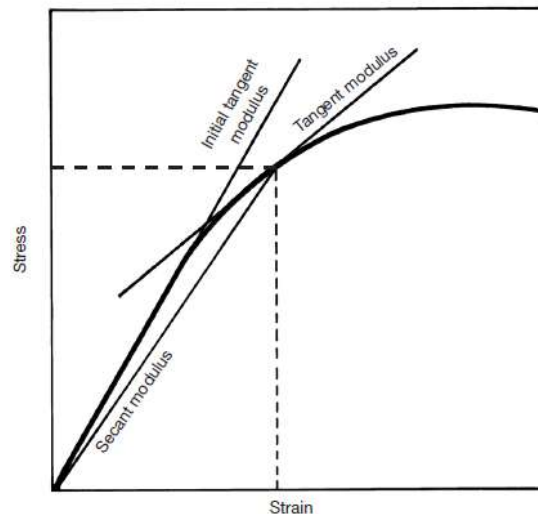


Figure 2-14: Three forms of elastic modulus - adopted from (Alexander & Beushausen, 2009).

Differences in the elastic moduli of the repair material and the substrate has been established to cause internal cracks and flaws to exist in a repair composite system. The compatibility in elastic moduli, therefore, becomes, in some cases, an important factor because incompatibility may lead to considerable stress concentration when widely differential volume changes of the repair material in relation to the concrete substrate occur. Since, in such situations, the interfacial bond region

(transition zone) is the weak link in the repair system, and cracks will tend to form in this region. In certain cases where the bond strength is high, cracks will occur in the matrix of the material which has the higher modulus of elasticity.

2.3.4 Thermal compatibility

The coefficient of thermal expansion (CTE), which gives a measure of dimensional contraction or expansion with changes in temperature, is an essential property of the composite repair system. When significant changes in temperature occur, a marked difference in the CTE will produce different volume changes between the repair material and the concrete substrate. Such differential volume changes may produce excessive stresses at the interface between the repair material and the concrete which causes bond failure or, in the case of high bond strength, failure within the lower strength material (Emmons & Vaysburd, 1995a). The greater the difference between CTE of aggregate and hardened cement paste, the greater the reduction of mechanical properties and durability of concrete if it is exposed to temperature changes.

The linear CTE, depends on the mix proportions and constituents of the concrete. This is because the CTEs of hardened cement paste and aggregates can be in a wide range and can differ markedly from each other. The volume concentration of aggregate in the mix also plays some part, albeit a minor one, and this is shown in Figure 2-15 (Browne, 1972).

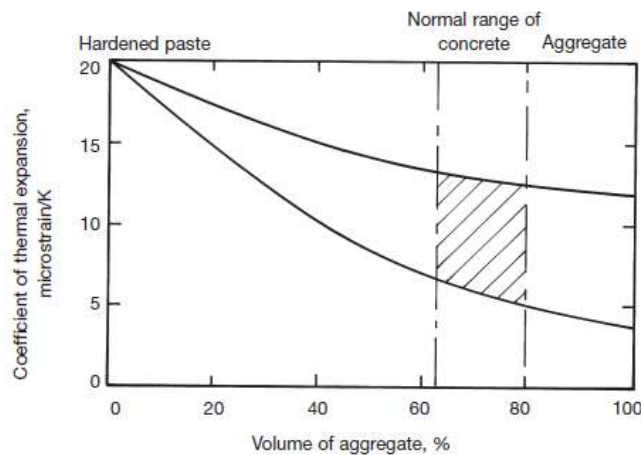


Figure 2-15: Thermal expansion of concrete having different aggregate types and contents - adopted from (Browne, 1972).

When concrete is exposed to temperature changes, unequal volume changes of its components cause tensile stresses and cracking of concrete and reduce its durability. This phenomenon is called thermal incompatibility of concrete components (TICC) which in practice appears if aggregate in concrete has a very low CTE (Emmons & Vaysburd, 1995a).

A study by Emmons & Vaysburd (1995a) reports that resinous repair materials have significantly higher CTE's compared to non-resinous materials. Non-resinous materials tend to have values about equal to that of many unmodified concretes, and the addition of polymers to unmodified materials has little effect on their coefficients of thermal expansion.

2.3.5 Creep and tensile relaxation

Creep is the increase in strain or deformation under a constant stress as shown in Figure 2-16. The main contributor to creep in concrete is the hardened cement paste. Creep in concrete occurs at all stress levels, and the creep strain can be several times larger than the initial strain on loading. Creep affects concrete ductility and relieves concrete of stresses due to differential structural movement and restrained shrinkage. However, creep also has detrimental effects on structures, such as increased deflections which can result in cracking, loss of pre-stress and creep buckling of long columns. (Alexander & Beushausen, 2009).

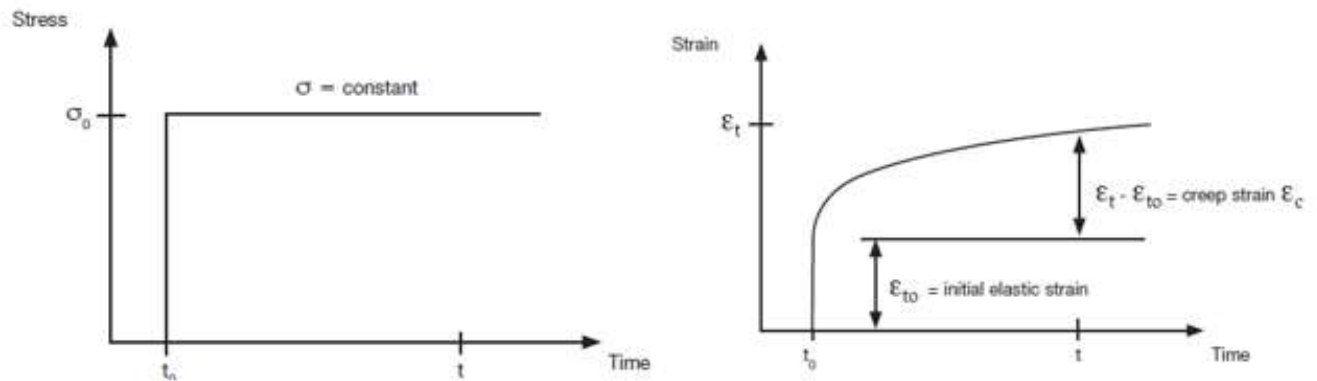


Figure 2-16: Characteristics of creep: time-dependent increase in strain under constant stress - adopted from (Alexander & Beushausen, 2009).

Creep effects have been shown to reduce the resulting tensile stress through relaxation. Most studies on tensile relaxation have used creep properties for the determination of relaxation in composite systems (Carlsward, 2006; Chilwesa & Beushausen, 2012; Ghali et al., 2006), this is

due to the lack of sufficient accumulated data on tensile stress relaxation (Alexander & Beushausen, 2009). Tensile relaxation is the time-dependent decrease in stress of the body under a sustained strain. This is illustrated in Figure 2-17.

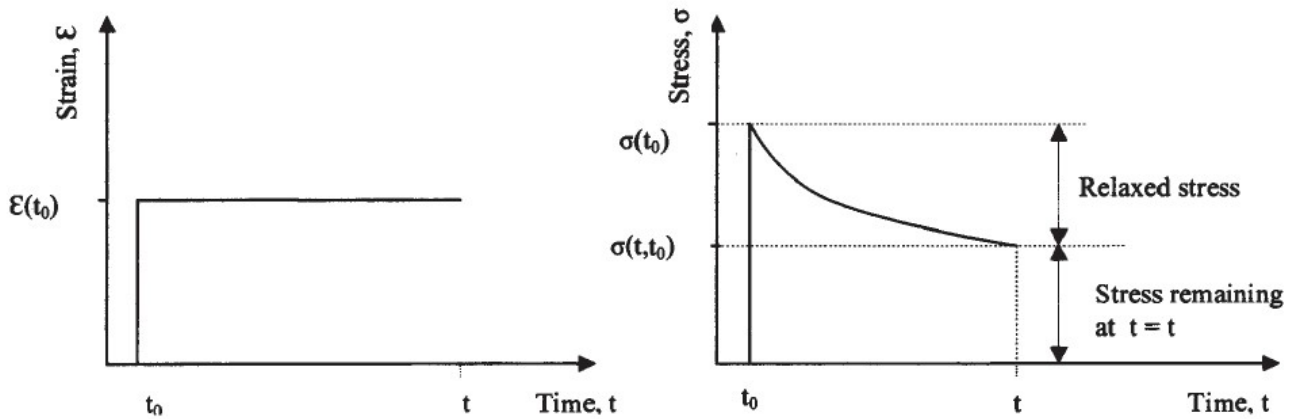


Figure 2-17: Characteristics of relaxation: time-dependent decrease in stress under constant imposed strain - adopted from (Alexander & Beushausen, 2009).

Creep and relaxation are manifestation of viscoelasticity, their source being in the cement paste. Creep has been attributed by some authors (Freudenthal, 1950; Reiner, 1960) to the viscous flow of the cement paste. These investigators attribute the reduction in the strain rate over time to the increasing viscosity of the paste and the gradual transfer of load from the cement paste to the aggregate. Contrary to this theory is the fact that the volume of concrete does not remain constant while it creeps and that there is partial recovery of creep when the load is removed (Emmons & Vaysburd, 1995a).

Creep in concrete occurs at all stress levels and imparts a degree of ductility to the concrete which is desirable for stress relief. Altoubat & Lange (2001) report that the tensile creep relaxes the shrinkage stress by as much as 50% and doubles the failure strain capacity. Beushausen & Alexander, (2006) have reported tensile relaxation values as high as 60%. In thin bonded overlays, tensile creep is the main stress relief mechanism (Bissonnette et al., 1999). A high level of relaxation helps reduce the tensile stress resulting from restrained shrinkage (Chilwesa & Beushausen, 2012).

2.4 Performance requirements for BCOs

Performance requirements for repair materials refers to a specific set of mechanical, physical and chemical properties for products and systems that would guarantee durability and stability for the repaired concrete structure. These requirements are based on a specific service environment and design objectives. A specific set of tests are usually performed on a material in accordance to a predetermined test standard to verify its required properties.

Arito et al. (2016b) and Jacobs (2006), report that prior to 1997 the repair of concrete structures was governed by numerous national standards and guidelines that varied from one locality to another. The wide variability in standards and guidelines necessitated the need to draft and adopt a more generalised standard of practice that could assist in creating harmony, especially in repair projects that involved the sourcing of materials and experts from different localities. To harmonise the repair of concrete structures, the EN 1504 series of standards and other standards were drafted to address specific forms of repairs such as re-alkalisation, cathodic protection and electrochemical chloride extraction. The repair industry mainly specifies appropriate repair treatment and product requirements for concrete repair products by the European Standards, EN 1504-3:2005. There, however, exists other standards such as the USA recommendations from the American Concrete Pavement Association (ACPA), Japanese requirements published by The Japan Highway Research Foundation and Swedish requirements by the Swedish National Road Administration. For this research EN 1504-3:2005 was considered because it is the guideline that is mostly used by manufacturers in South Africa. It is also the basis for CEN certification that is usually branded on many proprietary repair products – whose parent companies (e.g. Sika, BASF, etc) are headquartered in Europe.

2.4.1 EN 1504

Concrete repair is usually carried out to the specifications of local or national standards and guidelines. Prior to the development of EN 1504, the characteristics, performances required, as well as the approval systems developed in most countries varied. However, with the introduction of the European Standards these differences were minimised (Tilly & Jacobs, 2007).

The EN 1504 Standard, '*Products and systems for the protection and repair of concrete structures*', is divided into 10 parts. It deals with all the phases of a repair project, from the

awareness of the problem to the maintenance and inspection after the completion of the repair work. Table 2-3 shows the parts of the EN 1504 standard, the year of publication and their titles.

Table 2-3: European standards related to concrete repair products and systems - adopted from (Arito, 2018; Tilly & Jacobs, 2007).

Number	Year	Title
EN 1504- 1	1998 (2006)	Part 1: Definitions
EN 1504- 2	2004 (2006)	Part 2: Surface protection systems for concrete
EN 1504- 3	2005	Part 3: Structural and non-structural repair
EN 1504- 4	2004	Part 4: Structural bonding
EN 1504- 5	2004 (2013)	Part 5: Concrete injection
EN 1504- 6	2007	Part 6: Anchoring of reinforcing steel bar
EN 1504- 7	2007	Part 7: Reinforcement corrosion protection
EN 1504- 8	2004	Part 8: Quality control and evaluation of conformity
EN 1504- 9	1997 (2009)	Part 9: General principles for the use of products and systems
EN 1504- 10	2003	Part 10: Site application of products and systems and quality control of works

The year in brackets refers to the year of revision of the specific standard

EN 1504-3:2005 classifies patch repair products into two categories, namely: structural and non-structural. It recommends specific performance characteristics that need to be specified in repair mortars. Structural and non-structural mortars are further categorized into two classes based on their compressive strengths: R1 and R2 (for non-structural repairs) and classes R3 and R4 (for structural repair). Table 2-4 summarises the recommended performance characteristics and their test methods.

Table 2-4: Performance characteristics for structural and non-structural repair products for all intended uses and certain intended uses - adopted from EN 1504-3:2005.

Performance Characteristics	Test Method	Field Application	
		All Intended Use (AIU)	Certain Intended Use (CIU)
Compressive strength	EN 12190	✓	
Chloride ion content	EN 1015-17	✓	
Adhesive bond	EN 1542	✓	
Restrained shrinkage/expansion	EN 12617-4	✓	
Durability			
a) Carbonation resistance	EN 13295	✓	
b) Thermal compatibility (Part 1 or Part 2 or Part 4 of EN 13687)	EN 13687-1-2-4		✓
Elastic Modulus	EN 13412		✓
Skid resistance	EN 160364		✓
Coefficient of thermal expansion	EN 1770		✓
Capillary absorption	EN 13057		✓

The performance requirements specified in EN 1504-3:2005 for structural and non-structural repair products are summarized in Table 2-5. These performance requirements are discussed in the subsequent subsections.

Table 2-5: Performance requirements for repair products - adopted from EN 1504-3:2005.

Performance Characteristic	Reference Substrate	Test Method	Requirement			
			Structural		Non-Structural	
			Class R4	Class R3	Class R2	Class R1
Compressive strength	None	EN 12190	≤ 45 MPa	≤ 25 MPa	≤ 15 MPa	≤ 10 MPa
Chloride ion content	None	EN 1015-17	≤ 0.05%		≤ 0.05%	
Adhesive bond	MC (0.40)	EN 1542	≥ 2.0 MPa	≥ 1.5 MPa	≥ 0.8 MPa	
Restrained shrinkage/expansion	MC (0.40)	EN 12617-4	Bond strength after test			No Requirement
			≥ 2.0 MPa	≥ 1.5 MPa	≥ 0.8 MPa	
Carbonation Resistance	None	EN 13295	$d_k \leq$ control concrete (MC (0.45))		No Requirement	
Elastic Modulus	None	EN 13412	≥ 20 GPa	≥ 15 GPa	No Requirement	
Thermal compatibility Part 1: freeze-thaw	MC (0.40)	EN 13687-1	Bond strength after 50 cycles			Visual Inspection after 50 cycles
			≥ 2.0 MPa	≥ 1.5 MPa	≥ 0.8 MPa	
Thermal compatibility Part 2: thunder-shower	MC (0.40)	EN 13687-2	Bond strength after 30 cycles			Visual Inspection after 30 cycles
			≥ 2.0 MPa	≥ 1.5 MPa	≥ 0.8 MPa	
Thermal compatibility Part 4: Dry cycling	MC (0.40)	EN 13687-4	Bond strength after 30 cycles			Visual Inspection after 30 cycles
			≥ 2.0 MPa	≥ 1.5 MPa	≥ 0.8 MPa	
Skid resistance	None	EN 13036-4	Class I: > 40 units wet tested Class II: > 40 units dry tested Class III: > 55 units wet tested		Class I: > 40 units wet tested Class II: > 40 units dry tested Class III: > 55 units wet tested	
Coefficient of thermal expansion	None	EN 1770	Not required if tests 7, 8 or 9 are carried out, otherwise the declared value.		Not required if tests 7, 8 or 9 are carried out, otherwise the declared value.	
Capillary absorption	None	EN 13057	≥ 0.5 kg.m ² .h ^{0.5}		≥ 0.5 kg.m ² .h ^{0.5}	No Requirement

Despite their widespread use, Arito (2018) reports that the current series of standards do not address the challenges that hinder the realization of durable and effective concrete repairs in service. Compliance to these tests – and the values therein – does not guarantee durable and

effective concrete repairs in service. EN 1504 fails to include requirements for rehabilitation of concrete structures damaged due to fire, defects and damage in post-tensioned concrete structures and the repair materials and systems used for purposes other than rehabilitation of damaged concrete structures, e.g. to improve aesthetic appearance (DANSK - Standard, 2004; Tilly & Jacobs, 2007). EN 1504-3:2005 does not specify some important material properties such as elastic modulus and tensile relaxation for non-structural and structural repair mortars, yet they are relevant for their performance against cracking and debonding. The DANSK - Standard (2004) recommends supplementary considerations to be made should the repair systems fail to meet any categories highlighted in EN 1504. Examples of such cases include: reinforced concrete structures - especially prestressed concrete - where the structure and chemistry of concrete, as well as the tensile strength of cold-drawn reinforcement have been changed due to fire and concrete which has been subjected to high heat exposure over a long period e.g. concrete in chimneys and in steelworks.

With the high failure rate of the new proprietary repair mortars, these standards need to undergo continuous revisions and modifications. There is a need to identify and specify material properties that directly contribute to the realization of durable and effective repairs. A critical review of the existing performance criteria - as specified in the EN 1504-3:2005 - needs to be done to provide a platform for the development of performance criteria for repair mortars which can be used for project specification and quality control in industry. The performance criteria as specified in EN 1504-3:2005 are discussed in the subsequent sub sections.

2.4.1.1 Bond strength

Bond strength is the amount of stress required to separate an overlay from its substrate. It can be used as a quantitative measure of the bond of a repair material to the substrate (Arito, 2018). Naderi et al. (1986) reports that there is no standard definition of bond strength because it depends on the state of stress a structure is subjected to. It is therefore a challenge to compare the magnitude of bond strengths obtained using various methods. The bond strength obtained in tension should not be compared with the one from shear tests because the stress mechanisms causing failure are different in both methods.

A good bond between the overlay and the existing substrate is the primary requirement for successful repair. Sufficient bond strength will always be provided by a properly prepared substrate. ICRI (2003) reports that bond failure between repair materials and a properly prepared concrete substrate are frequently caused by drying shrinkage and are not as a result of inadequate bond strength. The following tests have been developed for testing bond strength. They include: the direct tensile test, slant shear test, direct shear strength test, splitting prism test, three-point bending test, tensile pull off test, push-out/push-off test and guillotine test (ICRI, 2013). For this research, the tensile pull-off test was used. EN 1504-3:2005 specifies that using EN 1542 test method, non-structural repair mortars should achieve an adhesive bond strength that is greater than 0.8 MPa while for structural repair mortars values of ≥ 2.0 MPa and ≥ 1.5 MPa for Class R4 and Class R3 respectively (see Table 2-5).

2.4.1.2 Elastic modulus

As discussed in detail in Section 2.3.3, elastic modulus is the measure of stiffness. It is the ratio of uniaxial stress to the resultant axial strain. The stiffness of concrete to an imposed load is determined by the stiffness of the individual phases of the concrete (Alexander & Beushausen, 2009). Elastic modulus is usually tested in compression. EN 1504-3:2005 does not provide any performance specifications for elastic modulus for non-structural repair mortars but for structural repair mortars it specifies values of ≥ 20 GPa and ≥ 15 GPa for Class R4 and Class R3 respectively. The test standard specified is EN 13412.

2.4.1.3 Restrained Shrinkage

Shrinkage, as explained in detail in Section 2.2.3, occurs from the movement of water within the cementitious material without imposed stresses from external loads. Restrained shrinkage occurs when the repair material bounded to a substrate produces tensile stresses in the repair material (ICRI, 2003). This results in cracking and debonding.

The ring test and a restrained bar test have been proposed to evaluate material performance under restrained shrinkage conditions. EN 1504-3:2005 bases the tests for restrained shrinkage on EN 12617-4. It has not specified any requirements for class R1 non-structural repair mortars, but it recommends a bond strength under tensile forces (pull off) of greater than 0.8 MPa for class R2.

For structural repair mortars it specifies values of ≥ 2.0 MPa and ≥ 1.5 MPa for Class R4 and Class R3 respectively. The bond strength are tested in accordance to EN 1542.

2.4.1.4 Compressive strength

The compressive strength of a repair material is the basic measure of its ability to resist compressive loads. ICRI (2003) reports that the compressive strengths of repair materials should be approximately equal to the substrate compressive strength. A difference in compressive strength also indicates a difference in modulus of elasticity. Substantial differences between these two properties may cause incompatible strains and excessive load transfer to the higher strength material. EN 1504-3:2005 specifies values of ≤ 15 MPa and ≤ 10 MPa for class R2 and Class R1 non-structural repair mortars respectively. The test standard specified is EN 12190.

The importance of this property needs to be weighed against other durability properties during specification as high compressive strengths may adversely affect other properties needed in some instances (Arito, 2018; Beushausen & Bester, 2016b). However, it is critical if the repair material is expected to be structural.

2.4.1.5 Tensile strength

Tensile strength is an indication of the ability of the material to withstand tensile stresses. ICRI (2003) recommends that in areas where repairs are likely to be subjected to tensile loads for example the top side of a cantilevered balcony, the tensile strength should be specified. EN 1504-3:2005 does not specify any values for the tensile strength for repair mortars.

2.4.1.6 Durability

ICRI (2003) defines durability of a Portland cement concrete as its ability to resist weathering action, chemical attack, abrasion and any other conditions of service. A durable repair will retain its original form, quality and serviceability when exposed to its environment. Durability of concrete is linked to the nature of its pore structure. Concrete with a refined pore structure will have lower porosity and permeability, making it less susceptible to aggressive agents that may cause deterioration (Beushausen & Bester, 2016).

There is lack of clearly defined performance requirements for repair mortars with regard to durability (Arito, 2018). The South African durability index (DI) testing method and specifications which are used in concrete could be adopted to help the development of performance requirements for repair mortars. Table 2-6 shows the concrete durability classification based on the UCT DI prediction tests. Hall & Hoff (2011) indicate that the sorptivity of a material can be used to aid specification and acts as a determinant of long-term durability.

Table 2-6: Concrete durability classification based on the UCT DI prediction tests – adopted from (Gillmer, 2012).

Durability Class	OPI (-log k m/s)	Sorptivity (mm/hr^{0.5})	Conductivity (mS/cm)
Excellent	>10	<6	<0.75
Good	9.5-10	6-10	0.75-1.50
Poor	9.0-9.5	10-15	1.50-2.50
Very Poor	9	>15	>2.5

2.4.2 Other standards

2.4.2.1 USA recommendations

Having recognized the need for longer-lasting concrete structures, the American Concrete Institute (ACI) published in 2013, the first U.S. code requirements specifically for the repair of reinforced concrete, ‘*Code Requirements for Evaluation, Repair and Rehabilitation of Concrete Buildings*’ (ACI 562-13). It was ACI’s first performance-based code. It is structured to afford licensed design professionals significant flexibility in selecting materials and devising customized repair strategies, while following a minimum baseline of code requirements. The second version of the code ACI 562 - 16 was published in June 2016 (Nahlawi & Paul, 2016; Paul, 2016). ACI 562-19 was published in 2019. ACI and the International Concrete Repair Institute (ICRI) have now published the ‘*Guide to the Code for Evaluation, Repair, and Rehabilitation of Concrete Buildings*’ as a companion to the code, which will help designers clearly and quickly interpret new, performance-based provisions of ACI 562 that directly impact the way they approach concrete repair.

Section 7.4 of the ACI code emphasizes the importance of proper bonding between the substrate and overlay. It states that the licensed design professionals should determine the factored interface shear and tension stresses across the bonded interfaces between the repair materials and existing substrates. They should then verify that the calculated horizontal shear strength is at least equal to the required bond strength or tensile strength of the concrete substrate, such that;

$$v_u \leq \phi v_m \dots\dots\dots (2.3)$$

Where v_u is the calculated bond demand shear stress based on mechanics, ϕ is the reduction factor obtained from ACI 562-16, Section 5.3.2, and v_m is the measured bond stress determined using a valid test method such as ASTM C1583/C1583M.

According to ACI 562-16, Section 7.4.2, for bonded interfaces with v_u values < 30 psi (0.2 MPa), only qualitative bond-integrity testing is required. For bonded interfaces with $v_u > 60$ psi (0.4 MPa) (per Section 7.4.4), or a repaired section that is subjected to a sustained tension force, reinforcement must be provided between the substrate and overlay.

American Concrete Pavement Association (ACPA) published in 1990 provides guidelines related to the design of BCOs, however, no updates are available (Bissonnette et al., 2013). According to ACPA, for a durable bonded overlay, it is sufficient to achieve a 0.7 MPa bond strength under a tensile load.

2.4.2.2 Japanese Requirements

The Japan Highway Research Foundation has published bonded concrete overlays guidelines in its *Design and Execution Manual for Bonded Concrete Overlays* for repairing bridge decks. It is the only commonly accepted design manual for concrete overlays in Japan (Bissonnette et al., 2013).

It comprises six chapters as shown in Table 2-7, with the design principles being presented in Chapter 4 of the manual. It specifies the use of ultra-rapid-hardening cement for mixture proportions of the overlay to be able to achieve a compressive strength of 24 MPa at the established age of 3 hours. This gives a higher value for the strength of about 40 MPa when the road is opened for the traffic.

Table 2-7: Contents of the design and execution manual from Japan – adopted from (Bissonnette et al., 2013).

Reference	Title
Chapter 1	General Principles
Chapter 2	Planning
Chapter 3	Materials
Chapter 4	Design
Chapter 5	Execution
Chapter 6	Quality Control

The Japanese requirements specify that a minimum thickness of 50 mm is required for the overlay. It was determined by considering the maximum aggregate size, shrinkage, and the quality of the workmanship. The standard thickness of the treated surface of the substrate concrete is specified as 10 mm. For surface treatment, shot blast methods are recommended because these surfaces can achieve a bond strength of 1 MPa. Shot blast methods are commonly used in Japan because of their cost although the use of high performance water jet method has been acknowledged by recent studies by Takuwa et al. (2000). The guideline further states that shear reinforcement is not necessary for overlay concrete. A bond strength under a tensile load of 1 MPa between overlay and substrate is sufficient for up to three times higher loads than the design value according to the experimental results of the research projects (Bissonnette et al., 2013).

2.4.2.3 Swedish Practice

The Swedish standards on concrete repair, Svensk Standard SS-EN 1504, borrows heavily from the EN 1504 already discussed in Section 2.4.1. Research organisations such as the Swedish Cement and Concrete Research Institute (CBI) also coordinates projects on concrete repair for instance the EU-project REHABCON ‘*Strategy for maintenance and rehabilitation in concrete structures*’ which began in May 2001 and ended in May 2004 (Fagerlund, 2004). The Swedish National Road Administration, which possesses extensive experience in concrete bridge repair (Bissonnette et al., 2013), has used the following requirements for BCOs.

The required tensile bond strength is $f_v = 1.0$ MPa. This requirement is satisfied if:

$$m \geq f_v + 1.4 \cdot s$$

$$x \geq 0.8 f_v$$

Where m and s are the average and the standard deviation ($s \geq 0.36s$ MPa) of the measuring values, respectively, and x is a single measuring value.

2.5 Closure

An introduction to BCOs and their use in extending the service life of concrete structures has been presented. The frequent deterioration of concrete structures has resulted in a need for their repair and protection. For more durable repairs, a better understanding of the performance of repairs and repair mortars in practice is required. An evaluation of the factors affecting the durability of concrete repairs has been presented. These include the process of substrate preparation; the overlay characteristics which are determined by the material selection process and application techniques. Various design and construction factors must be considered to ensure sufficient bond strength and crack resistance of bonded concrete overlays.

It has been observed that a repaired structural member is a three-phase composite system consisting of the substrate, overlay and the transition zone. Failure in repair mortars is mainly manifested by cracking and debonding. BCOs crack due to the tensile stresses induced by the restrained shrinkage deformations. The factors influencing restrained shrinkage cracks have been presented. They comprise: fineness and composition of cement, aggregate type and content, water and paste content, w/b ratio, cement extenders, admixtures, fibres, member geometry, environmental conditions and curing.

The formulation of proprietary repair materials varies from one manufacturer to another. Literature reveals that differences in properties will always exist between repair materials and the substrate concrete, and it is impossible to match all properties of the substrate material, because at the time of repair a large percentage of the ultimate shrinkage has already taken place. While compatibility has been reported to be necessary for the realisation of effective repairs, it is impossible to achieve the reviewed compatibility requirements for BCOs in practice. The material properties that influence dimensional compatibility include shrinkage, modulus of elasticity, creep, thermal expansion, tensile strength and tensile relaxation. These properties have been presented in Section 2.3. The correlation between compressive strength and durability of repair mortars as reported in literature should be avoided.

Finally, the performance requirements for BCOs have been presented. They refer to a specific set of mechanical, physical and chemical properties for products and systems that would guarantee durability and stability for the repaired concrete structure. The repair industry mainly specifies appropriate repair treatment and product requirements for concrete repair products by the European Standards, EN 1504. Despite their widespread use, Arito (2018) reports that the current series of standards do not address the challenges that hinder the realization of durable and effective concrete repairs in service. Compliance to these standards – and the values therein – does not guarantee durable and effective concrete repairs in service. EN 1504 fails to include requirements for rehabilitation of concrete structures damaged due to fire, defects and damage in post-tensioned concrete structures and the repair materials and systems used for purposes other than rehabilitation of damaged concrete structures, e.g. to improve aesthetic appearance. EN 1504-3:2005 does not provide any performance specifications for elastic modulus, tensile relaxation and creep which has been reported to be critical to cracking. The code does not also specify any durability and workability performance properties for BCOs. EN1504, therefore, requires modifications and/or revisions to make them more responsive to the realisation of effective repairs with respect to cracking and durability.

There are numerous other technical guidelines and recommendations. These guidelines and standards specify properties that differ from each other. The most common material properties that were observed to differ comprise shrinkage, strength and bond strength. There is therefore a need to resolve these differences in the performance requirements among the existing guidelines and standards so that the potential conflicts and confusion in the specification of performance requirements in practice are avoided.

3. Experimental methodology

3.1 Introduction

The factors that affect the performance of BCOs as well as the standards, codes and technical guidelines for repair mortars were presented in Chapter 2. It was established that overlay cracking depends on the interaction between the tensile stress from the restrained shrinkage and the time-dependent material properties such as elastic modulus, tensile relaxation, compressive and tensile strength. It is therefore important to understand how these material properties affect the performance of repair mortars. This chapter describes the experimental work, the testing philosophy, experimental design and the experimental variables under investigation. Material property tests were conducted in line with the objective of this research which was to investigate the performance requirements for proprietary repair mortars on cracking resistance and durability with respect to EN 1504-3:2005. This involved an investigation of the mechanical properties of proprietary repair mortars in their hardened state and an investigation of their durability and transport properties. The test methods and standards that were used are also discussed.

3.2 Testing philosophy and experimental approach

The mechanical properties that were investigated comprised: compressive strength, tensile strength, elastic modulus, tensile relaxation, restrained shrinkage cracking, bond strength and drying shrinkage. Durability index tests - specifically OPI, CCI and WSI - were also performed on the repair mortars.

Twelve repair mortars from four different manufacturers were tested. Major suppliers and manufacturers of repair products in South Africa provided their most used products in the industry to be tested in this study. A study of the data sheets from manufacturers indicated only some known characteristics of selected products to have been recorded. The property details were briefly described on the data sheets which were full of descriptions of methods of preparation and placement. The more detailed information on ingredients and relevant technical data regarding tensile strengths, shrinkage, bond strength to both concrete and steel, strain capacity, and creep are invariably unavailable, un-researched, or not revealed. Compressive strength was however quoted. It was also noted that they do not always use the same tests to determine the material properties

for their various products. The use of different test methods from another manufacturer makes it difficult to determine if the products are similar.

The specimens for the different tests in this study were exposed to a controlled laboratory environment with a mean temperature and relative humidity of $23^{\circ}\text{C} \pm 2^{\circ}\text{C}$ and $50\% \pm 4\%$ respectively. The range of temperature and relative humidity chosen is consistent with the requirements for various tests such as drying and restrained shrinkage. Other tests e.g. compressive strength and elastic modulus deviated from the specific laboratory environment to comply with their respective test standards.

The experimental procedure involved casting of cubes for compressive strength of the proprietary repair mortars. They were tested at 7, 14 and 28 days to monitor their strength gain. Dog-bone specimens were used to test for tensile strength and tensile relaxation. Elastic modulus was also tested at 7 and 28 days using cylindrical specimens. The time-development of the elastic modulus of the repair mortars was also monitored. To determine the age at cracking, width and area of the cracks, ring tests were performed. The ring tests were selected for the restrained shrinkage tests due to their simplicity as discussed in Section 3.7.6. Tests for drying shrinkage were conducted on 100 x 100 x 200 mm prism specimens. Drying shrinkage was monitored over 60 days after curing in a water bath for 28 days. The 60-day duration corresponded to the point where no significant change in the shrinkage measurements on most of the proprietary repair mortars was observed.

3.3 Test equipment

The following equipment was used;

- a) 50 and 25 litre pan mixers: to produce fresh mortar.
- b) Amsler hydraulic testing machine: for compressive strength tests.
- c) Zwick Roell Z020 Universal Testing Machine (UTM): for testing the tensile relaxation after 48 hours and direct tensile strength.
- d) DI tests equipment: for testing the durability indexes - OPI, WSI and CCI.
- e) Steel rings: to test for restrained shrinkage cracking under the ring tests.
- f) Electronic scales: for weighing specimens and materials

- g) Drying ovens: for drying wet materials and specimen preparation for DI and pull-off tests.
- h) Tamping rod: manual compaction of freshly-cast mixes.
- i) Crack meter: for measuring crack widths.
- j) Proceq dy-216 Pull-off test testing machine: for tensile bond test.
- k) Vibrating table: for compacting freshly-cast specimens.

3.4 Test materials – proprietary repair mortars

The most widely used proprietary repair materials in the Western Cape were sourced from four different manufacturers for testing. Twelve different proprietary repair mortars were supplied, three from each manufacturer. The mix proportions and key mix properties for the repair mortars as provided by the manufacturers are given in Table 3-1.

Table 3-1: Mix proportions and mix property for the commercial repair mortars.

Mix constituents												
Mix ID	PS	PFS	SA	S1	S2	G1	PF	G2	P1	PF	P2	A
Packaging per bag (kg)	25	25	20	25	25	25	25	25	25	20	20	20
Density (kg/m ³)	1650	2100	2300-2400	*	*	*	*	2265	1875	2200	1800	*
Water used (ℓ)	3.7	3.25	3.06	3.5	2.9	3.75	4.2	2.7	5	2.6	5.6	3.5
Volume Yield per bag (litres)	15	12	11	14	14	14	13	12	16	10	12.8	12.5
Material properties												
7-Day Compressive Strength (MPa)	*	*	55	27	40	30	35	*	*	40	*	38
28-Day Compressive Strength (MPa)	35 - 40	40	75	-	-	-	> 45	58	35	60	20	52
Thesis Measured 28-Day Compressive Strength (MPa) according to SANS 5863:2006a	35	43	88	37	50	54	53	56	35	65	20	55

‘*’ indicates that the specific material property was not provided

The summarised product description for each mix as described in their product data sheets is presented in Table 3-2. These materials vary significantly from one manufacturer to the other based on the available technical and health and safety data sheet.

Table 3-2: Mix Property description as per the product data sheets.

Mix ID	Product description	Uses
PS	Cementitious, polymer-modified, one component repair and re-profiling mortar containing silica fume.	Designed for thick layer concrete repairs, especially for overhead and vertical applications.
PFS	Cementitious, polymer-modified, low permeability, high-strength mortar containing silica fume and synthetic fibre reinforcement.	Designed as a high strength repair and reprofiling system for concrete substrates. It is particularly suitable for application on overhead and vertical surfaces using the wet spray method and can also be placed by hand.
SA	One component, free-flowing, high strength, cement-based concrete with a maximum aggregate size of 9 mm. Contains cement, crystalline free Silica, aggregate and additives.	Used for the structural repair of deteriorated concrete. It is ideal for casting sections or members where the volumes required are too large for conventional grouts, and too small and inaccessible for normal concreting procedures.
S1	Structural concrete vertical overhead repair and migrating corrosion inhibitor. Contains cementitious material and crystalline-free silica.	Used for rapid repair of load-bearing structures.
S2	Structural concrete plus mitigating corrosion inhibitors. Contains cementitious material and crystalline free silica.	General repair of concrete structures.
G1	Grout with mitigating corrosion inhibitors.	Grouting of machinery base plates to maintain precision alignment. Non-shrink grouting of structural steel and pre-cast concrete.
PF1	Polymer-modified, fibre-reinforced, cement-based mortar, which is chloride-free, ready-to-use, non-shrink and of a single component.	Used to repair voids and honey-combed areas, potable water-retaining structures and bedding mortar for concrete planks i.e. seats at sports stadiums, suspended flooring.

Table 3-2: Mix property description as per the product data sheets – cont'd.

Mix ID	Product description	Uses
G2	Shrinkage compensated Fluid Micro-Concrete. Cement based non-shrink concrete reinstatement grout, which can be applied by pouring or pumping.	Reinstatement of large sections of structural concrete with greater than 50 mm thickness. Can be applied in excess of 250 mm depending on the nature of the repair and the reinforcing.
P1	Single-component, polymer-modified, cementitious repair mortar containing a migrating corrosion inhibitor (MCI).	Suitable for use in hot climatic conditions for repairs to concrete and masonry. Used for patching in vertical and overhead applications without formwork as well as for large area rendering.
PF2	High-strength, rapid setting, shrinkage-compensated, fibre-reinforced, structural repair mortar with active corrosion inhibition. Contains Portland cement, graded sands, selected polymer fibres and special additives to significantly reduce the risk and incidence of shrinkage cracking.	Used for the structural repair of concrete elements such as, columns, piers and cross beams of all bridges, cooling towers and chimneys and other industrial environments.
P2	Single component acrylic polymer-modified repair mortar for use as a "fairing coat" or cosmetic mortar.	Used as a fairing or skim coat to cover and make good blemishes in concrete surfaces such as slight honeycombing, blowholes, defects caused by 'sand runs', patch repairs, shutter movement and grout loss.
A	Shrinkage controlled micro-concrete for all types of structural repairs. Contains a 6- 9 mm coarse aggregate.	Used where repairs require high fluidity e.g. heavily congested steel or repairs, to repair soffits where heavy loadbearing is required and in restricted access areas, where use of hand applied mortars would prove impractical.

Table 3-3 compares the test methods performed by the different manufacturers for the products they supplied. ‘*’ indicates where the same manufacturer uses a different test method which makes comparing those properties challenging for the specifier. The table includes EN 1504-3:2005

recommended test methods and the test method/standard used during this study for reference and comparison. Most repair mortars that were tested did not have data from the manufactures on their recommended test method.

Table 3-3: Property test methods for the proprietary repair mortars

Mix ID	Compressive strength	Bond strength	Elastic modulus	Drying shrinkage	Restrained shrinkage tests (Ring test)
PS	EN 12190	EN 1542	EN 13412	No Data	EN 12617-4
PFS	No Data	No Data	No Data	No Data	No Data
SA	No Data	No Data	No Data	No Data	No Data
S1	ASTM C-109	ASTM C-882	No Data	No Data	No Data
S2	ASTM C-109	ASTM C-882	No Data	No Data	No Data
G1	ASTM C-942*	ASTM C-882	No Data	No Data	No Data
PF1	ASTM C-109	ASTM C-882	No Data	No Data	No Data
G2	ASTM C-109	No Data	No Data	No Data	No Data
P1	ASTM C-109	No Data	No Data	No Data	No Data
PF2	EN1260	EN 1542	EN 13412	No Data	No Data
P2	No Data	No Data	No Data	No Data	No Data
A	No Data	No Data	No Data	No Data	No Data
EN 1504-3	EN 12190	EN 1542	EN 13412	No Data	EN 12617-4
Test Method					
Used	SANS 5863	D7234-12	BS 1881	SANS 6085	ASTM C1581

3.5 Specimen preparation

3.5.1 Mix design

Each of the twelve proprietary repair mortars was mixed according to the manufacturer specifications (i.e., with respect to water contents and mixing duration). Although such variation is not usually adopted in studies on material properties, it was necessary in this case to ensure that the products were prepared in accordance with the corresponding manufacturer’s guidelines (Torney et al., 2014).

Most of the manufacturers (in their product data sheets) recommend both the minimum and the maximum amount of water that should be added during casting. The actual amount of water that was used is presented in Table 3-4. It is important to note that this amount was the average of the manufacturers recommended water content range. The mid-point values were chosen due to the workability of the mixes.

Table 3-4: Amount of water used, w/b ratio and the mixing time.

Material	PS	PFS	SA	S1	S2	G1	PF1	G2	P1	PF2	P2	A
Packaging per bag (kg)	25	25	20	25	25	25	25	25	25	20	20	20
Recommended Amount of Water (ℓ)	3.4 - 4.0	3.0 - 3.5	3.0 - 3.12	3.0 - 4.0	2.6 - 3.2	3.5 - 4.0	4.2	2.7	5	2.4 - 2.8	5.6	3.5
Water (ℓ) Used	3.7	3.25	3.06	3.5	2.9	3.75	4.2	2.7	5	2.6	5.6	3.5
Water /product ratio	0.15	0.13	0.15	0.14	0.12	0.15	0.17	0.11	0.20	0.13	0.28	0.18
Mixing time	3 mins	3 mins	3 mins	3- 5 mins	5 mins	*	3- 4 mins	3- 4 mins	5 mins	3 mins	*	*

‘*’ indicates that the specific material mixing time was not provided

3.5.2 Casting and curing

The mixes were prepared using either the 50 or 25-litre pan mixer, as per the mix proportions presented in Table 3-4. Freshly-cast mortar mixes were placed in moulds and compacted using a vibrating table until no air bubbles could be seen on their surface. No compaction was performed on the flowable mortars. The freshly cast-mortar in the moulds was thereafter covered with a black polythene sheet and left for 24 ± 2 hours in the laboratory at $23 \pm 2^\circ \text{C}$ before demoulding. All the specimens, except for the ring test specimens, were cured in the water bath for a period of 7 and 28 days after casting prior to testing. The procedure for curing the ring tests samples is described in Section 3.7.6.

3.6 Material characterisation

Common variations in proprietary repair mortars include binder, aggregate components and additives. It is expected that these differences would be reflected in the different physical and material properties. The characterization of the repair mortars was through the product description

as stated by the manufacturers, grading analysis and the test results from Energy Dispersive Spectrometry (EDS).

The supplied product datasheets and additional information obtained from the internet was used to classify the repair products as follows: polymer-modified, fibre-reinforced, aggregate inclusion and the presence of silica fume in the mortars. The mix property description and the uses for each repair mortar under investigation has been presented in Table 3-2.

3.6.1 Grading

Grading of the material by sieve analysis was carried out in accordance with SANS 201:2008. Since the repair mortars are supplied as formulated mortar, sieve analysis incorporated aggregate, binder and fillers. For Mix 3, the aggregate was analysed in isolation.



Figure 3-1: Sieve Analysis

3.6.2 Energy Dispersive Spectrometry (EDS)

Microscopic analysis of the structure of a material is valuable for many applications, such as the its development and improvement, quality control, reverse engineering, and evaluation of performance (Garcia-Salinas & Donald, 2010). In scanning electron microscopy (SEM), the image is formed by electronic processing of the wave nature. Microanalysis of characteristic X-rays in the SEM is a powerful method to assess the chemical composition of phases in cement pastes, in particular the calcium silicate hydrate containing alumina (C-A-S-H). SEM is considered among the most used, fast and accurate method of microscopic analysis of construction materials. It has been extensively used in material characterization, especially in combination with Energy Dispersive Spectrometry (EDS) (Stefanidou & Pavlidou, 2018). EDS is routinely used because it

conveniently records the full chosen range of characteristic X-rays which are usually processed and quantified.

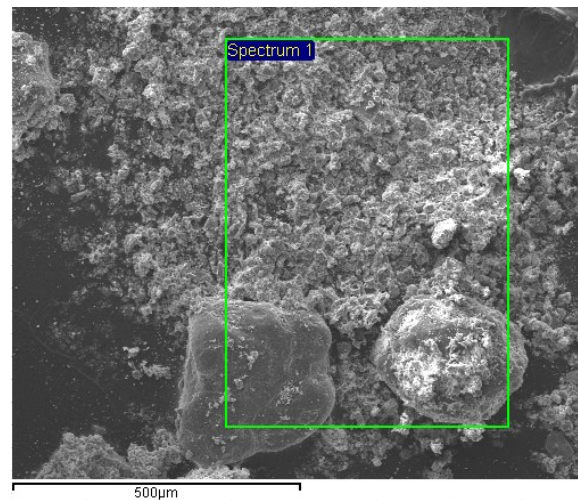


Figure 3-2: X-ray analysis of the repair mortar.

3.7 Tests

The tests that were conducted in this study comprise: compressive and direct tensile strength tests, elastic modulus, bond strength tests, drying shrinkage, restrained shrinkage tests, tensile relaxation tests and the durability indexes tests. A detailed description of these tests is provided in the subsequent subsections. For each test, the number and size of specimens, test setup and testing procedure is provided. Additional information on the tests and testing procedure can be found in the Appendix A.

3.7.1 Compressive strength

The compressive strength test was carried out on the mortars to monitor their strength development and to provide input data for elastic modulus test in compression. This test was also used to assess whether the repair mortars meet the performance requirements for strength as specified in the EN 1504-3:2005. Standard $100 \times 100 \times 100$ mm cubes were cast and tested according to SANS 5863:2006a at 3, 7, and 28 days from the date of casting.

An Amsler hydraulic compression testing machine with a load capacity of 3000 kN, shown in Figure 3-3, was used for testing. The test entailed the application of a compressive axial load continuously, and without shock, to cube specimens at a uniform rate of 0.3 ± 0.1 MPa/s until

failure. The compressive load was applied through square steel platens. The compressive strength was calculated by dividing the maximum load attained during the test by the cross-sectional area of the specimens. Three specimens were tested for each mix and their average reported.



Figure 3-3: Amsler compression testing machine.

3.7.2 Tensile strength

The tensile strength of a cementitious material can be tested in different ways. These include: direct tensile strength, flexural strength, the splitting tensile strength and the ring/hoop tension test. Direct tensile strength tests were conducted. It is however reported that there exists difficulties in the fixation of the specimens to the testing equipment (Carlswärd, 2006). These tests were conducted at 7 and 28 days after the day of casting. Notched dog-bone shaped prismatic specimens with extended dovetail ends - as shown in Figure 3-4 were used. The specimens had cross-sectional dimensions of 40×40 mm. The notches of 1 mm thick by 5 mm wide on two sides were created by protrusions on the side of the mould used to cast the specimens. The notching of the specimens

resulted in the concentration of stresses within the notched cross-section which helped in localizing failure at the notch (Masuku, 2009).

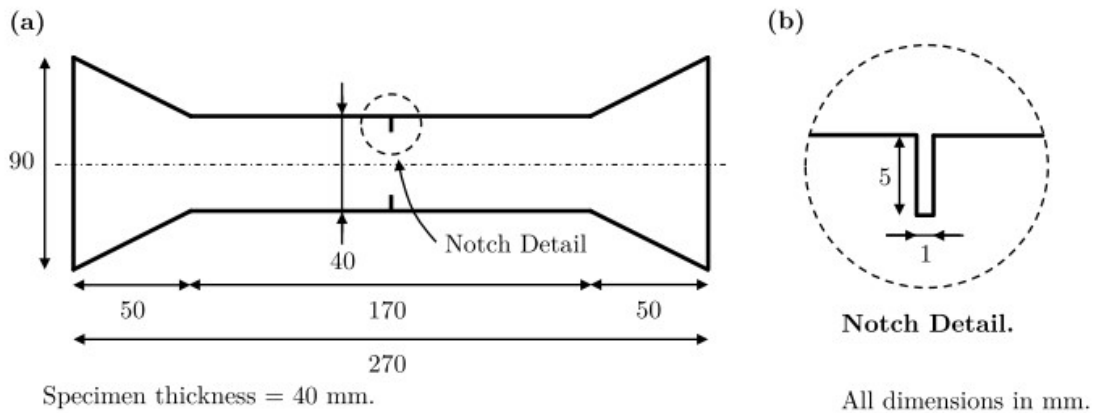


Figure 3-4: (a) Notched dog-bone specimen dimensions and (b) notch detail – adopted from (Beushausen & Bester, 2016).

Three specimens were tested for direct tensile strength in a Zwick Roell Z020 Universal Testing Machine (UTM) (shown in Figure 3-5) which has a maximum load capacity of 20 kN. The load was applied at a constant rate of 0.2 mm/minute until failure (Arito et al., 2016b; Masuku, 2009). This loading rate is also recommended in SANS 863-5:1994 which specifies a time envelope of between three to ten minutes for concrete material tests. The tensile strength of the repair mortars was calculated as the load at failure divided by the effective cross-sectional area of the specimen. The average of tensile strength of three specimens was recorded.

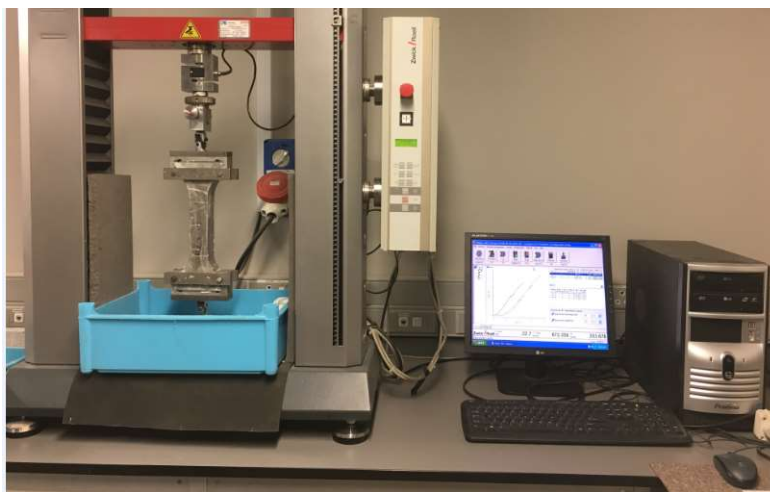


Figure 3-5: Zwick Roell Z020 Universal Testing Machine (UTM).

3.7.3 Tensile relaxation

Tensile relaxation tests were conducted using un-notched dog-bone shaped prismatic specimens. These specimens were not loaded to failure. Before testing, each specimen was sealed with paraffin wax on all surfaces to ensure that they do not undergo additional stress build up due to drying shrinkage during testing. Two specimens were tested in a Zwick Roell Z020 Universal Testing Machine (UTM) with each specimen being loaded up to 80% of its ultimate direct tensile strength at the beginning of the test. The number and availability of the test equipment in the laboratory limited the test specimens to two. Beushausen et al. (2012) report that the 80% of the ultimate direct tensile is more realistic in simulating the behaviour of bonded overlays under service conditions or members that are close to cracking. The resulting tensile strain remained constant and the stress decay in the specimen was recorded by a computer software. Due to the limitations in the number and availability of the test equipment in the laboratory, the test was automatically stopped after 48 hours and the residual stress value (σ_t /MPa) was recorded. Furthermore, Atrushi (2003) reports that under isothermal temperature of 20 °C, the relaxation increases to about 40% of the fictive elastic stresses after 3 days and remains about constant after that.

Tensile relaxation was determined at 7 and 28 days after the date of casting of the specimens. The tests were conducted in an environmental controlled room at a temperature of 21 ± 1 °C and relative humidity of $50 \pm 4\%$.

3.7.4 Elastic modulus

Elastic modulus in compression was tested using cylindrical specimens of diameter and height 100 mm and 200 mm respectively. Three cylinders were tested at the age of 7 and 28 days after casting, in accordance with BS 1881: Part 121:1983. The Instron Machine with a load capacity of 3000 kN was used. It is equipped with LVDTs and data acquisition system as shown in Figure 3-6. The top and bottom of each cylinder was ground to help ensure that the circumferential axis is perpendicular to the longitudinal axis and to provide a smooth contact surface with the loading plates. The specimens were loaded at a rate of 0.6 ± 0.4 MPa/s until the stress equal to one-third of the compressive strength of the repair mortar mix was reached. The average of three tests was reported.



Figure 3-6: Instron; elastic modulus under compression testing machine.

3.7.5 Drying shrinkage

This test involves the determination of length changes produced by causes other than externally applied forces and temperature changes in prismatic mortar specimens exposed to controlled temperature and moisture conditions. Prism specimens 100 x 100 x 200 mm in dimension were used with the test being conducted in accordance with SANS 6085:2006. Three specimens from each repair mortar mix were tested and their mean reported. Two strain targets were attached onto the specimen at a gauge length of 100 mm on two opposite faces of each specimen after curing in a water bath for 28 days. The shrinkage strain was measured using a strain extensometer (shown in Figure 3-7) on the four targets on each specimen thus providing two longitudinal strain readings per specimen. The drying shrinkage was monitored daily for a period of 60 days. This duration of testing was chosen as it corresponded with the period of no change in length between the set targets on most of the specimens.

Drying shrinkage was calculated by dividing the change in length between a set of targets measured using a strain extensometer over the duration of measurement by the gauge length of the targets (100 mm).

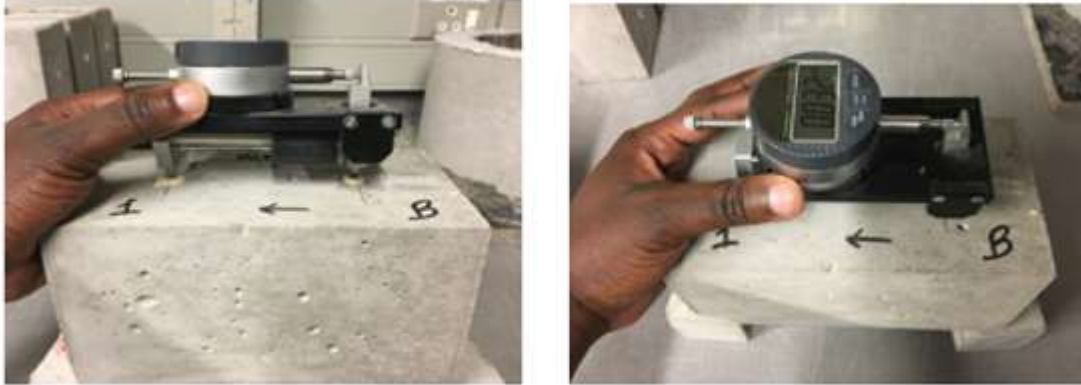


Figure 3-7: Strain extensometer on two strain targets measuring the shrinkage.

3.7.6 Restrained shrinkage cracking

Many tests that have been developed to assess restrained shrinkage cracking. They include: ring tests with a restraining core, longitudinal tests where the restraint is applied at the edge of the specimen, panel tests which have the restraint along the circumference and tests in which the substrate offers the restraint (Bentur & Kovler, 2003). The ring test is the most commonly used for estimating the cracking potential of repair mortars under restrained shrinkage because it is simple and economical (Bentur & Kovler, 2003; Carlswärd, 2006). It has various limitations such as failure to account for the restraint type, overlay geometry and the need for a minimum curing period of 24 hours in the mould (Beushausen & Bester, 2016). Bentur & Kovler (2003) while quoting other studies report that the test has limitations with respect to size effects and non-uniform drying.

This test involves the casting of a mortar annulus around a cylindrical steel ring. The steel ring provides the restraint to the shrinkage that the mortar will undergo, leading to stress development within the specimen. When these stresses exceed the tensile strength of the mortar the specimen cracks. Arito (2018), while citing other studies, reports that the ring test has been used to evaluate autogenous shrinkage, effect of alkalis on the cracking of cementitious materials, plastic shrinkage cracking of fresh concrete and the shrinkage cracking of hardened concrete.

The ring test was performed in accordance with ASTM C 1581 although it had some modifications due to the lack of the strain gauges and their accompanying data acquisition systems. Figure 3-8 shows the ring test apparatus and test specimen dimensions that were used. Once assembled, the ring moulds were sealed with a silicone gel to prevent the leakage of fresh concrete through the contact surfaces of the outer steel ring and base. The silicon was allowed to set for approximately 24 hours before casting. Figure 3-9 shows the assembled ring mould before casting.

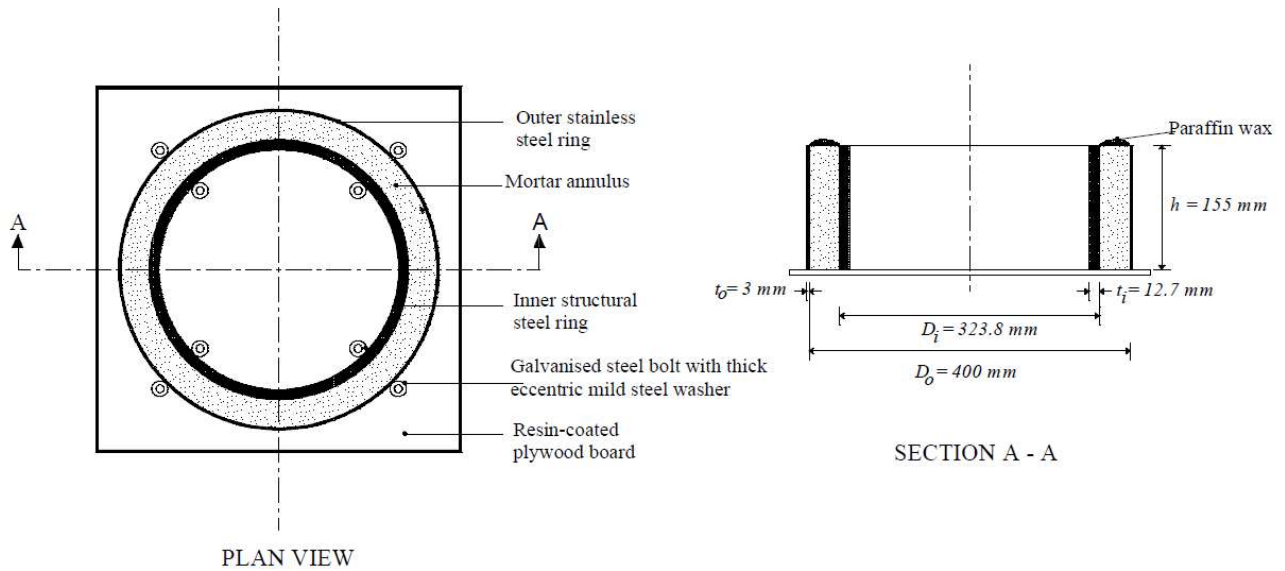


Figure 3-8: Ring Test Apparatus and test specimen dimensions - Adopted from ASTM, C1581/C1581M).



Figure 3-9: Ring mould preparation.

Three specimens were cast for each repair mortar mix. For stiff mortars mechanical vibration was performed for about 30 seconds while for flowable mortars no compaction was performed. The specimens were demoulded after 1 day, and then transferred to an environmental room that was maintained at a temperature and relative humidity of 23 ± 2 °C and $50 \pm 4\%$ respectively. The top surface of the test specimen was coated with molten paraffin wax. This ensured that the test specimen dries from the outer circumferential surface only. Precaution was taken to ensure that the outer circumference of the test specimen was not coated with the paraffin wax. In the environmental room, a plastic sheeting was then wrapped around it for 2 more days for curing. The age at which the first crack appeared was recorded as the ‘age at cracking’. After 14 days from the date at which the first crack appeared, the average width of the cracks on each specimen was measured using a crack meter as shown on Figure 3-10. The average age at cracking and crack width of three specimens was recorded.



Figure 3-10: Ring specimen showing crack width measurement and hand microscope.

3.7.7 Bond strength

Pull-off tests were carried out to determine the interfacial tensile bond strength between the overlay and the concrete substrate. The tests were performed in accordance with ASTM C1583. The 150 x 150 x 150 mm cubes were cured in a water bath for 7 and 28 days before testing. Three samples per mix were cored from 150 x 150 x 150 mm mortar cubes and used to perform this test. Coring was done perpendicular to the interfacial bond between the overlay and substrate and resulted in cores consisting of both overlay and substrate material. The cored specimens were 49 ± 1 mm in

diameter and 149 ± 1 mm in height. They were then cut to approximately 30 mm of substrate and 10 mm of overlay material for testing as shown in Figure 3-11.

Bai et al. (2009), reports that while the pull off test was initially developed to evaluate the in-situ strength of concrete structures, it has been accepted in the field of concrete repairs as a standard test for assessing the bond strength between overlays and substrate concrete in several countries, with South Africa included (British Standards Institution, 1999; Centre for Civil Engineering Research Codes and Specifications, 1990).



Figure 3-11: (a) Overlay casting (b) Cored specimen dimensions after shortening.

A Proceq[®] pull off machine (shown in Figure 3-12) was used to perform this test. The cored specimens were glued onto a steel plate while aluminium disks were glued to the top of the overlay end of the cored specimen which provided suitable anchorage points for the Proceq[®] machine. The adhesive used was X60 – a cold curing glue for experimental tests. X60 consisting of methylmetacrylate, is mostly used to attach/fix strain gauges on concrete specimens during testing for shrinkage.

The dolleys were connected to the pull-off tester by means of a metal pin. The turning knob was then screwed tight, to secure the connection between the pull-off machine and the cored specimen. To avoid the application of an initial tensile load, the turning knob is finger tightened. The whole apparatus was then levelled to ensure that the tensile force coincided with the longitudinal axis of the specimen. The failure load and zone of each sample was recorded. The tensile bond strength for

each mix was then determined from the average failure load of three specimens divided by the cross-sectional area of the specimens.



Figure 3-12:(a) Pull off test set up (b) Aluminium disks glued to the shortened cored samples.

3.7.8 Durability indexes.

Durability is the ability of a structure to withstand the design environment over the design life without undue loss of serviceability or need for major repair. It is associated with the deterioration of the material over the intended service life of a structure in a given environment (Alexander & Beushausen, 2009). The durability index tests were used to predict whether a repair mortar will prevent the ingress of aggressive chemicals which could lead to corrosion of reinforcing steel and degradation.

Durability index tests were used to characterise the repair mortars. These tests comprise: Oxygen Permeability Index (OPI), Water Sorptivity Index (WSI) and the Chloride Conductivity Index (CCI). The tests were done at 28 days after curing in accordance to the Durability Index Testing Procedure Manual 2017 (Ver. 4.2, July 2017). 7-day tests were also performed to determine the early age properties of the repair mortars.

3.8 Closure

This chapter has presented a detailed description of the experimental methodology in this study, the testing philosophy and other relevant information pertaining to the experimental work. The time-dependent material properties that influence the susceptibility of repairs to undergo cracking

were tested on proprietary repair mortars. The test equipment used, and the materials tested have been presented. Twelve products from four different manufacturers were tested.

The test standards that were used to prepare and the various specimen types and sizes have been presented. No information was found in literature on a code of practice for the testing of direct tensile strength and tensile relaxation in mortar specimens. Material characterization of the tested products was performed. This was through the product description as outlined in the product data sheets, through grading analysis to determine the amount of fines and through the energy dispersive spectrometry (EDS). All mixes were cast according to the manufacture's specifications. The tests conducted included compressive and direct tensile strength tests, elastic modulus, bond strength tests, drying shrinkage, restrained shrinkage tests, tensile relaxation tests and the durability index tests. The results of the tests presented in this chapter are discussed in Chapter 4.

4. Results and discussion

4.1 Introduction

This chapter presents an in-depth analysis and discussions of the results from the tests that have been presented in Chapter 3. The results are presented in graphs, figures and tables. Detailed test results are provided in Appendix B.

4.2 Material characterization

The properties of the constituent materials for the proprietary repair mortars were determined. The properties included sieve analysis, EDS and the product description. The coding system adopted to identify the proprietary repair mortars was as follows:

- a) PS - repair mortar that is polymer modified and containing silica fume.
- b) PFS - polymer modified fibre reinforced mortar containing silica fume.
- c) SA – repair mortar containing silica fume and a maximum aggregate size of 9 mm.
- d) S1 and S2 mixes having silica fume.
- e) G1 - formulated grout mortar with corrosion inhibitor.
- f) PF1 - polymer modified fibre reinforced repair mortar.
- g) G2 - concrete reinstatement grout.
- h) P1 – polymer modified repair mortar.
- i) PF2 – polymer modified fibre reinforced repair mortar
- j) P2 – polymer modified repair mortar.
- k) A – repair mortar containing 6 - 9 mm coarse aggregates.

4.2.1 Product description

Product classification based on constituents as specified in the product datasheet is as shown in Table 4-1. The mixes were categorised as polymer-modified (P), fibre-reinforced (F), silica fume (S) and containing aggregates (A) as specified by the manufacturers. Some mixes had a combination of these materials. Due to the proprietary nature of these repair mortars, the author believes that some information – such as admixtures - was not stated in the product data sheets from the manufacturers. Two proprietary repair mortars' product data sheets did not describe their constituents and only referred to them as repair grouts (referenced here as G1 & G2).

Table 4-1: Classification of the repair mortars based on the product datasheets.

Mix ID	Polymer-modified	Fibre-reinforced	Aggregates	Silica fume
PS				
PFS				
SA				
S1				
S2				
G1				
PF1				
G2				
P1				
PF2				
P2				
A				

4.2.2 Sieve analysis

The sieve analysis was done to establish the particle size distribution and the amount of filler in the mixes. The grading curves presented in Appendix B.9 were used. These curves indicate that the proprietary repair mortars show a narrow range of particle size. Table 4-2 shows the cumulative percentage retained and passing the 0.075 μm sieve. Mix A has the highest amount of fines with 28.28% passing the 0.075 mm sieve. Mixes G1 and P2 have 6.30% and 3.01% respectively passing the 0.075 mm sieve. The rest of the repair mortar products except PF2 and S2, have an amount less than 1% passing through the 0.075 mm sieve.

Table 4-2: Cumulative % retained and passing the 0.075 mm sieve.

Mix ID	Cumulative % retained	Cumulative % passing	Sdv. Dev
PS	99.77	0.23	0.2
PFS	99.78	0.22	0.1
SA	99.78	0.22	0.2
S1	99.13	0.87	0.1
S2	98.53	1.47	0.2
G1	93.70	6.30	0.3
PF1	99.61	0.39	0.2
G2	99.59	0.41	0.2
P1	99.85	0.15	0.1
PF2	98.84	1.16	0.3
P2	96.99	3.01	0.3
A	71.62	28.38	0.6

The fineness of cementitious materials has an important bearing on the rate of hydration and hence on the rate of gain of strength and also on the rate of evolution of heat. Finer materials offer a greater surface area for hydration and hence faster the development of strength (Mehta & Monteiro, 2006 and Neville, 2011). Larger proportions of fine particles increases the water demand. An increase in water demand increases the susceptibility to cracking. Crosswell (2009) reports that the higher the water content, the higher the susceptibility of materials to drying shrinkage and the greater the tendency to crack.

4.2.3 Energy Dispersive Spectrometry (EDS)

Proprietary repair mortars vary in their formulation. The common variations observed included binder, aggregate components and additives. These differences would be expected to be reflected on the different physical properties. There were differences in the physical properties of the repair mortars. Table 4-3 shows the different elemental composition for the analysed repair mortars.

Table 4-3: Analysed spectrum showing the elemental composition of proprietary repair mortars under investigation.

Mix ID	All results in weight%									
	O ₂	Mg	Al	Si	S	K	Ca	Ti	Fe	Total
PS	41.05	0.47	2.21	6.01	0.74	0.19	17.87	0.18	0.81	100
PFS	39.04	0.47	1.01	6.62	0.87	0.23	19.92	0	0.8	100
SA	44.24	0.41	0.85	9.83	0.88	0.13	17.0	0	0.82	100
S1	35.67	0.21	5.88	1.39	1.68	0	13.47	0.32	3.78	100
S2	45.45	0	5.02	7.86	1.19	0	8.65	0.3	3.19	100
G1	28.65	0.25	0.78	3.57	0.41	0.1	9.26	0	0.91	100
PF1	30.9	0.14	0.65	4.12	0.34	0	5.19	0.43	0.35	100
G2	29.85	0.19	0.94	4.34	0.58	0	8.75	0	0.42	100
P1	26.09	0.21	0.41	2.08	0.43	0	7.32	0	0.4	100
PF2	30.82	0.15	0.48	5.84	0.76	0.12	4.49	0	0.38	100
P2	38.38	0.23	0.53	10.52	0.53	0	10.78	0	0.6	100
A	37.13	0.55	0.9	4.96	1.07	0.14	17.53	0	0.95	100

Meaning of symbols: O₂ – Oxygen, Mg – Magnesium, Al – Aluminium, Si – Silicon, S – Sulphur, K – Potassium, Ca – Calcium, Ti – Titanium, Fe – Iron.

Figure 4-1 shows the photomicrographs of the proprietary repair mortar products. The important phases of ettringite (acicular crystals), portlandite (plate-like) and calcite (grainy) can be seen.

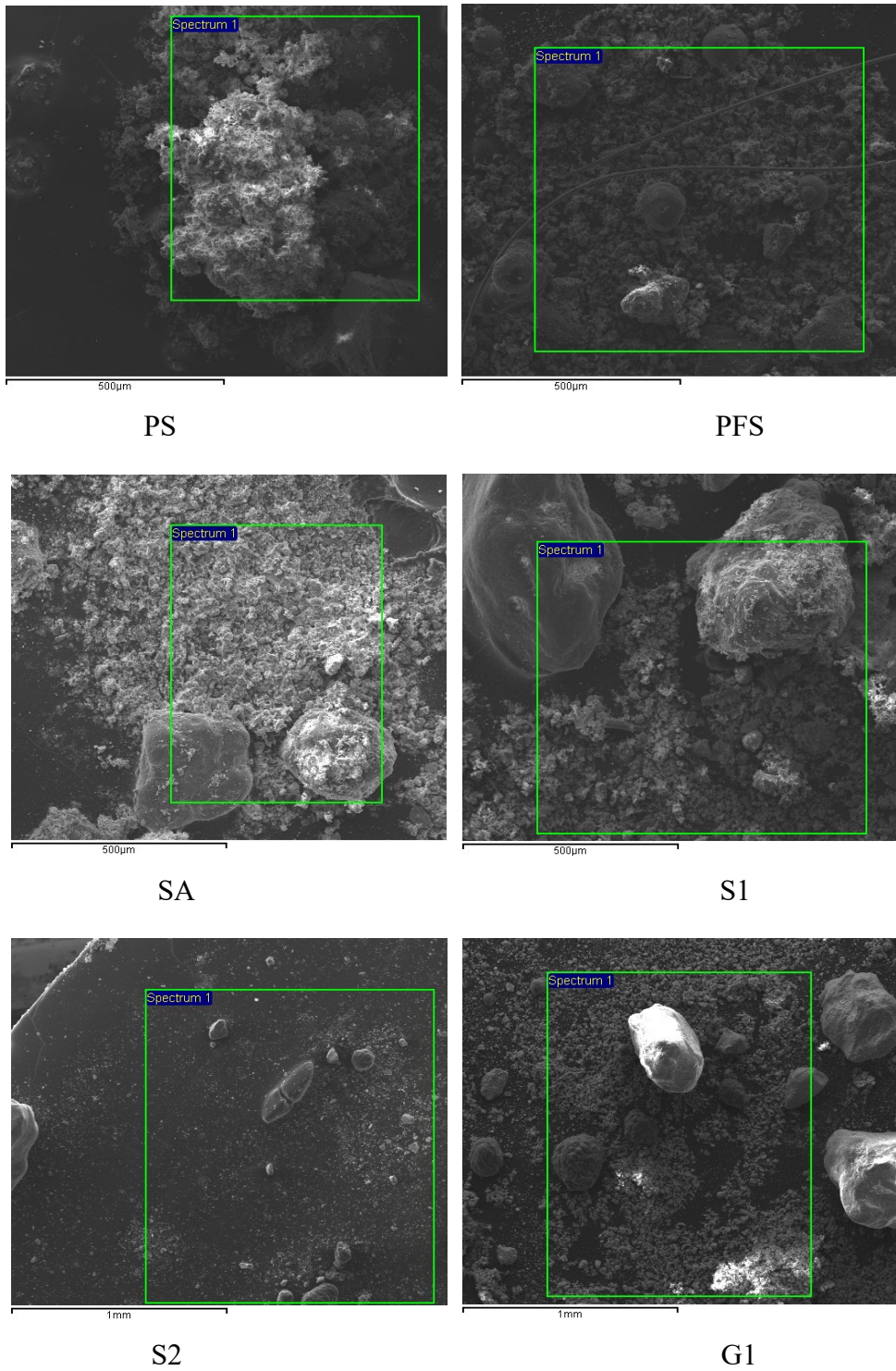
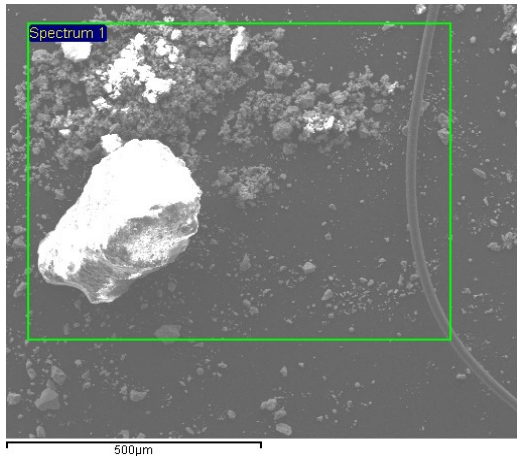
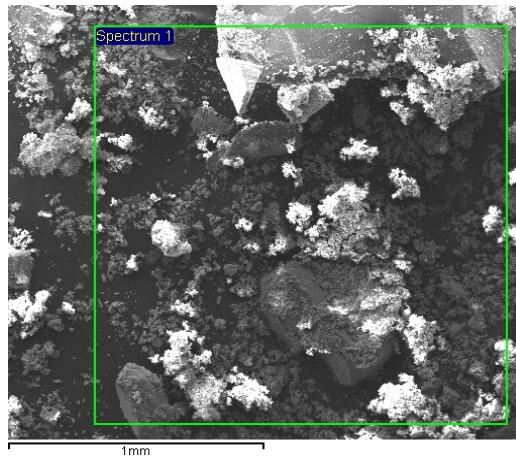


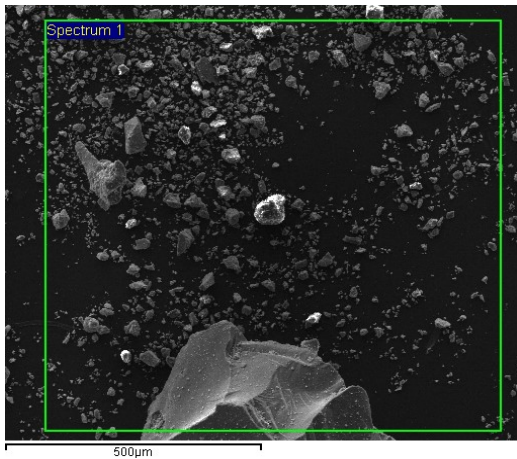
Figure 4-1: Photomicrographs for the proprietary repair mortars.



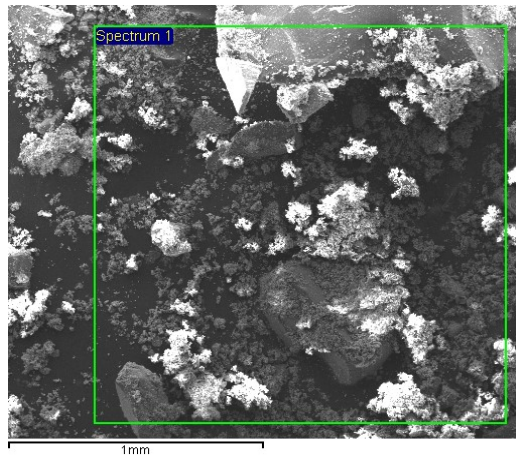
PF1



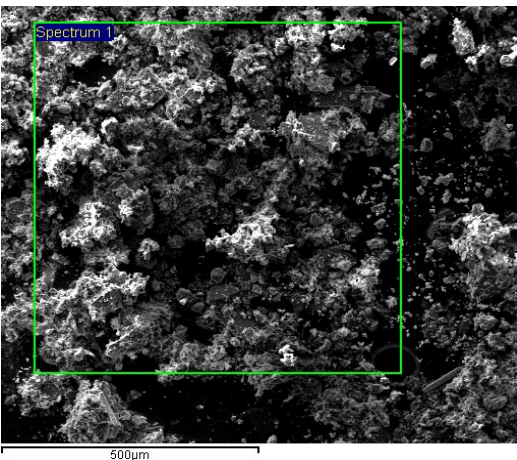
G2



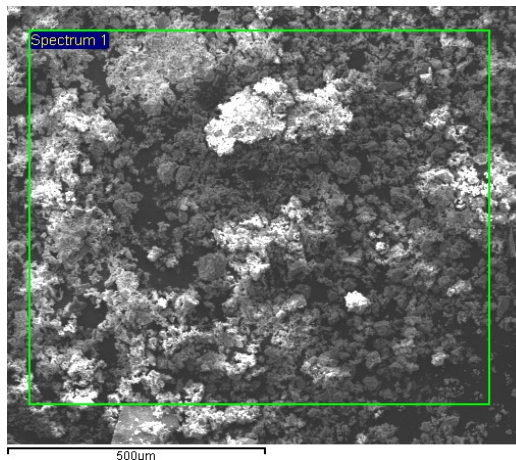
P1



PF2



P2



A

Figure 4-1: Photomicrographs for the proprietary repair mortars – cont'd.

Table 4-3 shows the element composition confirming the presence of these phases. As expected, it shows high concentrations of calcium and oxygen, but also significant amounts of silicon and sulphur. This is probably due to the electron beam volume interaction with other phases, possibly located underneath the portlandite layers; these phases would be CSH and ettringite (Brasileiro, 2014). The fibres incorporated in the repair mortars in mix PFS and PF1 can be seen from the photomicrographs in Figure 4-1 as indicated in Table 4-1.

4.3 Compressive strength

The compressive strength tests were carried out on 100 mm cubes as described in Section 3.7.1. Some researchers, Arito (2018) and Beushausen & Bester (2016a) report that compressive strength has little relevance to cracking of overlays. These tests were however performed to fulfil the requirements of the EN 1504-3:2005 which explicitly state that the compressive strength of repair mortars must always be specified for all intended uses (AIU). The test was also performed to obtain the magnitude and monitor the strength development for material characterization purposes and for the determination of elastic modulus in compression. The 3, 7 and 28-day compressive strength results for the 12 repair mortars is shown in Figure 4-2. Detailed compressive strength results are presented in Appendix B.1.

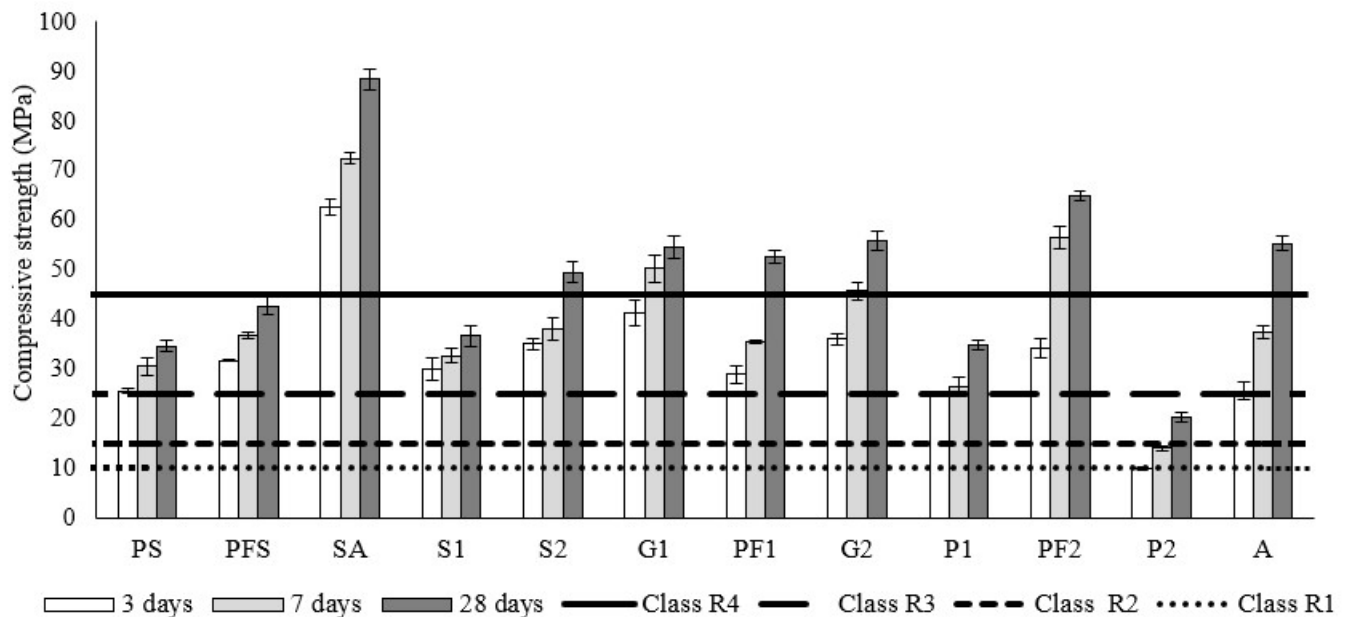


Figure 4-2: Compressive strength results.

From the requirements of EN 1504-3:2005 it can be deduced that all the proprietary repair mortars under investigation, except for mix P2 were structural, with the compressive strengths ≥ 25 MPa (Class R4 and Class R3). P2 is a non-structural mortar, Class R2 with a compressive strength ≥ 15 MPa. This product is marketed as cosmetic repair mortar to be used as a fairing or skim coat to cover and remediate blemishes in concrete surfaces. The other repair mortars are specified as high strength mortars to be used for structural repairs. This implies that most of the repair work being performed in the South African industry make use of structural repair mortars while they might not be serving any structural role. It is noted from Table 3-4, that manufacturers specify low amounts of water leading to very low w/b ratios. Reducing the w/b ratio increases the compressive strength. This is consistent with literature (Alexander & Beushausen, 2009; Yurdakul et al., 2013). Lower w/b ratios increase the susceptibility to cracking (Sayahi & Emborg, 2017). Sayahi & Emborg (2017) further report that the optimum range of w/b ratio to decrease the risk of early-age cracking in concrete ought to range between 0.45 and 0.55.

Comparing the compressive strength results in Figure 4-2, mix SA has the highest 28-day compressive strength of 88.4 MPa. This high strength can be attributed to the presence of both silica fume (SF) and aggregates. SF contributes to the high strength in two ways. First, because of its small particle size, SF can act as a filler for the spaces between binder grains. This results in a reduction in the size of the individual pores and voids in the paste, although the total porosity is not affected. Since pores are discontinuities in the cement paste matrix, reduced pore sizes require a higher stress to initiate a crack; thus, the strength is increased. Secondly, the pozzolanic nature of SF which is slower than normal cement hydration but continues over time. As more calcium hydroxide is converted to CSH, the strength of the material will continue to increase (Cong et al., 1990; Singh & Bansal, 2015). The aggregates generate a strong bond with the paste creating a higher strength. Figure 4-3 shows that the 7-day compressive strength for mix SA (72.4 MPa) is higher than the 28-day compressive strength for all the mixes. This can be attributed to the time development of the strength of the cement paste and the ITZ. At 7 days, the development of the paste and aggregate-paste interface strength is limited and therefore the influence of aggregate volume is more apparent. However, mix A containing aggregates did not have such high strengths.

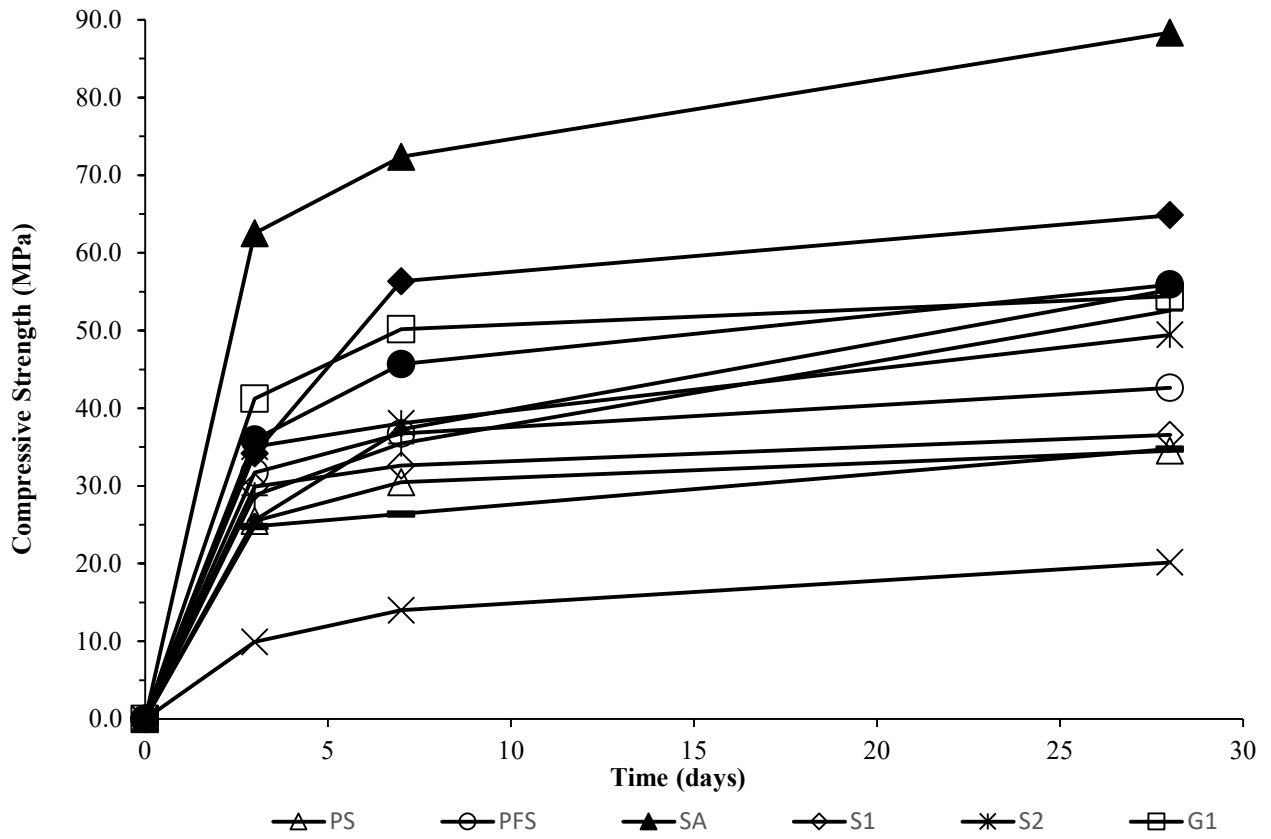


Figure 4-3: Compressive strength development of the repair mortars

Mix PF2 has a 28-day compressive strength of 64.9 MPa. This high strength can be attributed to the polymers and fibres incorporated in the mix. This agrees with studies by Kalwane & Dahake (2015) who state that the incorporation of fibres and polymers increases the compressive strength of concrete. The inclusion of polymers in concrete usually increases the mechanical properties of the ITZ, resulting in concrete with better mechanical properties as a whole (Bezerra et al., 2011). However, this is the opposite to the observations made by Arito (2018). Arito (2018) noted that polymer-modification reduced compressive strength at all ages with the magnitude of this reduction, in EVA polymer-modified mixes, increasing with an increase in polymer content from 10% to 20%. Mix P2 had the lowest compressive strength of 20.2 MPa. It is a non-structural mortar and thus does not require the high strength as the rest of the mortars. All the proprietary repair mortars tested had the same or higher compressive strength than the one stated by the

manufacturer, see Table 3.1. SF incorporated in mixes PS, PFS, SA, S1 and S2 repair mortars can be attributed to their high compressive strength of > 30 MPa.

All test specimens for the proprietary repair mortars exhibited an hour glass shear failure pattern when subjected to compressive forces. A typical failure pattern is shown in Figure 4-4.



Figure 4-4: Acceptable hour glass shear failure shape of the repair mortar cubes.

From Figure 4-3, it can be observed that there is an increase in compressive strength for all the mixes with the increase in the age after casting from 3-day to 28-day. This observation is consistent with literature that the time-strength relations for cementitious materials in moist curing conditions and normal temperatures, at a given water-cement ratio, the longer the moist curing period the higher the strength, assuming that the hydration of anhydrous cement particles is still going on.

4.4 Tensile strength

The direct tensile strength tests were carried out at 7 and 28 days on dog-bone specimens as described in Section 3.7.2. The results are provided in Appendix B.2 and Figure 4-5. The EN 1504-3:2005 standard does not provide any performance requirements for tensile strength.

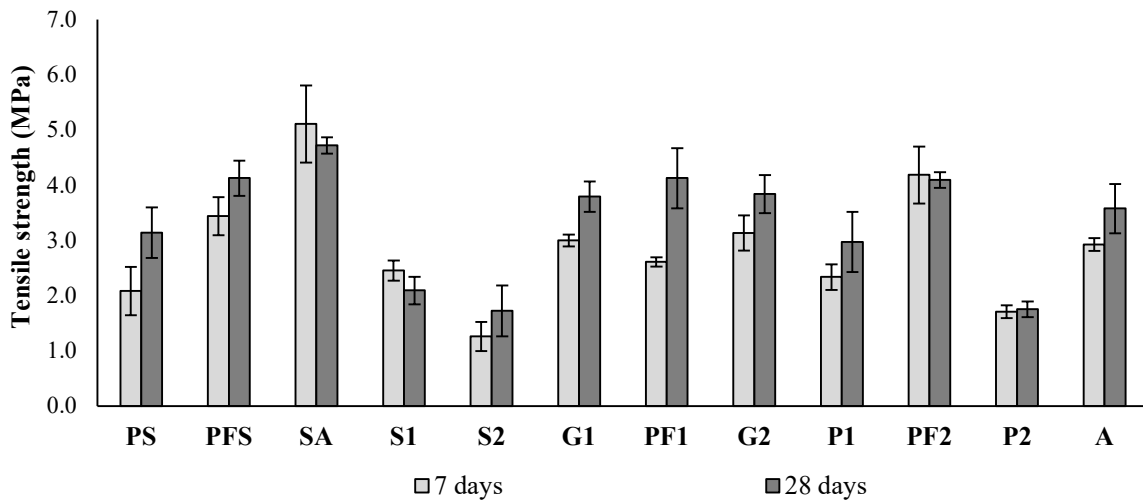


Figure 4-5: Tensile strength results.

The high variability of the results as shown by the error bars in Figure 4-5 shows the difficulty in performing the direct tensile test as pointed out by Mehta & Monteiro (2006) & Neville (2011). While most of the specimens failed at the notched areas (Figure 4-6), some of them failed below the tapered section or within the gripping jaws (Figure 4-7) of the Zwick Roell Z020 Universal Testing Machine (UTM). Arito (2018), Masuku (2009) & Chilwesa & Beushausen (2012) attribute the mode of failure at the dovetail ends to the high stress concentrations occurring at these points and the nature of holding mechanism of the UTM. This could have resulted from eccentricity in loading due to problems with the swivel heads. The results from the specimens which had failure below the tapered section were disregarded.



Figure 4-6: Failure mode within the prismatic section.



Figure 4-7: Failure below the tapered section within the gripping jaws.

Figure 4-5 shows the tensile strength across the different mixes for the specimens subjected to 7 and 28-days curing. SA had the highest 28-day tensile strength of 4.7 MPa, followed by PFS, PF1 and PF2 which had a tensile strength of 4.1 MPa. S2 recorded the lowest tensile strength of 1.7 MPa. Results for the 7 days cured specimens indicate a similar trend as observed for the 28 day cured specimens. The manufacturers make use of SF in mixes PS, PFS, SA, S1 and S2 to increase their tensile strength. Toutanji, et. al. (2006) reports that the addition of SF increases the tensile strength of cement-based materials. However, SF seemed to have little effect on S1 and S2. This result though unexpected and can be attributed to the corrosion inhibitors included in the mortars.

Figure 4-5 shows the effect of age at testing on the tensile strength of repair mortars. 9 of the mortars tested showed that the tensile strength either stayed the same or decreased (shown by the error bars) with increase in curing period. This strange result seems to suggest that the age at testing had no effect on the proprietary repair mortars. This was also noted by Chilwesa & Beushausen (2012). This could, however, be attributed to the large scatter of results observed in tests probably caused by the difficulty in performing the tests. It's only PS, G1 and PF1 that showed an increase in strength with increase curing age from 7 days to 28 days. Oluokun et al. (1990) notes that while tensile strength develops slightly faster than compressive strength in the early ages, he observed that the faster the early-age development of a particular physical property, the slower its development at later ages. Tensile strength therefore has slow development at ages greater than 3 days.

4.5 Elastic modulus

The Elastic modulus in compression tests were carried out using cylindrical specimens of 100 mm diameter and 200 mm height as described in Section 3.7.4. Figure 4-8 shows the results of the elastic modulus tests for 7 and 28 day cured specimens. The elastic modulus of 11 out of the 12 proprietary repair mortars lie within the expected range as stated in EN 1504-3:2005 for structural mortars (≥ 15 GPa for Class R3). This was for both 7 and 28 day cured specimens. It is only mix P2 that had an elastic modulus value of 9.7 GPa. The standard EN 1504-3:2005 does not provide any requirement for elastic modulus for non-structural repair products. It is important to note that the values stated in EN 1504-3:2005 are obtained using EN 13412 test method. This study made use of BS 1881.

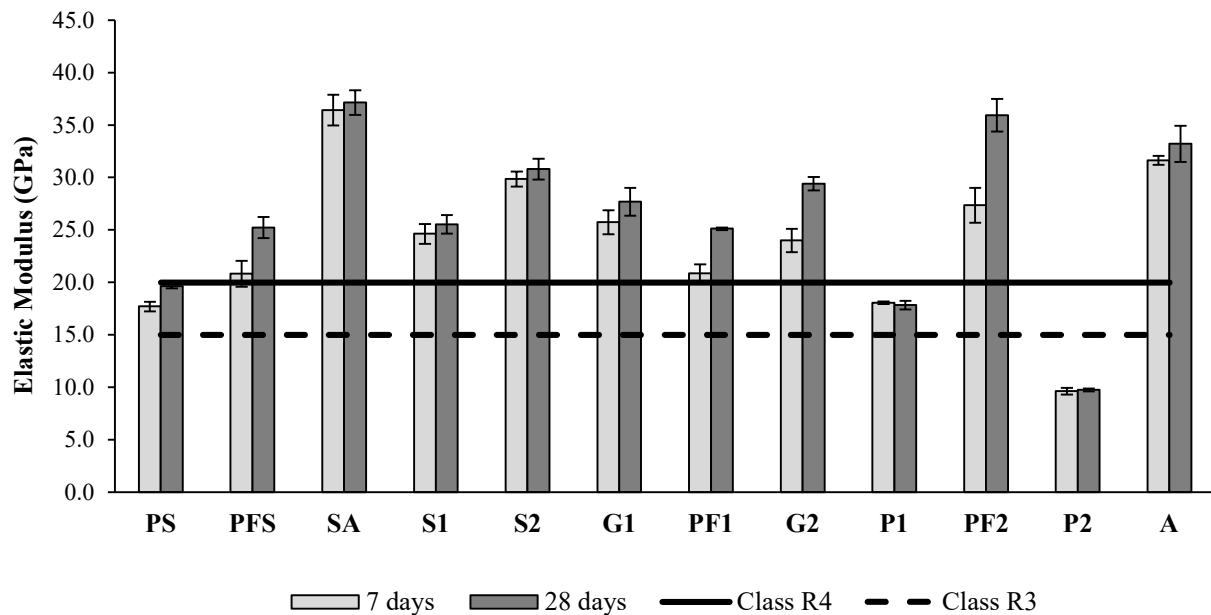


Figure 4-8: Elastic modulus for 7 and 28-day cured specimens

SA had the highest 28-day elastic modulus value of 37.1 GPa. It was also noted that the 7-day elastic modulus for mixes SA and A of 36.4 GPa and 31.6 GPa respectively was the highest compared to the rest of the mixes. This can be attributed to the presence of aggregates in the two mixes. The elastic modulus of mortar is influenced by the elastic properties and volume fraction of the aggregate and transition zone. The elastic modulus of mortar increases with an increase in

volume fraction of fine aggregate with the volume of transition zone depending on the total aggregate surface area and the interface thickness.

Polymer-modified mixes had a lower elastic modulus compared to the mixes that had a combination of fibres and polymers. Mixes P1, P2 and PS had low values of elastic modulus. Arito, (2018) attribute this reduction to the poor bonding and the presence of discontinuities within the matrix. The low elastic modulus in polymer-modified mixes are further reported by Amba, et al. (2010).

The effect of age of curing on elastic modulus is shown in Figure 4-8. There was no detectable increase in elastic modulus with increased curing age from 7 to 28 days for mixes SA, S1, S2, G1, P1, P2 and A. This was consistent with observations of lack of change in elastic modulus with curing on proprietary repair mortars made by Chilwesa & Beushausen (2012). Mehta, et. al (2010) reports that with high strength concrete a prolonged period of moist curing beyond the initial 7 days is not needed for improvement of mechanical properties of concrete. However, this study shows that there is an improvement in elastic modulus for mixes PS, PFS, PF1, G2 and PF2.

4.6 Tensile relaxation

Relaxation tests were conducted on 7 and 28-day mortar specimens to capture the influence of relaxation on early age and older specimens. The tests were conducted over a 48-hour period as stated in Section 3.7.3. The standard EN 1504-3:2005 has not specified performance requirements for tensile relaxation for repair products. The results for tensile relaxation are as shown in Figure 4-9.

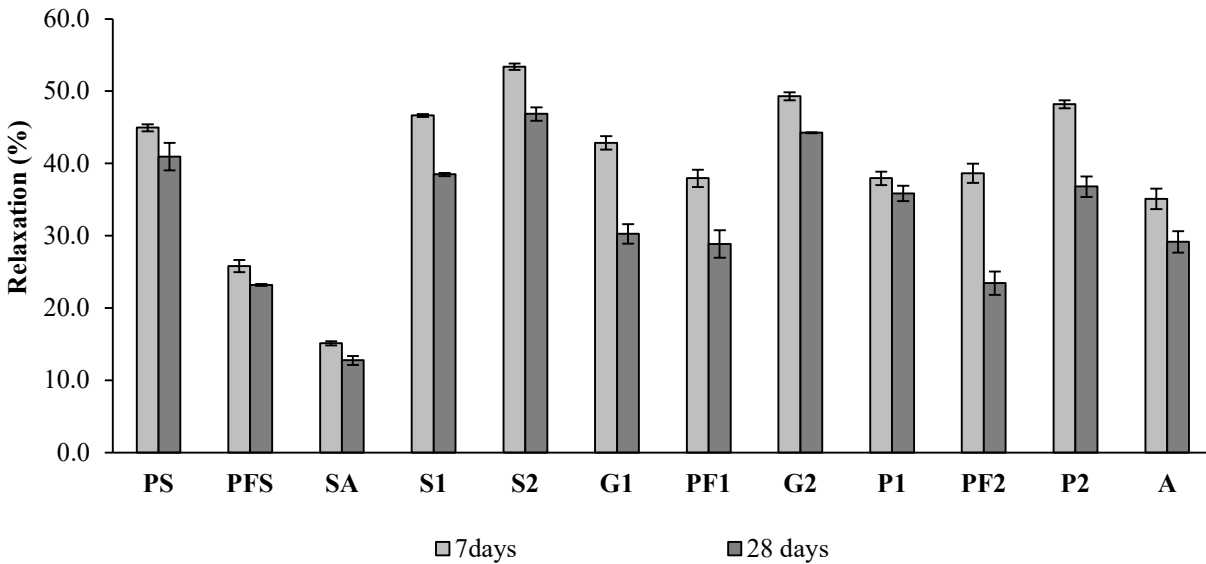


Figure 4-9: Tensile relaxation results for 7 and 28-day cured specimens.

Mix S2 had the highest value of tensile relaxation at all ages compared to the rest of the repair mortars. It had a tensile relaxation value of 46.85% and 53.40% at 7 and 28 days respectively. It is unexpected for a mix containing SF to have a high value of relaxation because SF has been reported to result in stiffer pastes. SA recorded the lowest tensile relaxation values of 12.75% and 15.10% at 7 and 28 days respectively. Mix A should have had similar values as SA due to the presence of aggregates in both mixes. However, the presence of SF in mix SA reduces its tensile relaxation performance. It was observed that the measured values of tensile relaxation decreased with an increase in age at loading. This was consistent with observations made by Masuku et al. (2009) and Chilwesa & Beushausen (2012). Neville (2011) reports that relaxation reduces with increasing age because relaxation is dependent on the degree of hydration. Hydration reduces gradually with time. There was a wide variation of relaxation values for the repair mortars tested. Ranging from a high of 53.4% for S2 to the lowest being 15.10% for SA at 7 days of curing and a high of 46.85% for S2 to 12.75% for SA at 28 days. Several authors also reported wide ranging differences in relaxation. Beushausen (2005) reported 40-50% stress relaxation in actual bonded overlays while Pigeon et al. (2000) reported a value of 67% in fully restrained specimens.

4.7 Drying shrinkage

The test results for drying shrinkage are presented in Figure 4-10 and Appendix B.4. The shrinkage measurements began immediately after water curing for 28 days as discussed in Section 3.7.5. Drying shrinkage was monitored for 60 days. This duration was chosen because it corresponded with the period of no change in length between the set targets on most of the specimens.

The reduction in drying shrinkage in mix SA and mix A compared to rest of the mixes, except mix PF2, can be attributed to the presence of aggregates which have dilution and restrain effects as reported by Arito (2018) and Dittmer and Beushausen (2013). The presence of aggregates leads to a decrease in the binder content. This consequently leads to the reduction of heat of hydration and overall reduction in shrinkage in these mixes (Fowler & Trevino, 2011). Bode & Dimmig-Osburg (2011) report that aggregates have a shrinkage-reducing effect in the mortar by disrupting the cement stone matrix, and by having a stress-relieving effect, thereby obstructing the spread of microcracks. Arito (2018) reports that this in turn reduces the susceptibility to shrink because microcracks create pathways through which pore water is lost to the environment.

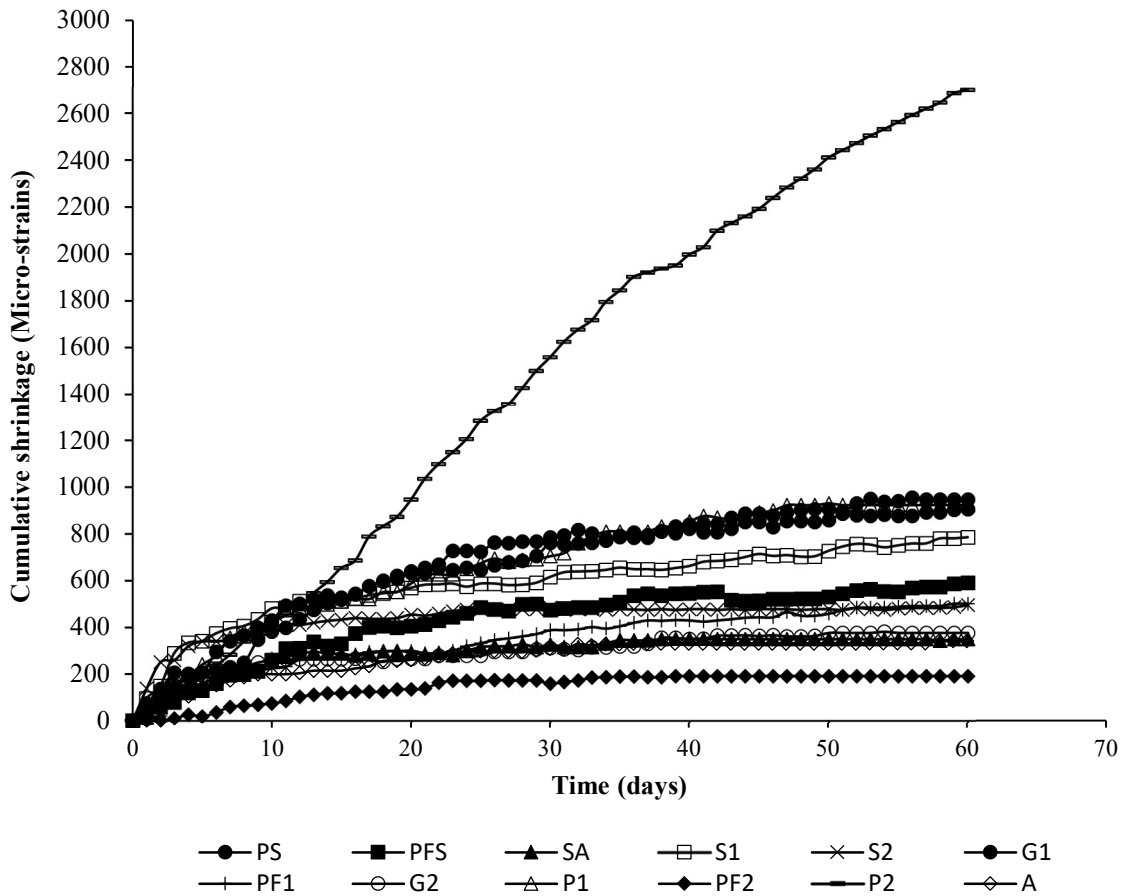


Figure 4-10: Scatter plot for drying shrinkage.

The polymer modified mixes, PS, P1 and P2 had the highest shrinkage values with P2 having a shrinkage value of 2697 micro strains. Figure 4-11 shows a reduction in shrinkage for polymer modified mixes that contained fibres. These are PFS, PF1 and PF2. Bode & Dimmig-Osburg (2011) reports that polymer modification increases drying shrinkage. Arito (2018) reports that an increase in polymer content in polymer-modified mixes results in an increase in voids within the pores of the specimens thereby increasing the drying shrinkage. Interconnected pores act as pathways through which moisture is lost from the mixes to the environment (Ohama, 1995). The increase in shrinkage on the polymer-modified mixes P1 and P2 can also be attributed to the evaporation of the large volume of water held in the form of capillary pores within its matrix and the one held within its polymer films. The observed difference in the values of drying shrinkage can be attributed to the differences in polymer types. This has however not been specified by the

manufacturers. Unmodified mixes only lose water held within the capillary pores of the hydrated cement matrix to the atmosphere.

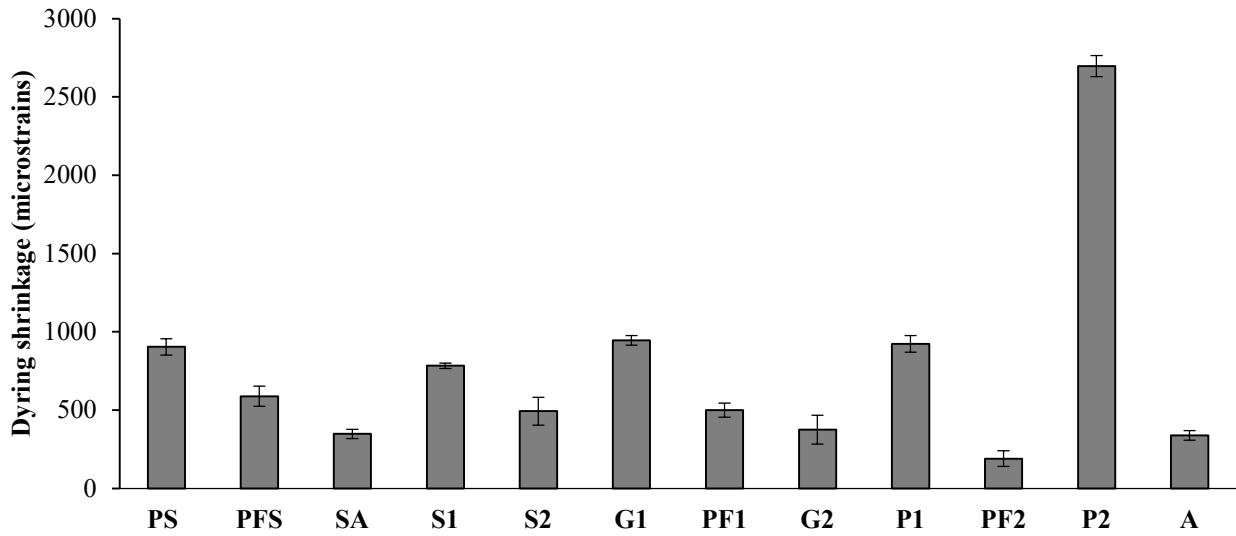


Figure 4-11: 60 day drying shrinkage test results.

4.8 Restrained shrinkage cracking

This test involved monitoring the surface crack widths and the age of cracking for the test specimens. This was in accordance with ASTM-C1581. The test results are presented in Figure 4-12 and in Appendix B.6.

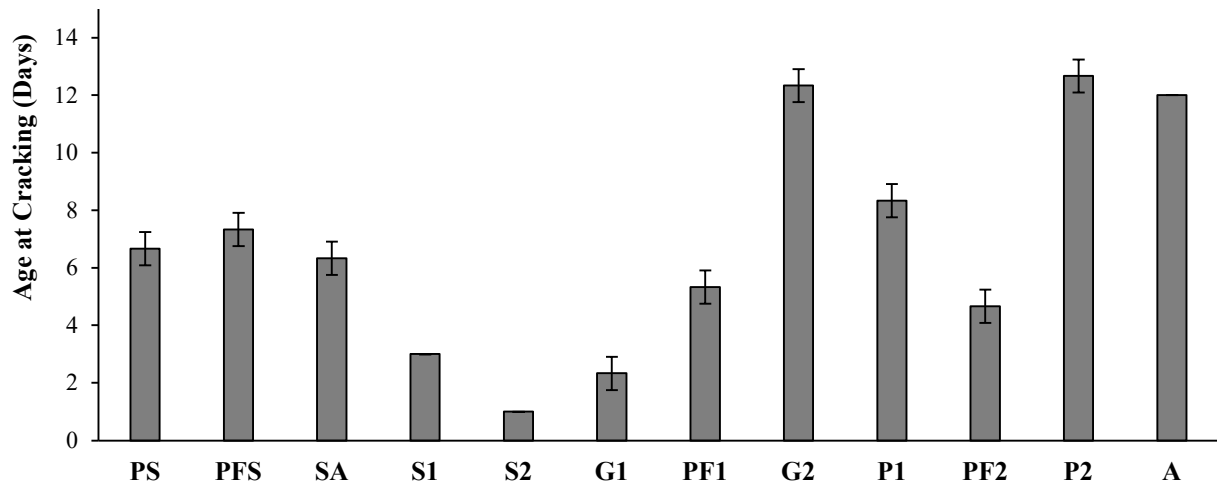


Figure 4-12: Average age at cracking test results for the repair mortars

4.8.1 Age at cracking

From the results presented in Figure 4-12, mix P2 took the longest time to crack i.e., 13 days - followed by mix A and mix G2 which had 12 days each. However, the larger scatter of the results shown by the error bars on these mixes indicate that there is no significant difference between the reported age at cracking. Mix P2 took the longest time to crack probably because of its high tensile relaxation, as well as the lowest elastic modulus compared to other specimens. This is despite the fact that mix P2 recorded the highest free shrinkage strain of 2797 micro-strain among the specimens by day 60. The opposite was observed for mix A and mix G2 which had very low values for drying shrinkage – 377 micro-strain and 340 micro-strain with high values of elastic modulus. This observation is inconsistent with literature, but their recorded high values of tensile relaxation explains their long time for crack initiation. Similar trends of having a delay in the age at cracking in mixes with high drying shrinkage have been observed by Arito (2018) and Chilwesa & Beushausen (2012).

Mix S2 had the lowest age at cracking of 1 day followed by mix G1 and mix S1 having 2 and 3 days respectively. It is interesting to note that mix S2 cracked first amongst the mixes, despite exhibiting the highest 7-day tensile relaxation of 53.4%. This suggests that crack resistance of repair mortars depends upon the combined influence of several factors. This agrees with studies

by Arito (2018) and Pigeon & Bissonnette (1999), who noted that crack resistance of concrete repair mortars is not just determined by one material property but the combined influence of various material properties and parameters. These interrelationships are complex and cannot be explained by looking at a singular material property, but rather, a holistic investigation into the material relationships is needed.

Despite having the highest compressive strength of 88.4 MPa at 28 days, mix SA cracked after 6 days. The high strength and high modulus of elasticity contributed to its increased brittleness, low tensile relaxation and therefore increased cracking (Dittmer and Beushausen, 2013; Vaysburd et al., 2001). Mix SA had a low relief of the tensile stresses induced by restrained shrinkage. Bloom & Bentur (1995) report that the presence of silica fume increases the free plastic shrinkage of concrete thus leading to earlier cracking. This explains the low age at cracking for mix S1 and mix S2.

4.8.2 Crack widths

The average crack width of all the ring specimens at an age of 14 days after the appearance of the first crack is shown in Figure 4-13. This was to monitor crack width development and to evaluate the performance of the repair mortar. A crack meter was used to measure the crack size up to an accuracy of 0.02 mm.

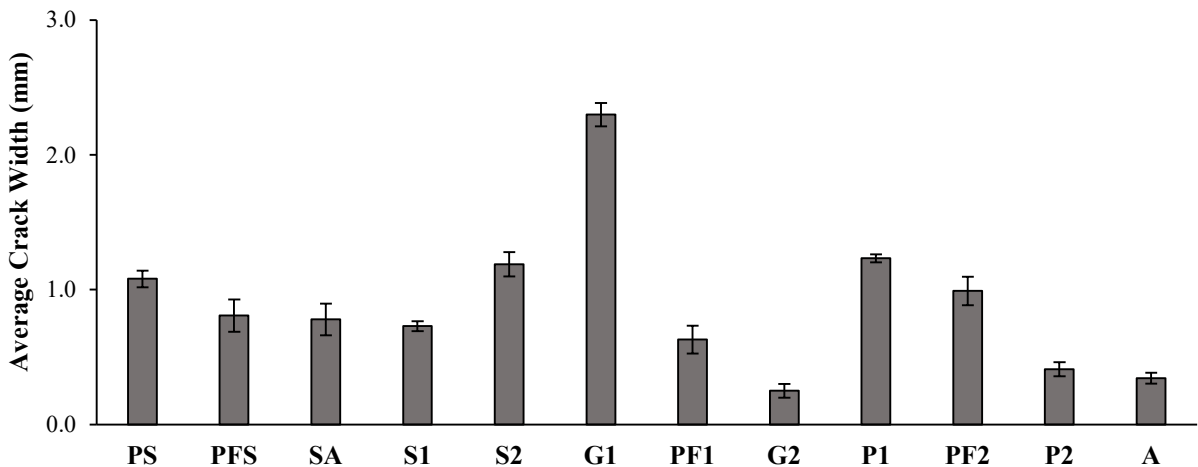


Figure 4-13: Average crack widths at 14 days after appearance of the first crack.

From Figure 4-13 it can be observed that mixes G2, P2 and A had the least crack widths of 0.25 mm, 0.41 mm and 0.34 mm respectively. This is consistent with these three mixes having the longest time to crack as observed in Section 4.8.1. The incorporation of aggregates in mixes SA and A could have bridged the existing microcracks consequently resulting in a reduction in surface crack widths. Polymer modified mixes of PS, PFS, PF1, P1 and PF2 had low values of surface crack widths compared to G1. This observation can be attributed to the increase in tensile relaxation in these mixes which results in a reduction of magnitude of displacement of the opposite crack faces. It was also observed that all the tested repair mortars had their crack widths increase with time from the appearance of the first crack. Arito, (2018) attributes this to the continuous shrinkage strains in the mixes which causes the displacement between opposite crack faces.

The variability in the results for the restrained shrinkage cracking was due to the challenges encountered with the test as some of the rings in the laboratory were not well aligned. Vaysburd et al. (2001) also noted that the ring test is not recommended for testing premixed grouts because the initial reading neglects the volume change during the first 24 hours, which can be very substantial, especially for rapid-hardening repair materials. For proprietary repair mortars, this is critical as they might have expanding admixtures/agents in them. The other challenge associated with this test is that the specimens are restrained from movement and the ratio of longitudinal to lateral dimensions is far greater than normally encountered in most repair installations.

4.8.3 Interrelationships between material parameters and age at cracking

The evaluation of the relationships between each of the investigated crack-determining material properties and the age at cracking is necessary as the performance of repairs in service can be improved through the understanding of the influence of governing properties and boundary conditions within a repair system (Arito, 2018; Lukovic, 2016). This in turn helps clarify the contradictions identified in literature regarding the relationships between the investigated material properties and the age at cracking. Furthermore, it provides us with an opportunity to critically review of the existing performance criteria as stated in EN 1504-3:2005. Scatter plots have been used to represent the relationships under investigation. They have been preferred due to their lack of bias in representing experimental data.

4.8.3.1 Compressive strength

The EN 1504-3:2005 recommends that compressive strength of repair mortars must be specified always for all intended use - see Table 2.4. It is, therefore, important that the relationship between 28-day compressive strength and age at cracking for the proprietary repair mortars be investigated.

Results from literature reveals that an inverse relationship exists between the age at cracking and compressive strength at 28 days. Several authors report a reduction in age at cracking with an increase in compressive strength (Arito, 2018; Dittmer and Beushausen, 2013). However, from the results presented in Figure 4-14, it is not possible to make the same conclusion for the proprietary repair mortars. This is shown by the weak negative linear correlation observed – with a correlation coefficient of -0.21 between the age at cracking and the compressive strength. This can be attributed to the composition and variations in binder, aggregate components and additives existing in the proprietary repair mortars. SF, polymers, fibres and their combination incorporated in the various repair mortars increases their compressive strength as discussed in Section 4.3. This results in low ductility and increased risk of crack formation (Wittmann, 2002). From the results however, it was noted that the repair mortar with the maximum compressive strength (mix SA) performed better than expected. This implies that high strengths repair mortars containing additives such as aggregates, improves their performance with regard to cracking.

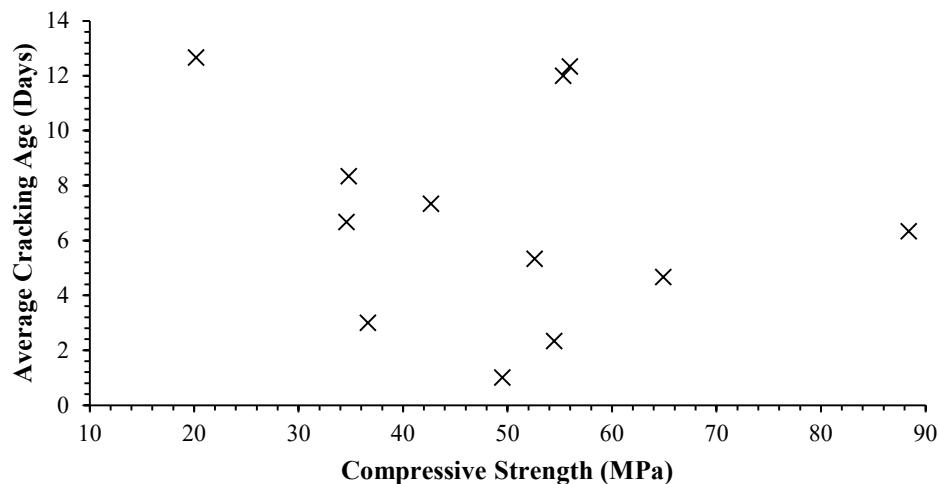


Figure 4-14: Average age at cracking vs. 28-day compressive strength.

4.8.3.2 Direct tensile strength

The EN 1504-3:2005 does not state the tensile strength that repair mortars must possess yet a critical review of literature suggests that repair mortars ought to have a high tensile strength for them to withstand the tensile stresses emanating from restrained shrinkage deformations (Emmons et al., 1993). This has however been disputed by some researchers such as Arito (2018).

From the results presented in Figure 4-15, no relationship could be established between the age at cracking and direct tensile at 28 days for proprietary repair mortars. The results are highly variable in nature and have a large scatter. No linear correlation was observed as a correlation coefficient of 0.01 was obtained between the age at cracking and direct tensile strength. Arito (2018) observed a reduction in age at cracking due to an increase in tensile strength. Ghezal and Assaf (2014) reported that an increase in tensile strength does not necessarily translate to an increase in resistance to cracking. These results however show high tensile strength mortars performing better with regard to cracking.

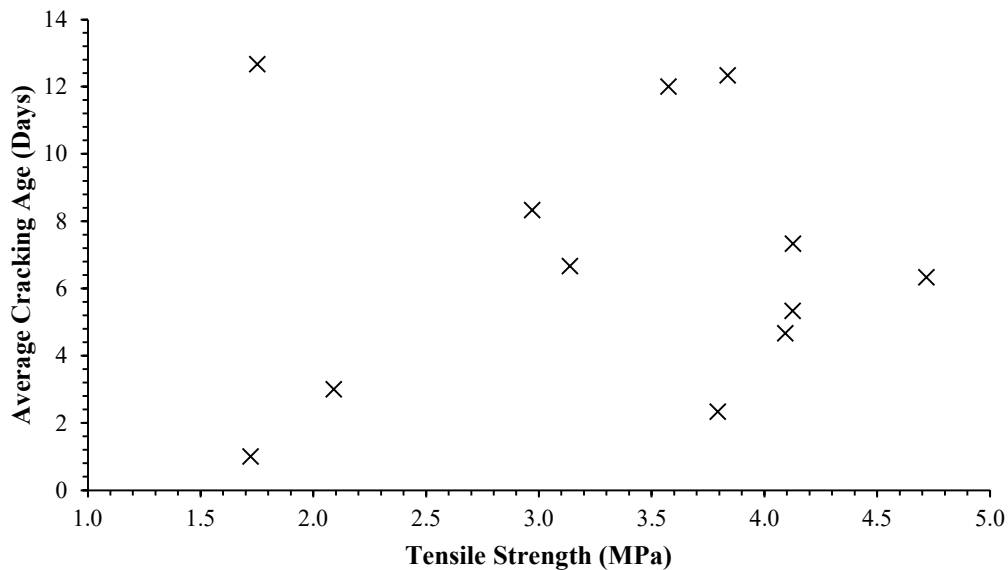


Figure 4-15: Average age at cracking vs. 28-day tensile strength.

4.8.3.3 Elastic Modulus

The scatter plots for the age at cracking versus the elastic modulus in compression at 28 days for proprietary repair mortars are presented in Figure 4-16. From the results presented, it is not clear that an increase in the modulus of elasticity resulted in a decrease in the age at cracking. A weak negative linear correlation was observed – with a correlation coefficient of -0.32 between the age at cracking and the elastic modulus. Arito (2018) observed that an increase in the modulus of elasticity resulted in a decrease in the age at cracking. This relationship was attributed to the increased tensile stresses due to restrained shrinkage deformations. Elastic modulus has been shown to have a direct influence on the elastic tensile stress that results from restrained deformation by Gilbert (1988).

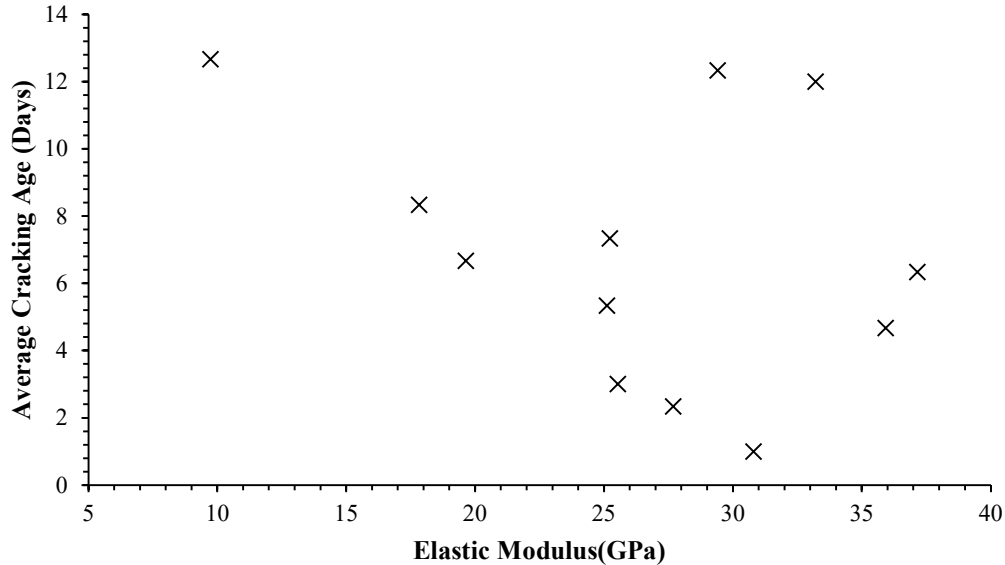


Figure 4-16: Average age at cracking vs. 28-day elastic modulus.

4.8.3.4 Drying Shrinkage

The interrelationship between the age at cracking and the drying shrinkage at 60 days is presented in Figure 4-17. No relationship could be established between the age at cracking and drying shrinkage. A weak positive correlation was observed - with a correlation coefficient of 0.33 between the age at cracking and drying shrinkage.

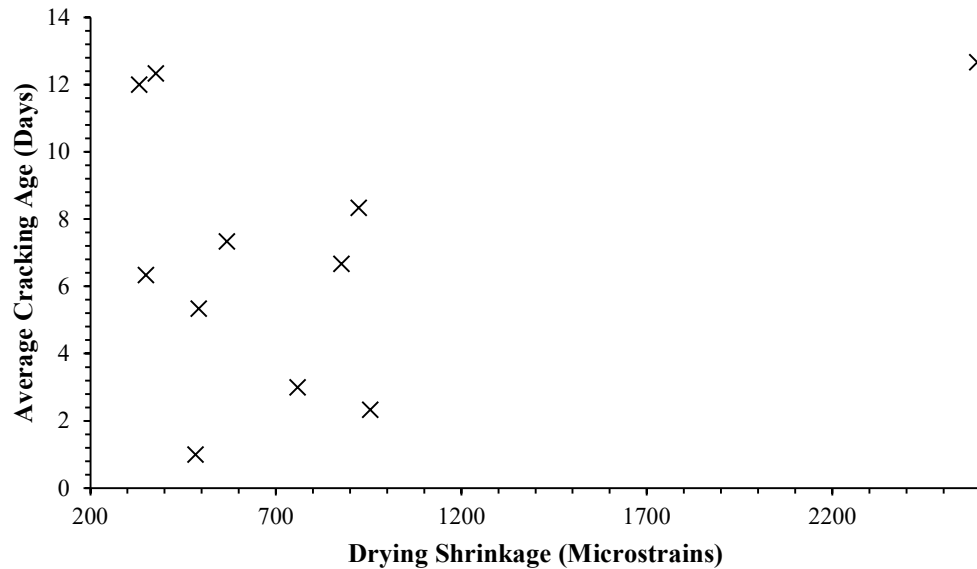


Figure 4-17: Average age at cracking vs. drying shrinkage.

Review of literature suggests that increase in drying shrinkage increases the susceptibility to cracking. This was the effect shown by mixes G2 and A that had low values of drying shrinkage and they each took 12 days to crack. This phenomenon wasn't true for mix P2 which exhibited a high drying shrinkage and took long to crack. It was characterised by a high tensile relaxation and low elastic modulus which delayed its cracking disapproving what is reported in literature.

4.8.3.5 Tensile Relaxation

The scatter plots for the interrelationship between the tensile relaxation and the age at cracking are presented in Figure 4-18. Information from literature suggests that increasing tensile relaxation delays cracking, this is consistent with results obtained by Arito (2018) and Ghezal, and Assaf (2014).

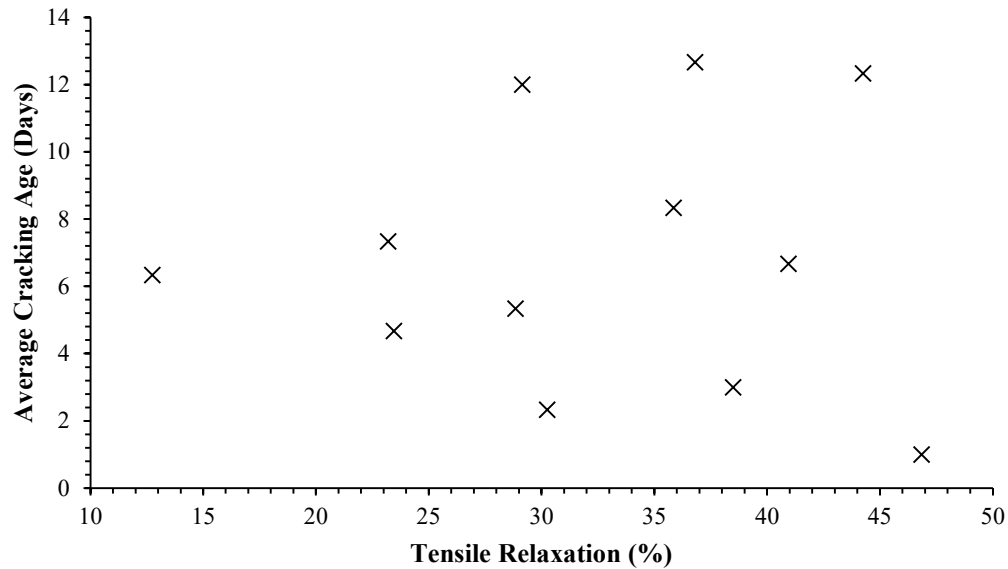


Figure 4-18: Average age at cracking vs. tensile strength.

Mix G2, with a tensile relaxation of 44% took 12 days for the first crack to appear while P2 with a tensile relaxation of 37% had an average age at cracking of 13 days. A high tensile relaxation is therefore desirable for a repair mortar as it enhances crack resistance and should therefore be considered during the design. However, from the results presented in Figure 4-18, this same trend is not consistent. No linear correlation was observed as a correlation coefficient of 0.02 was obtained between the age at cracking and tensile relaxation. Mix S2 which had the highest tensile relaxation of 47% took the least amount of days to crack, 1 day. This suggests that even with a high value of tensile relaxation other factors such as its high compressive strength and elastic modulus affected its performance. This affirms the realisation that the performance of repair mortars with regard to cracking depends upon a combination of several factors and not just one.

4.9 Bond strength

Bond strength tests were performed at 7 and 28 days on the repair mortars to determine the tensile bond strength between the overlay and substrate. The results for the tensile bond strength tests are as shown in Figure 4-19. From the results mix A had the highest bond strength of 2.88 MPa after 28 days followed by PFS and PF2 with 2.33 MPa and 2.21 MPa respectively. PF1 had the lowest tensile bond strength of 0.61 MPa with PS having 1.52 MPa. The standard, EN 1504-3:2005 specifies an adhesive bond strength of ≥ 2.0 MPa for class R4 and ≥ 1.5 MPa for class R3. It specifies a value of \geq

0.8 MPa for class R2. The values stated in EN 1504-3:2005 are obtained using EN 1542 test method. This study made use of ASTM C1583. From the results, while PF1 was categorised as a structural mortar due to its compressive strength, it fails to meet the structural requirement for adhesive bond for both the 7-day and the 28-day. This indicates that the properties indicated by the manufacturers on their product data sheets are not always correct and tests should be done to verify them. Mix P2 which is a non-structural mortar due to its compressive strength, has 28-day adhesive bond for structural mortars.

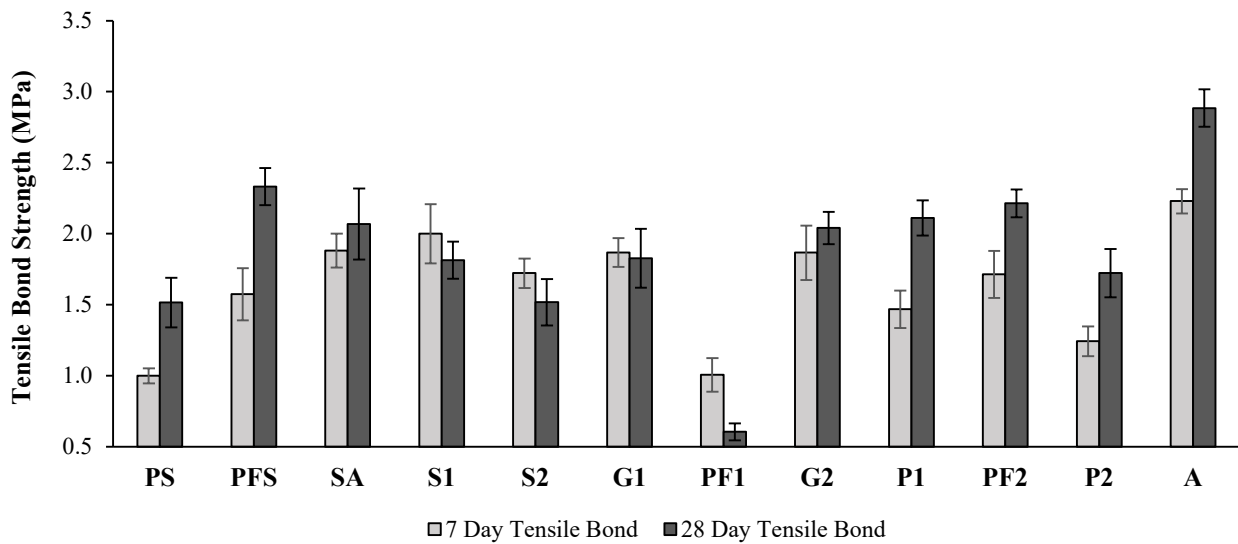


Figure 4-19: 7 and 28-day pull off test results

The analysis of the CoV of the twelve repair mortars at 28 days shows that it varies from 4.5% to 12.1 %. The CoV for PS, SA and G1 are relatively high and suggest that the test data are quite variable while the CoV's of the other repair mortars are acceptable taking into consideration that the pull off test being a tensile test, significant scatter on the results is expected. A few challenges are associated with this test. First, rarely was the failure occurring at the interface plane. Most of the cores failed in the substrate or overlay which was consistent with what is reported in literature regarding the material failure. This makes the test be of little value regarding the identification of the actual interface bond strength. Secondly, the damage of the bond between the substrate and the overlay caused by the coring procedure could have resulted in premature failure. This could explain the

variability of the results and by the overlapping error bars in Figure 4-19. Further testing therefore, needs to be performed to draw final conclusions to this test.

4.9.1 Effect of mix type

It can be observed from Figure 4.19 and Figure 4-2 that a high compressive strength of the overlay does not result to an increase in pull-off strength. Mixes SA and PF2 repair mortars which had the highest overlay compressive strength did not result in the highest tensile bond strength. This can be explained by the failure location as described in section 4.9.2. The strength of the substrate plays a major role in the pull-off strength. From Table 4-5, the repair materials that had a failure location in the substrate indicates that the overlay and the adhesive layer are stronger than the substrate concrete.

The bond strength increased with the increase in age at curing from 7 to 28-day except for mix PF1 as shown in Figure 4-19. These findings are also consistent with those reported previously by Sugo et al. (2008), Drysdale and Gazzola (1985) and Reda and Shrive (2000). This can be attributed to the maturing CSH structure. Mixes S1, S2 and G1, despite having lower 28-day tensile bond strength have overlapping error bars which indicate that there is no significant difference between the reported pull off strength. The reduction in strength might have resulted from drying shrinkage and changes in the fracture toughness of the cementitious paste (Sugo et al., 2008).

From the bond quantification in Table 4-4, adopted from Sprinkel & Ozyildirim, (2000) it can be observed that the repair mortars that contained polymers existed in almost all the categories from excellent to poor. Mix PF1 having a poor adhesive bond is inconsistent with existing literature. Ohama (1995) reports an increase in bond strength with the addition of polymers. The development of the adhesive is attributed to the high adhesion of polymers and the adhesion is usually affected by the polymer-cement ratio and the properties of substrates used.

Table 4-4: Bond strength quantification - adopted from (Sprinkel & Ozyildirim, 2000)

Bond Strength (MPa)	Label	Repair Products Tested
≥ 2.1	Excellent	PFS, P1, PF2, A
1.7 - 2.1	Very Good	SA, S1, S2, G1, G2, P2
1.4 - 1.7	Good	PS
0.7 - 1.4	Fair	-
0 - 0.7	Poor	PF1

4.9.2 Failure modes

Failure occurred at three distinct zones namely the interface, substrate and within the overlay. Failure can also occur at the epoxy used to bond the disk to the core. A combination of these failures can also occur although this was not the case in any of the specimens. Failure occurring between the steel plate, the applied glue and the substrate (adhesive failure) was considered invalid and the test repeated. Adhesive failure was a rare occurrence. The magnitude and location of the failure and fracture surface gives valuable information about the performance of the repair system (overlay, adhesive and substrate). Table 4-5 shows the failure zones for both the 7 day and 28 days after curing in a water bath. 50% of the tested repair mortars - mixes SA, G1, PF1, G2, P1 and P2, had the same failure location at either the substrate or interface for both the 7-day and 28-day. Failure in these two locations indicated that the bond strength is greater than the tensile strength of the substrate and the overlay. The other mixes investigated had varying failure locations. This can be attributed to the general variability in pull off tests and the intrinsic heterogeneity of concrete as a material. Failure occurring in the overlay material indicates that the repair material is the weakest part of the system. It is referred to as the cohesive failure of the overlay. Mix A had cohesive failure of the overlay after 7 days of curing. The fracture surface in the substrate, also referred to as cohesive failure of the substrate, indicates that the overlay concrete and the adhesive layer are stronger than the existing concrete. The pull-off stress is the tensile strength of the concrete substrate in this case. Mixes SA, G1, G2 and A exhibited this type of failure on all the three specimens tested on the 28-day after curing. In some cases the failure occurs partially along the bond surface and partially in either the overlay or the substrate and the fracture surface is a combination of two or more of the failure modes mentioned (Sprinkel & Ozyildirim, 2000).

The crack surface for mixes PF1, P1 and P2 was initiated in the interface adhesive-concrete overlay from the zone where high percentage of voids and network voids were visible. This high percentage of voids visible for PF1 might be related to the agglomeration and non-favourable fibre orientation. This apparent weakness could explain why, the pull-off strength of this specimen was the lowest one of the specimens tested (Bonaldo & Barros, 2004). Repair mortar failure at the interface was characterised by the incomplete separation of the overlay from the substrate. When failure occurred at the substrate-overlay interface, a layer of overlay was seen on the surface of the substrate (Figure 4-20). This result was also observed by Beushausen (2005) who states that for early

bond strength development, failure would occur within the overlay, close to the substrate-overlay interface. This phenomenon can be attributed to the formation of mechanical keys within the substrate surface which are impossible to remove.



Figure 4-20: Typical failure at the interface for the pull off test.

Table 4-5: 7 and 28-day cohesive failure location.

Mix ID	Specimen	Failure Location	
		7 Day	28 Day
PS	1	Substrate	Interface
	2	Substrate	Interface
	3	Substrate	Substrate
PFS	1	Interface	Interface
	2	Interface	Substrate
	3	Interface	Substrate
SA	1	Substrate	Substrate
	2	Substrate	Substrate
	3	Substrate	Substrate
S1	1	Substrate	Interface
	2	Substrate	Interface
	3	Substrate	Substrate
S2	1	Substrate	Interface
	2	Interface	Substrate
	3	Substrate	Substrate
G1	1	Substrate	Substrate
	2	Substrate	Substrate
	3	Substrate	Substrate
PF1	1	Interface	Interface
	2	Interface	Interface
	3	Interface	Interface
G2	1	Substrate	Substrate
	2	Substrate	Substrate
	3	Substrate	Substrate
P1	1	Interface	Interface
	2	Interface	Interface
	3	Interface	Interface
PF2	1	Interface	Interface
	2	Substrate	Substrate
	3	Substrate	Interface
P2	1	Interface	Interface
	2	Interface	Interface
	3	Interface	Interface
A	1	Overlay	Substrate
	2	Overlay	Substrate
	3	Overlay	Substrate

4.10 Durability indexes

The durability index tests were used to characterise the quality of the tested repair mortars as affected by choice of material and mix proportions, compaction, curing techniques and environment, as well as assess their penetrability. These tests comprise: Oxygen Permeability Index (OPI), Water Sorptivity Index (WSI) and the Chloride Conductivity Index (CCI). The tests were done at 28 days in accordance with the South African Durability Index Testing Approach, Procedure Manual 2017 (Ver. 4.2, July 2017). They were used to qualitatively assess whether a repair material will prevent the ingress of aggressive chemicals which could lead to corrosion of reinforcing steel and degradation.

4.10.1 Oxygen Permeability Index (OPI)

OPI is the negative log of the coefficient of permeability of the specimens from the mixes under investigation. The results from the 28-day OPI test are presented in Figure 4-21 and Appendix B.7.1. A high OPI value translates into low permeability. From the results, 10 of the tested repair mortars have a durability class of ‘Excellent’ according to the durability classification based on the UCT DI prediction tests as presented in Table 2-6. Only mixes PFS and A that had an OPI of less than 10 but still had a durability class of ‘Good’. The tested repair mortars have a relatively high value of OPI representing the low permeability of the proprietary repair mortars.

It was observed that there was no significant comparison in the effect of incorporation of polymers and the fibres in the repair mortars on OPI considering the scatter of the results. PS is polymer-modified and has an OPI of 10.55 while PF2 is fibre-reinforced and has an OPI of 10.75. Mix A characterised by a high aggregate content in their formulation has the highest value of permeability compared to the rest of the mixes. The reduction in binder content and the increase in aggregate content results in a porous microstructure with interconnected voids which enhances the rate at which oxygen permeates through the mixes. This could also be due to the state of compaction and the presence of bleed voids and channels. Mix SA which also incorporated aggregates had a high OPI value, this observation though unexpected might have resulted from the inherent variability in the testing.

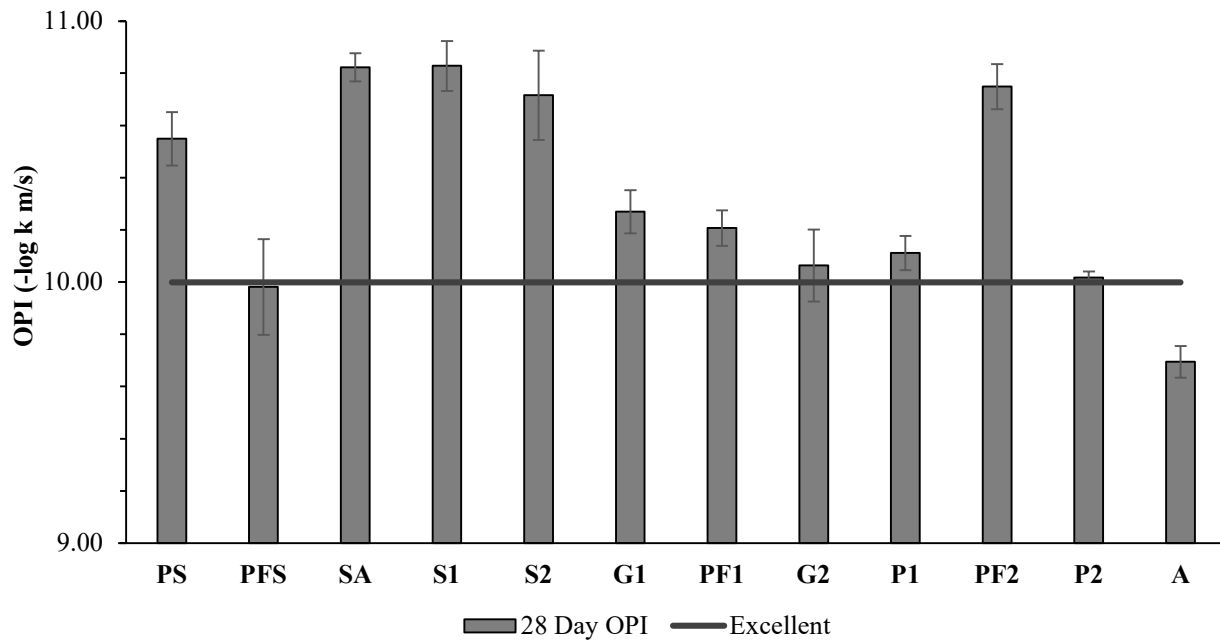


Figure 4-21: OPI test results.

4.10.2 Water Sorptivity Index (WSI)

The test results for WSI are presented in Figure 4-22 and Appendix B.7.2. From the results 8 out of 12 of the tested repair mortars have a durability class of ‘Excellent’ according to the durability classification based on the UCT DI prediction tests as presented in Table 2-6. Mix SA with a WSI value of 10.8 has a durability class of ‘Poor’ while mix A with a WSI value of 9.6 were the worst performing mortar mix. These mixes had incorporated aggregates. The presence of aggregates leads to the reduction in paste content making them porous. It is however noted other factors such as compaction could affect the porosity of these mixes. The mixing duration and the compaction of the repair mortars was done according to the manufacturers guidelines thus having an influence on the porosity. This also explains the high range of the porosity results (7.9 - 25.4%) as shown in Table 4-6. An increase in voids enhanced the sorption of water through the specimens due to the poor packing and subsequently translating to a low WSI. Mix A which had the highest porosity of 25.4 % has the lowest WSI value of 9.69.

Table 4-6: Porosity results for the repair mortars

Mix ID	28 Day Porosity (%)
PS	14.3
PFS	14.8
SA	22.7
S1	9.4
S2	8.6
G1	14.1
PF1	15.7
G2	14.5
P1	10.8
PF2	7.9
P2	14.5
A	25.4

Polymer-modified mixes – i.e. PS, PFS, PF1, P1, PF2 and P2 - had low WSI values. Polymer-modification resulted in a reduction in WSI. This was observed by Arito (2018) and is consistent with the observations of Soufi et al. (2016) who reported that an increase in polymer dosage decreases capillary absorption significantly. This has been described in section 4.10.1.

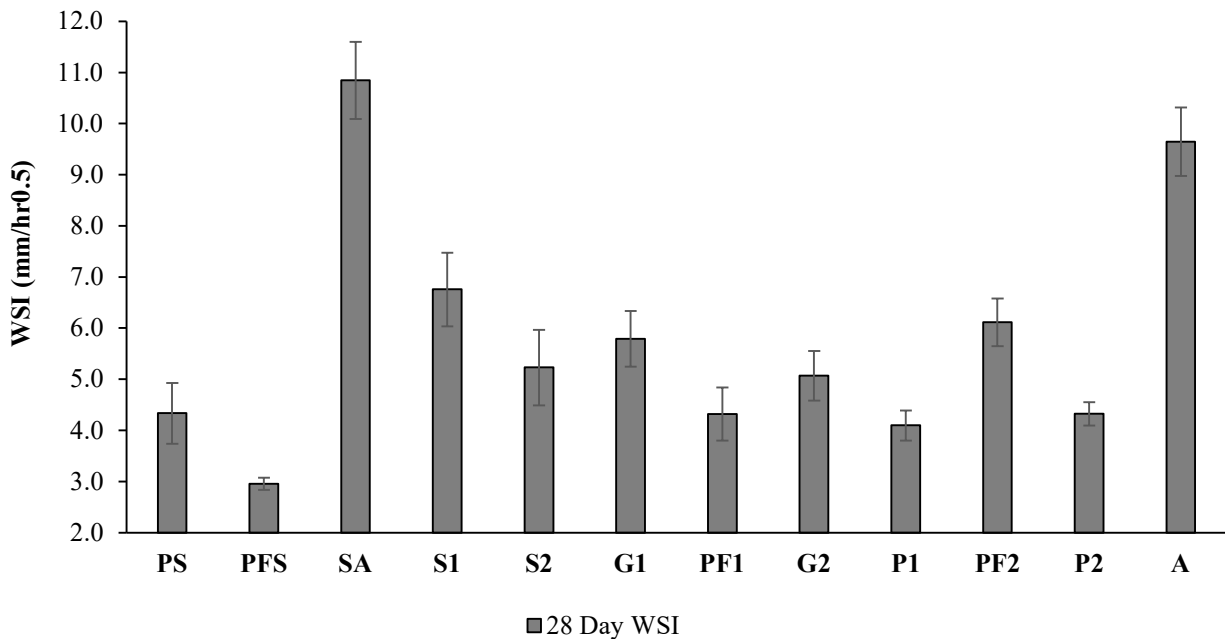


Figure 4-22: WSI test results

4.10.3 Chloride Conductivity Index (CCI)

The test results for CCI are presented in Figure 4-23 and Appendix B.7.3. The lowest and highest conductivity results differed by an order of magnitude of 0.3 mS/cm to 5.3 mS/cm. 50% of the mortars that were tested have a durability class of ‘Excellent’ according to the durability classification based on the UCT DI prediction tests as presented in Table 2-6. Mix P2 had the highest value of CCI of 5.3 mS/cm with a durability classification of ‘Very Poor’. As a guideline, common durability specifications in South Africa, for environmental class XS3 (marine environment: tidal, splash and spray zones) and a minimum cover depth of 50 mm, demand CCI values less than 0.35 for concrete containing silica fume (10%) (“EN 206-1:2000 Concrete - Part 1; Specification, performance, production and conformity,” 2000). PS, PFS, S1 and S2 which contain silica fume, therefore, do not meet this requirement. However due to the proprietary nature of the product the exact quantity of silica fume added to the products could not be identified.

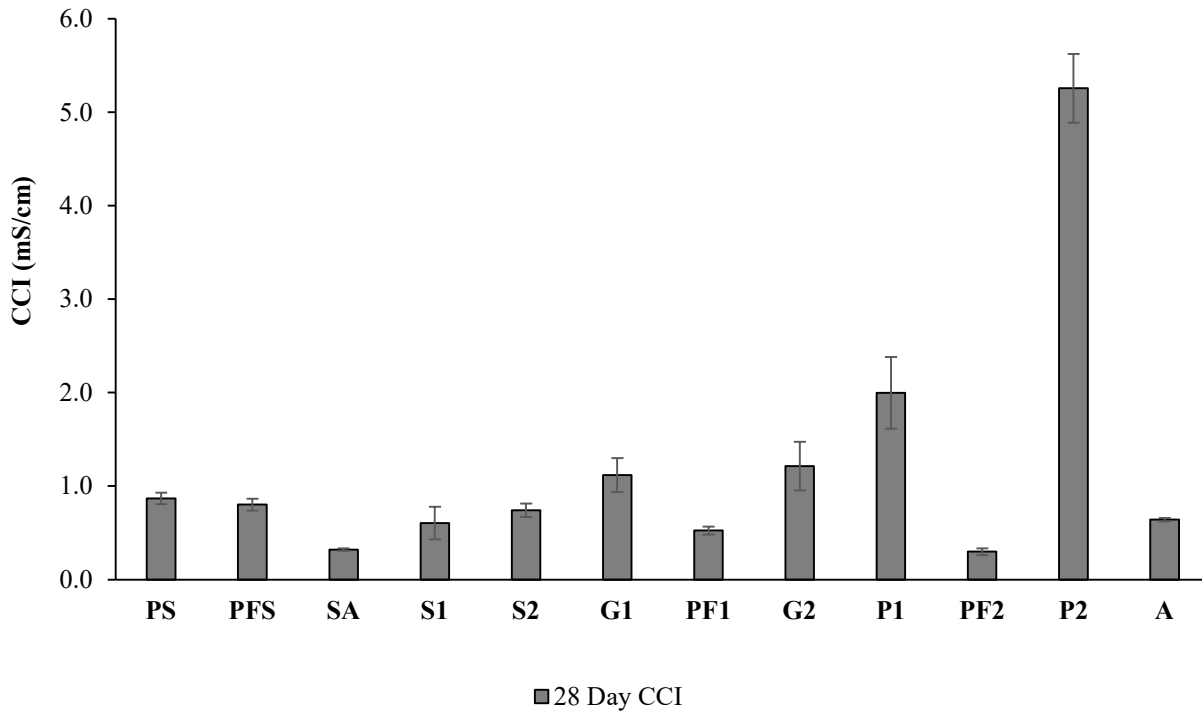


Figure 4-23: CCI test results

4.11 Closure

Results from the experimental work has been presented, analysed and discussed in this chapter. Material characterization of the twelve proprietary repair mortars that were tested was investigated. The mortars were categorised by their product description as presented in the manufacturer’s data sheets, by sieve analysis and by the Energy Dispersive Spectrometry (EDS). The sieve analysis was done to determine the amount of filler contained in the mixes. Mix A had the highest amount of fines with 28.28% passing the 0.075 mm sieve while 58% of the repair mortars had an amount less than 1% passing through the 0.075 mm sieve. The gradation curves showed that the mixes contain a narrow range of particles. EDS analysis was used to show the element composition of the repair mortars as shown in Table 4.3.

Compressive strength results for the repair mortars showed that all the tested mortars except for mix P2 were structural with the compressive strength ≥ 25 MPa (Class R4 and Class R3). Mix P2 is a non-structural repair mortar, Class R2, with a compressive strength ≥ 15 MPa. This is

according to EN 1504-3:2005. Mix SA had the highest 28-day compressive strength of 88.4 MPa. This high strength can be attributed to the presence of aggregates which generate a stronger bond between the paste and the aggregate creating a higher strength. Mix PFA, which was polymer and fibre modified, had a 28-day compressive strength of 64.9 MPa. This high strength was attributed to the polymer-fibres incorporated in the mix. The inclusion of polymers in concrete increases the mechanical properties of the ITZ, resulting in concrete with better mechanical properties. Silica fume incorporated in mixes PS, PFS, and S1 repair mortars is attributed to their high compressive strength of > 30 MPa.

Mix SA had the highest 28-day tensile strength of 4.7 MPa, followed by PFS, PF1 and PF2 which had a tensile strength of 4.1 MPa. S2 recorded the lowest tensile strength of 1.7 MPa. It was noted that the incorporation of SF contributed to high tensile strength of PS and PFS. 9 out of the 12 tested repair mortars showed that the tensile strength either remained the same or decreased with increase in age at testing from 7 day to 28 day suggesting that that increase in curing period had no effect on the proprietary repair mortars. For elastic modulus, 11 of the 12 tested repair mortars values lie within the expected range as stated in EN 1504-3:2005 for structural mortars (≥ 15 GPa for Class R3). The standard EN 1504-3:2005 does not provide any requirement for elastic modulus for non-structural repair mortars. SA had the highest value of elastic modulus of 37.16 GPa. It was noted as well that the elastic modulus for mixes SA and A developed much faster than the other mortars. This can be attributed to the presence of aggregates in the two mixes.

Tensile relaxation tests were conducted on 7 and 28-day mortar specimens to investigate the influence of relaxation on early age and older specimens. EN 1504-3:2005 does not provide any performance requirements for tensile strength. Mix S2 had the highest tensile relaxation at all ages compared to the rest of the specimens. It had a tensile relaxation value of 46.85% and 53.40% at 7 and 28 days respectively. SA recorded the lowest tensile relaxation values of 12.75% and 15.10% at 7 and 28 days respectively. It was observed that the measured values of tensile relaxation decreased with an increase in age at loading. This was consistent with observations made by Masuku et al. (2009) and Chilwesa & Beushausen (2012).

Drying shrinkage measurements on the repair mortars were monitored for 60 days. Mix A had the least shrinkage at 332 Micro-strains while mix P2 recorded the maximum value of 2591 Micro-

strains. The reduction in drying shrinkage in mixes SA and A compared to rest of the mixes except mix PF2, can be attributed to the presence of aggregates which have dilution and restraint effects. The polymer-modified mixes, PS, P1 and P2 exhibited the highest shrinkage. A reduction in shrinkage in polymer-modified mixes that contained fibres was observed. These are PFS, PF1 and PF2. Bode & Dimmig-Osburg (2011) reports that polymer modification increases drying shrinkage.

For the ring tests mix P2 took the longest time to crack of 13 days followed by mixes A and G2 which had 12 days each. P2 took the longest time to crack probably because of its high tensile relaxation, as well as the lowest elastic modulus compared to the other mortar specimens. The opposite was observed for mixes A and G2 which had very low values for drying shrinkage – 377 micro-strain and 340 micro-strain with high values of elastic modulus. This observation is inconsistent with literature, but their recorded high values of tensile relaxation explains their long time for crack initiation. Despite having the highest compressive strength of 88.4 MPa at 28 days, SA cracked after 6 days. The high strength and high modulus of elasticity contributed to its increased brittleness, low tensile relaxation and therefore increased susceptibility to cracking. Mixes G2, P2 and A had the least crack widths of 0.25 mm, 0.41 mm and 0.34 mm respectively. This is consistent with these three mixes having the longest time to crack. The incorporation of aggregates in mixes SA and A could have bridged the existing microcracks and consequently resulting in the reduction in the surface crack widths.

Tests for bond strength in tension were performed at 7 and 28 days on the proprietary repair mortars. Mix A had the highest bond strength of 2.88 MPa after 28 days followed by mixes SA and PFS with 2.36 MPa and 2.33 MPa respectively. Mix PF1 had the lowest tensile bond strength of 0.61 MPa with PS having 1.52 MPa. The standard EN 1504-3:2005 specifies an adhesive bond strength of ≥ 2.0 MPa for class R4 and ≥ 1.5 MPa for class R3. It specifies a value of ≥ 0.8 MPa for class R2. Mix PF1, categorised as a structural mortar due to its compressive strength, fails on the structural requirement for adhesive bond for both the 7-day and the 28-day. From the bond quantification table adopted from Sprinkel & Ozyildirim (2000) it can be observed that the polymer modified repair mortars of PFS, P1, PF2 and A had an excellent bond strength which was ≥ 2 MPa.

Finally, the durability index tests were used to characterise the repair mortars as well as assess their penetrability. For OPI, 10 of the tested repair mortars have a durability class of ‘Excellent’

according to the durability classification based on the UCT DI prediction tests. Only mixes PFS and A that had an OPI of less than 10 but still had a durability class of 'Good'. The tested repair mortars have a relatively high OPI representing low permeability. 8 out of 12 of the tested repair mortars have a durability class of 'Excellent' for WSI with mix SA having a WSI value of 10.8 has a durability class of 'Poor' while mix A with a WSI value of 9.6 were the worst performing mortar mixes. 50% of the tested mortars have a durability class of 'Excellent' for CCI. Mix P2 had the highest value of CCI of 5.3 mS/cm with a durability classification of 'Very Poor'.

5. Conclusions and recommendations

5.1 Introduction

This chapter contains the conclusions arrived at during this study and recommendations for further research. The overarching objective of the research was to provide a platform for the development of performance requirements for proprietary repair mortars on cracking resistance and durability with respect to EN 1504-3:2005 which can be used in project specifications. These requirements have been arrived at by the laboratory testing of proprietary repair mortars that are commonly used in South Africa. The objective was achieved through the following sub-objectives:

- a) An investigation of the proprietary repair mortars' mechanical properties in the hardened state.
- b) An investigation of durability and transport properties of the proprietary repair mortars.

These objectives were met through a critical review of literature and a laboratory test program that comprised testing twelve proprietary repair mortars from four different manufacturers. It is acknowledged that studying a wide scope of properties, including compressive strength, tensile strength, tensile relaxation, restrained shrinkage tests, adhesive (bond) strength and durability indexes of the repair materials is beneficial in understanding the holistic performance of the material. Whilst not all parameters have been investigated in this research, the study collectively fills gaps in knowledge to enable the understanding of the performance requirements for proprietary concrete repair materials.

The performance of proprietary repair mortars with regard to durability and cracking resistance in repair works differs. These differences are primarily associated with variations in the formulation of the material. Literature has highlighted the importance of using a specification framework in selecting the product to be used. There is emphasis on the need for a thorough understanding of material properties and site conditions in order to provide an understanding of how repair materials will perform. This must be viewed in conjunction with an appreciation of appropriate specification criteria for conservation work. The results provide an indication of material performance and a platform for objective decision-making on the suitability and specification of these materials.

5.2 Effect of time-dependent material properties on crack resistance and durability

5.2.1 Compressive strength

From the test results it has been noted that the tested proprietary repair materials achieved the compressive strengths as stated by the standard EN 1503-4:2005. 11 of the tested repair materials were categorised as structural with only mix P2 being a non-structural repair mortar. These results also confirmed the specifications/categorisation from the manufacturers. Mixes PS, PFS, SA, S1, S2, G1, PF1, G2, P1, PF2 and A were categorised as high strength mortars to be used for structural repairs. Mix P2, having a low compressive strength is to be used as a cosmetic repair mortar. It was observed that despite mixes S1, S2 and G1 being manufactured by the same company, they use different test methods for their compressive strength measurements which makes comparing this property challenging for engineers or the specifier. They use ASTM C-109 for S1 and G1, and C-942 for S2 as indicated in Table 3-3. It was further observed that the proprietary repair materials have high compressive strengths. This fails to deviate from using compressive strength as a measure the effectiveness in performance of repair mortars in service.

The characterization of repair mortars through their product description from the manufacturer revealed common variations in the proprietary repair mortars. As stated by the manufacturers in their product data sheets the tested repair mortars included polymers, fibres, aggregates and silica fume while some contained a combination of these products. The different formulations had an influence in the compressive strength of the repair mortars. The high compressive strengths of mixes SA and A was attributed to the presence of aggregates. The inclusion of polymers in the repair mortars resulted in higher strengths except for mix P1. Silica fume incorporated in mixes PS, PFS, SA, S1 and S2 repair mortars contributed to their high compressive strength.

5.2.2 Tensile strength

The incorporation of polymers, fibres and SF in the proprietary repair mortars contributed to their high tensile strength. From the results it was shown that a high tensile strength was not a guarantee for better performance with regard to cracking. This was the case for mix SA with a high 28-day tensile strength of 4.7 MPa while it cracked after 7 days. It was noted that an increase in age at

testing had no effect on tensile strength. EN 1504-3:2005 does not specify any requirements for tensile strength.

5.2.3 Elastic modulus

EN 1504-3:2005 provides performance requirements with regards to the elastic modulus for structural mortars but does not provide any requirements for non-structural repair mortars. 11 of the 12 tested repair mortars lie within the expected ranges as stated in EN 1504-3:2005. The presence of aggregates in mixes SA and A repair mortars contributed to their high elastic modulus. Polymer modification leads to lower elastic modulus compared to mixes that contained a combination of polymers and fibres.

5.2.4 Tensile relaxation

The EN 1504-3:2005 does not provide any requirement for tensile relaxation for repair products. It was observed that the measured values of tensile relaxation decreased with an increase in age. A high tensile relaxation is desirable for a repair mortar because it enhances its crack resistance and should therefore be considered during the design. Mix G1, with a tensile relaxation of 44% took 12 days for the first crack to appear while mix P2 with a tensile relaxation of 37% had an average age at cracking of 13 days, although there is no significant difference between the reported age at cracking.

5.2.5 Drying shrinkage

The presence of aggregates leads to a reduction in drying shrinkage as noted on repair mortars mixes SA and A. Although this did not lead to better performance with regard to cracking. An increase in drying shrinkage does not necessarily translate into an increase in the susceptibility to cracking. This was observed in mix P2 which had the highest shrinkage value but took the longest time to crack. Polymer-modified mixes had the highest shrinkage values although there was a reduction in shrinkage in mixes containing a combination of polymers and fibres.

5.2.6 Restrained shrinkage cracking

Arito (2018) reports that high tensile relaxation values, as well as the lowest elastic modulus results in an increase in age at cracking for repair mortars. This was observed for mix P2 despite the fact that it recorded the highest free shrinkage strain. Mixes SA and S2 recorded low age at cracking

despite the fact that they had the highest compressive strength and tensile relaxation respectively. This shows that crack resistance of repair mortars depends on the combined influence of several factors. This agrees with Arito (2018) and Pigeon & Bissonnette (1999) who noted that crack resistance of concrete repair mortars is not just determined by one material property but the combined influence of various material properties and parameters. Crack widths are directly proportional to the age at cracking with the mixes that took longest time to crack recording the least crack widths. The incorporation of aggregates in the repair mortars leads to a reduction in surface crack width. Polymer modification leads to a reduction in surface crack widths. This observation can be attributed to the high tensile relaxation that results in a reduction of magnitude of displacement of the opposite crack faces.

5.2.7 Bond strength

The standard, EN 1504-3:2005 specifies an adhesive bond strength of ≥ 2.0 MPa for class R4 and ≥ 1.5 MPa for class R3. Mix PF1 fails on the structural requirement for adhesive bond for both the 7-day and the 28-day despite being categorised as a structural mortar due to its compressive strength. This indicates that the properties indicated by the manufacturers on their product data sheets should always be verified before the product can be specified. A High compressive and tensile strength of the overlay does not necessarily translate into a high bond strength. Mixes SA and PF2 repair mortars which had the highest overlay compressive strength did not result in the highest tensile bond strength. There is an observed increase in the bond strength as the age at testing increases from 7 day to 28 day.

5.3 Durability and permeability performance of proprietary repair mortars

The repair mortars under investigation have high OPI values representing their low permeability. It was observed that the incorporation of polymers and the fibres in the proprietary repair mortars did not result in a significant effect in their comparative performance with respect to OPI. CCI tests on the repair mortars revealed that 50% of the tested mortars have a durability class of 'Excellent'. Repair mortars PS, PFS, S1 and S2 containing silica fume did not meet the durability specifications in South Africa, for environmental class XS3 (marine environment: tidal, splash and spray zones) and a minimum cover depth of 50 mm as stated in EN 206-1:2000 Concrete - Part 1. It is only mix SA that met these requirements.

5.4 Recommendations for further research

The results presented highlight the importance of using a specification framework in selecting the product to be used. These results emphasize the need for a thorough understanding of material properties in order to provide an understanding of how repair materials will perform. This must be viewed in conjunction with an appreciation of appropriate specification criteria for repair work.

The number of proprietary repair mortars used in the experiments was limited to twelve due to the large number of tests and the extensive amount of time required for the full range of tests that needs to be conducted on each mix. Further detailed investigation therefore needs to be performed in order to draw further conclusions. The following recommendations are suggested to improve the experimental outcome:

- Further research into the microstructural properties of these materials may give additional insights into the causes of their different physical properties.
- On-site observation and testing should be considered to identify any potentially problematic macro-scale issues associated with repair mortars, particularly in relation to moisture transmission and retention. Understanding these factors amongst others, are essential to prevent damage to repaired structures by the use of incompatible repair materials.
- Analytical models should be used to predict and assess the cracking potential of the commercial repair mortars.
- Nomographs to be developed to assist in the design of mixes and the prediction of the susceptibility of mixes to cracking to make the results of this study more relevant in practice. The parameters used to develop these nomographs ought to be kept at a minimum to make it an ‘easy-to-use’ tool for the material manufacturer, repair engineers and contractors.

6. References

- Alexander, M. G. (1994). Deformation properties of blended cement concretes containing blastfurnace slag and condensed silica fume. *Advances in Cement Research*, vol.6, no., pp.73-81.
- Alexander, M., & Beushausen, H. (2009). Deformation and Volume change of Hardened Concrete. In Owens, G., editor, *Fulton's Concrete Technology*. *Fulton's Concrete Technology*. Cement & Concrete Institute, Ninth edition.
- Alexander, Mark G, & Mindess, S. (2005). *Aggregate in Concrete*. Taylor & Francis, New York.
- Alexander, M. G, Jaufeerally, H., & Mackechnie, K. (2003). Structural and Durability Properties of Concrete made with Corex Slag. *Research Monograph*, (6), 1–28.
- Altoubat, S.A & Lange, D. . (2001). Creep, Shrinkage and Cracking of Restrained Concrete at Early Age. *ACI Materialsjournal*. 98(4):323.
- Amba, J. C., Balayssac, J. P., and Détriché, C. H. (2010). Characterisation of differential shrinkage of bonded mortar overlays subjected to drying. *Materials and Structures*, (43(1-2):), 297-308.
- Arito, P. A., Beushausen, H., and Alexander, M. G. (2016b). Barriers to the realisation of effectiveness in the performance of concrete patch repair mortars in service. *Proceedings of the fib SYMPOSIUM 2016: Performance-Based Approaches for Concrete Structures, Cape Town, South Africa, 21-23 November 2016*.
- Arito, P. A. (2018). Influence of Mix Design Parameters on Restrained Shrinkage Cracking in Non-Structural Concrete Patch Repair Mortars. PhD Thesis, University of Cape Town.
- Atrushi, D. S. (2003). *Tensile and Compressive Creep of Early Age Concrete: Testing and Modelling*. PhD thesis, The Norwegian University of Science and Technology.
- ASTM-C1581 (2004). Standard test method for Determining the Age at Cracking and Induced Tensile Stress Characteristics of Mortar and Concrete under Restrained Shrinkage.
- Bai, Y., Basheer, P. A. M., Cleland, D. J., & Long, A. E. (2009). State-of-the-art applications of the pull-off test in civil engineering. *International Journal of Structural Engineering*, 1(1), 93.

- Baldwin, N. J. R. & E. S. King. (2003). Field studies of the effectiveness of concrete repairs, 42. Phase 1 report: Desk study and literature review. Technical Report 175, Mott MacDonald Ltd.
- Banthia, N. & Gupta, R. (2006). Influence of polypropylene fiber geometry on plastic shrinkage cracking in concrete. *Cement and Concrete Research, Volume 36*, 1263-1267.
- Banthia, N. and Gupta, R. (2009). Plastic shrinkage cracking in cementitious repairs and overlays. *Materials and Structures, 42(5)*, 567-579.
- Bentur, A., & Kovler, K. (2003). Evaluation of early age cracking characteristics in cementitious systems. *Materials and Structures/Materiaux et Constructions, 36(3)*, 183–190.
- Bentz, D. P. (2005). Curing with Shrinkage Reducing Admixtures. *Concrete International*, pages 55–60.
- Bentz, D. P., Sant, G., and Weiss, J. (2008). Early-Age Properties of Cement- Based Materials. I: Influence of Cement Fineness. *Journal of Materials in Civil Engineering, 20(7)*, 502-508.
- Bentz, D. P., & Haecker, C. J. (1999). An argument for using coarse cements in high performance concretes. *Cement and Concrete Research, 615–618*.
- Beushausen, H.-D., & Alexander, M. (2005). Crack development in bonded concrete overlays subjected to differential shrinkage: a parameter study. In *Proceedings of the international conference on concrete repair, rehabilitation and retrofitting ICCRRR, Cape Town* (pp.393-394).
- Beushausen, H., & Alexander, M. G. (2006). Failure mechanisms and tensile relaxation of bonded concrete overlays subjected to differential shrinkage. *Cement and Concrete Research, 36(10)*, 1908–1914.
- Beushausen, H., Masuku, C., & Moyo, P. (2012). Relaxation characteristics of cement mortar subjected to tensile strain. *Materials and Structures, 45*, 1181–1188.
- Beushausen, H. (2005). Long term performance of bonded concrete overlays subjected to differential shrinkage. PhD Thesis, University of Cape Town.
- Beushausen, H, & Bester, N. (2016a). The influence of curing on restrained shrinkage cracking of

- bonded concrete overlays. *Cement and Concrete Research*, 87, 87–96.
- Bezerra, U. T., Ferreira, R. M., & Castro-gomes, J. P. (2011). The effect of latex and chitosan biopolymer on concrete properties and performance, In Aguiar, J. and Czarnecki, L., editors, *Polymers in Concrete*, volume 466, 37–46.
- Bissonnette, B., Courard, L., Beushausen, H., Fowler, D., Trevino, M., & Vaysburd, A. (2013). Recommendations for the repair, the lining or the strengthening of concrete slabs or pavements with bonded cement-based material overlays. *Materials and Structures/Materiaux et Constructions*, 46(3), 481–494.
- Bissonnette, Benoît, Courad, L., Fowler, D. W., & Granju, J.-L. (2013). *Bonded Cement-based Materials Overlays for the Repair, the Lining or the Strengthening of Slabs or Pavements. Journal of Chemical Information and Modeling* (Vol. 53).
- Bissonnette, Benoît, Pierre, P., & Pigeon, M. (1999). Influence of key parameters on drying shrinkage of cementitious materials. *Cement and Concrete Research*, 29(10), 1655–1662.
- Bissonnette, Benoît, & Pigeon, M. (1995). Tensile creep at early ages of ordinary, silica fume and fiber reinforced concretes. *Cement and Concrete Research*, 25(5), 1075–1085.
- Bloom, R., & Bentur, A. (1995). Free and restrained shrinkage of normal and high strength concrete. *ACI Materials Journal*, (92(2)), 211–217.
- Bode, K. A., & Dimmig-Osburg, A. (2011). Shrinkage Properties of Polymer-Modified Cement Mortars (PCM). *Key Engineering Materials*, In Aguiar, J. and Czarnecki, L., editors, *Polymers in Concrete*, volume 466, pages 29–36. Trans Tech Publ, Trans Tech Publications.
- Bonaldo, E., & Barros, J. O. (2004). Bond characterization between concrete base and repairing SFRC by pull-off tests, *Report 04-DEC/E-13*, Universidade do Minho.
- Brandt, A. M. (2009). *Cement-Based Composites: Materials, Mechanical Properties and Performance*, Taylor and Francis, Second edition.
- Brasileiro, C. (2014). Microstructural Characterization of Phases and Interfaces of Portland Cement Mortar Using High Resolution Microscopy, *Congresso Brasileiro de Engenharia*, pages 440–448.

- British Standards Institution. (1999). *Product and systems for the protection and repair of concrete structures - test methods - measurement of bond strength by pull off, BS EN 1542:1999*.
- Browne, R. D. (1972). Thermal movement of concrete. *London: Concrete Society*.
- BS EN 206-1:2000 Concrete - Part 1; Specification, performance, production and conformity. (2000).
- BSI (2005). BS EN 1504-3:2005: Products and systems for the protection and repair of concrete structures - definitions, requirements, quality control and evaluation of conformity - Part 3: Structural and non-structural repair.
- Carette, G. G., & Malhotra, V. M. (1983). Mechanical properties, durability and drying shrinkage of portland cement concrete incorporating silica fume. *Cement, Concrete and Aggregates, vol.5, no., pp.3-13*.
- Carlswärd, J. (2006). *Shrinkage cracking of steel fibre reinforced self compacting concrete overlays. test methods and theoretical modeling*. PhD Thesis, Lulea University of Technology Sweden.
- Centre for Civil Engineering Research Codes and Specifications. (1990). *Determination of bond strength of mortars of concrete, CUR Recommendation 20*, Gouda, the Netherlands.
- Chilwesa, M., & Beushausen, H. (2012). Assessing The Age At Cracking Of Concrete Repair Mortars/Overlays Subjected To Restrained Drying Shrinkage. Masters Thesis, University of Cape Town.
- Cong, X., Gong, S., Darwin, D., & McCabe, S. L. (1990). Role of Silica Fume in compressive strength of cement paste, mortar and concrete, Technical Report University of Kansas Center for Research, Inc.
- Courard, L., Piotrowski, T., & Garbacz, A. (2014). Near-to-surface properties affecting bond strength in concrete repair. *Cement and Concrete Composites, 46*, pages 73–80.
- Crosswell, S. (2009). Sand-cement - mortars, plasters and screeds. In Owens, G., editor, *Fulton's Concrete Technology*, chapter 26, pages 381–392. Cement & Concrete Institute, Ninth edition.

- DANSK-Standard (2004). Repair of Concrete Structures to EN 1504. Elsevier.
- Dawood, E. T. and Ramli, M. (2011). High strength characteristics of cement mortar reinforced with hybrid fibres. *Construction and Building Materials*, 25(5), 2240–2247.
- Draft report, Bahrain: The Concrete Society Bahrain and the Bahrain Society of Engineers (2000). *Guide to the maintenance and repair of reinforced concrete structures in the Arabian Peninsula*.
- Drysdale, R.G., and Gazzola, E. A. (1985). Influence of mortar properties on the tensile bond strength of brick masonry. In *In Proceedings of the 7th International Brick Masonry Conference, Melbourne, Australia*, (pp. 927–938.). Brick Development Research Institute and University of Melbourne, Melbourne, Australia.
- Emmons, E. H., Vaysburd, A. M., and Mac-Donald, J. (1993). “A rational approach to durable concrete repairs.” *Concrete International*, 15(9), 40–45.
- Emmons, P. H., & Vaysburd, A. M. (1995a). Performance criteria for concrete repair materials, Phase I. *Performance Criteria for Concrete Durability*.
- Emmons, P. H., & Vaysburd, A. M. (1995b). Performance Criteria for Concrete Repair Materials, Phase II Field Studies, pages 15–18.
- Emmons, P., & Sordyl, D. (2006). The state of the concrete repair industry, and a vision for its future. *Concrete Repair Bulletin*, pages 7–14.
- Fagerlund, G. (2004). *REHABCON Manual - Strategy for Maintenance and Rehabilitation in Concrete Structures*.
- Fidjestol, P. and Lewis, R. (1998). *Microsilica as an addition, Lea's Chemistry of Cement and Concrete*,. (L. Editor, P.C. Hewlett & Arnold, Eds.) (4th ed.).
- Filho, R. D. T., Ghavami, K., Sanjuan, M. A., and England, G. L. (2005). Free, restrained and drying shrinkage of cement mortar composites reinforced with vegetable fibres. *Cement and Concrete Composites*, 27(5), 537–546.
- Fowler, D. W., & Trevino, M. (2011). Overlay Design Process. In Bissonnette, B., Courard, L.,

- Fowler, D. W., and Granju, J.-L., editors, *Bonded Concrete materials overlays for repair, the Lining or strengthening of slabs or pavements.*, Volume 3, Chapter 2, Pages 5-16. Springer Netherlands
- Freudenthal, A. M. (1950). The inelastic behaviour of engineering materials and structures. *Wiley, New York.*
- Fujiwara, H., Maruoka, M., Kawato, T., Sugawara, T., Yoshikawa, K., Abe, T., ... Kasahara, H. (2016). Development of new types of repair materials by imparting thixotropic properties. In M. Grantham (Ed.), *Concrete Solutions: Proceedings of Concrete Solutions, 6th International Conference on Concrete Repair*. Thessaloniki, Greece: CRC Press.
- Garcia-Salinas, M. J., & Donald, A. M. (2010). Use of Environmental Scanning Electron Microscopy to image poly(N-isopropylacrylamide) microgel particles. *Journal of Colloid and Interface Science*, 342(2), 629–635.
- Ghali, A, Favre, R. & Elbadry, M. (2006). *Concrete Structures: Stresses and Deformations. Analysis and Design for Sustainability*, Third Edition.
- Ghezal, A. F. and Assaf, G. J. (2014). Restrained Shrinkage Cracking of Self-Consolidating Concrete. *Journal of Materials in Civil Engineering*, 27(10):04014266.
- Gillmer, M. (2012). Investigating repair mortars containing superabsorbent polymers as a method of internal curing to improve concrete patch repair performance. Masters Thesis. University of Cape Town.
- Gilbert, R.I. 1988. Time Effects in Concrete Structures. Netherlands: ELSEVIER.
- Granju, J. L (2001). Debonding of Thin Cement Based Overlays, *Journal of Materials in Civil Engineering*, 13(2): 114–120.
- Grieve, G. R. . (1991). The influence of two South African fly ashes on engineering properties of concrete. University of the Witwatersrand.
- Grzybowski, M. & Shah, S. P. (1990). Shrinkage cracking of fibre-reinforced concrete. *ACI Materials Journal*, 87(2), pages 138-148.
- Hammer, T. A. (1999). Test methods for linear measurement of autogenous shrinkage before

- setting. In: E. Tazawa, Ed. *Autogenous Shrinkage of Concrete*. New York, United States of America: E&FN Spon and Routledge, 143–154.
- Harrell, S., Joy, W., & Fay, K. Von. (2017). *Evaluation of Packaged Concrete Repair Materials - Scoping Study* (Vol. 01).
- Holl, C. H., & O'Connor, S. A. (1997). Cleaning and preparing concrete before repair. *Concrete International*, 19, 60–63.
- Holt, E. E. (2001). Early age autogenous shrinkage of concrete. *VTT Publications*, (446), 2–184.
- Jacobs, J. (2006). Current industry practice, research and repair. In Grantham, M. G., Jaubertie, R. M., and Lanos, C., editors, *Concrete Solutions: Proceedings of the Second International Conference, June 2006, St Malo, France*, 16–24. IHS BRE Press.
- Johansen, R. (1981). Silica in Concrete, *Report 6: Long term effects*, FCB/SINTEF Norwegian Institute of Technology, Trondheim, Norway. (Report STF65 A81031)
- Kalwane, U. B., & Dahake, A. G. (2015). Effect of Polymer Modified Fibers on Strength of Concrete, *Journal of Polymer & Composites*. Volume 3, Issue 1, pages 15-24.
- Kosmatka, S., & L.wilson, M. (2003). *Design and Control of Concrete Mixtures*. The guide to applications, methods, and materials. 15th Edition. Portland Cement Association.
- Laurence, O., Bissonnette, B., Pigeon, M. & Rossi, P. (2000). Effect of steel macro fibers on cracking of thin repairs. In: *Proceedings of the 5th International RILEM Symposium on Fibre-Reinforced Concretes (BEFIB 2000)*. Lyon, France: Sept 13-15, 213-222.
- Lukovic, M. (2016). Influence of interface and strain hardening cementitious composite (SHCC) properties on the performance of concrete repairs. PhD thesis, Delft University of Technology.
- Mangat, P. S., & O'Flaherty, F. J. (2000). Influence of elastic modulus on stress redistribution and cracking in repair patches. *Cement and Concrete Research*, 30(1), pages 125–136.
- Masuku, C, Beushausen, H., & Moyo, P. (2008). Proposal of an experimental programme for determining tensile relaxation in bonded concrete overlays, In Alexander, M. G., Beushausen, H.-D., Dehn, F., and Moyo, P., editors, *Concrete Repair, Rehabilitation and Retrofitting II*:

- 2nd International Conference on Concrete Repair, Rehabilitation and Retrofitting, ICCRRR-2, 24-26 November 2008, Cape Town, South Africa, pages 369–370. CRC Press.
- Masuku, Crispin. (2009). Tensile Relaxation of Bonded Concrete Overlays. Master's Thesis, University of Cape Town.
- Matthews, S. (2007). CONREPNET: Performance-based approach to the remediation of reinforced concrete structures: Achieving durable repaired concrete structures. *Journal of Building Appraisal*, 3(1): 6–20.
- Mehta, P., Asselanis, J., Aitcin, P.-C. (2010). Effect of Curing Conditions on the Compressive Strength and Elastic Modulus of Very High-Strength Concrete. *Cement, Concrete and Aggregates*, 11(1):80.
- Mehta, P. K., & Monteiro, P. J. M. (2006). *Concrete: microstructure, properties, and materials*. McGraw-Hill, Third edition
- Mehta, P. K. (1997). Durability - Critical issues for the future. *Concrete International*, 27–33.
- Miller, M. (2005). Polymers in cementitious materials. *Rapra Technology Limited*.
- Mindess, S., Young, J. F., & Darwin, D. (2003). *Concrete*. Prentice Hall, Pearson Education, Inc. Upper Saddle River, NJ 07458. Second Edition
- Mukheibir, P. V. (1990). *The deformation properties of concrete with classified Lethabo fly ash*. Masters Thesis, University of Cape Town.
- Naderi, M., Cleland, D., and Long, A. E. (1986). Insitu Test Methods for Repaired Concrete Structures. In Sasse, H., editor, *Adhesion between Polymers and Concrete / Adh'esion entre polym'eres et b'eton - Bonding, Protection, Repair. Proceedings of an International Symposium Organised by RILEM Technical Committee 52 - Resin Adherence to Concrete and Laboratoire Central Des Pont*, 19(6), 707–718.
- Nahlawi, K., & Paul, J. H. (2016). Evolution of ACI 562 Code — Part 9. Interface bond provisions in ACI 562-16 *Concrete International* 39(11), pages 52-56.
- Neville, A. M. (2011). *Properties of Concrete*. *Journal of General Microbiology*, 5th Edition. Pearson Education Limited

- Ohama, Y. (1995). *Handbook of Polymer-Modified Concrete and Mortars: Properties and Process Technology*. Noyes Publications.
- Oluokun, F. A., Burdette, E. G., & Deatherage, J. H. (1990). Rates of development of physical properties of concrete at early ages. *Transportation Research Record*, (1284), 16–22.
- Paul, J. H. (2016). Navigating New Concrete Repair Standards, pages 10–12.
- Pierard, J., Pollet, V., & Cauberg, N. (2006). Mitigating autogenous shrinkage in HPC by internal curing using superabsorbent polymers. In *International RILEM Conference on Volume Changes of Hardened Concrete: Testing and Mitigation, Lyngby, Denmark*.
- Pigeon, M., & Saucier, F. (1992). Durability of repaired concrete structures. *Proceedings, International Symposium on Advances in Concrete Technology*, 741–773.
- Pigeon, M., & Bissonnette, B. (1999). Tensile Creep and Cracking Potential. *Concrete International*, pages 31–35.
- Powers, T. C. (1959). Cause and control of volume change. *Journal of the PCA Research and Development Laboratories*, 1(1), pages 29-39.
- Radlinska, A., Pease, B., & Weiss, J. (2007). A preliminary numerical investigation on the influence of material variability in the early-age cracking behavior of restrained concrete. *Materials and Structures*, 40(4), pages 375–386.
- Radlinska, Aleksandra, & Weiss, J. (2012). Toward the Development of a Performance-Related Specification for Concrete Shrinkage. *Journal of Materials in Civil Engineering*, 24(1):64–71.
- Reda Taha, M.M., and Shrive, N. G. (2000). Enhancing masonry bond using fly ash. In *Masonry International*, 14:9–17.
- Reiner, M. (1960). Deformation strain and flow. *H.K. Louis and Co., Ltd.*
- Rixom, R., & Mailvaganam, N. (1999). *Chemical Admixtures for Concrete*. E. & FN Spon Ltd, Third Edition.
- SABS (2006a). SANS 5863: Concrete Tests - compressive strength of hardened concrete. SABS Standards Division.

- SABS (2006b). SANS 6085: Concrete tests - Initial drying shrinkage and wetting expansion of concrete. SABS Standards Division.
- Salvoldi, B. G., Beushausen, H., & Alexander, M. G. (2015). Oxygen permeability of concrete and its relation to carbonation. *Construction and Building Materials*, 85, pages 30–37.
- Sayahi, F., & Emborg, M. (2017). Effect of Water-Cement Ratio on Plastic Shrinkage Cracking in Self Compacting Concrete, XXIII Nordic Concrete Research Symposium
- Sellevoid, E.J. and Nilsen, T. (1987). Condensed silica fume in concrete: a world review. Supplementary cementing materials for concrete. *Ed. Y.M. Malhotra, Ottawa: CANMET, Chapter 3.*
- Shah, H. R., & Weiss, J. (2006). Quantifying shrinkage cracking in fiber reinforced concrete using the ring test. *Materials and Structures/Materiaux et Constructions*, 39(293), pages 887–899.
- Silfwerbrand, J., & Petersson, Ö. (1993). Thin concrete inlays on old concrete roads. *5th International Conference on Concrete Pavement Design & Rehabilitation*, PP. 255-260.
- Singh, H., & Bansal, S. (2015). Effect Of Silica Fume On The Strength Of Cement Mortar, 623–627.
- Soufi, A., Mahieux, P.-Y., Aït-Mokhtar, A., and Omiri, O. (2016). Influence of polymer proportion on transfer properties of repair mortars having equivalent water porosity. *Materials and Structures*, 49.
- Sprinkel, M., & Ozyildirim, C. (2000). *Evaluation Of High Performance Concrete Overlays Placed On Route 60 Over Lynnhaven Inlet In Virginia*. Virginia Transportation Research Council.
- Stefanidou, M., & Pavlidou, E. (2018). Scanning Mortars to Understand the Past and Plan the Future for the Maintenance of Monuments. *Scanning*, 2018, pages 1–8.
- Sugo, H., Page, A. W., & Lawrence, S. (2008). Influence of age on masonry bond strength and mortar microstructure This article is one of a selection of papers published in this Special Issue on Masonry. *Canadian Journal of Civil Engineering*, 34(11), pages 1433–1442.
- Takuwa, I., Shitou, K., Kamihigashi, Y., Nakashima, H. and Yoshida, A. (2000). The application

- of water-jet technology to surface preparation of concrete structure,. *Journal of Jet Flow Engineering*, (17(1)), pages 29–40.
- Tazawa, E.-I., Miyazawa, S., and Kasai, T. (1995). Chemical shrinkage and autogenous shrinkage of hydrating cement paste. *Cement and Concrete Research.*, 25(2), 288-292.
- The Concrete-Society. (2003). Concrete Society Technical Report No. 22 - Non structural cracks in concrete. In *Concrete Repair Manual*, volume 1 pages 507-551. American Concrete Institute and Building Research Establishment and The Concrete Society and The International Concrete Repair Institute. Second Edition.
- Thomas James Dittmer. (2013). *The Effect of Aggregate on the age at Cracking of Bonded Concrete Overlays Subjected to Restrained Deformation*. Masters Thesis, University of Cape Town.
- Tilly, G. P., & Jacobs, J. (2007). *Concrete Repairs. Performance in Service and Current Practice*. IHS BRE Press.
- Torney, C., Forster, A. M., & Szadurski, E. M. (2014). Specialist “restoration mortars” for stone elements: A comparison of the physical properties of two stone repair materials. *Heritage Science*, 2(1), pages 1–12.
- Toutanji, H. A., Liu, L., & El-Korchi, T. (2006). The role of silica fume in the direct tensile strength of cement-based materials. *Materials and Structures*, 32(3), pages 203–209.
- Troxell, G. E., Raphael, J. M., & Davis, H. E. (1958). Long-time creep and shrinkage tests of plain and reinforced concrete. *Proceedings American Society for Testing and Materials*, vol.58, pp.1101-1120.
- Turatsinze, A., Granju, J. L., Sabathier, V., & Farhat, H. (2005). Durability of bonded cement-based overlays: Effect of metal fibre reinforcement. *Materials and Structures*, 38(277), pages 321–327.
- Uys, A. J. (1983). The influence of fly ash on the strength, elastic modulus, shrinkage and creep of concrete made with Cape Town aggregates, with particular reference to alkali-aggregate reaction. Master’s thesis, University of Cape Town.

- Vaysburd, A. M., Consulting, V., Emmons, P. H., Group, S., & Pigeon, M. (2001). Some Aspects of Evaluating Cracking Sensitivity of Repair Materials. *RILEM Proceedings PRO 23 "Early Age Cracking in Cementitious Systems—EAC'01*, pages 169–185.
- Weiss, W. J. (2002). Restrained shrinkage cracking: the role of shrinkage reducing admixtures and specimen geometry. *Materials and Structures*, 35(246), 85–91.
- Wittmann, F. (2002). Crack formation and fracture energy of normal and high strength concrete. *Sadhana*, 27(4):413–423.
- Yurdakul, E., Taylor, P. C., Ceylan, H., & Bektas, F. (2013). Effect of Water-to-Binder Ratio, Air Content, and Type of Cementitious Materials on Fresh and Hardened Properties of Binary and Ternary Blended Concrete. *Journal of Materials in Civil Engineering*, 26(6),

Appendix A: Testing procedure

The standard procedures followed during the testing for the various material properties are summarised in the subsequent subsections.

A.1 Sieve analysis

The sieve analysis was done according to EN 13139:2002 and SANS 201:2008. The procedure for sieve analysis is hereby summarised.

- a) Sieves with the following openings - 4.75 mm, 2.36 mm, 1.18 mm; 0.60 mm, 0.30mm; 0.15 mm and 0.075 mm - were used. The sieves were nested in order of decreasing size of opening from top to bottom and 320 g of the sample placed on top of the sieve. The sample in the sieve was agitated using a mechanical sieve shaker for a period of five minutes.
- b) The mechanical sieve shaker was stopped. Thereafter, the sieves were removed from the shaker.
- c) Both the mass of material retained in a specific sieve as well as the mass of the sieve was measured using a balance and recorded.
- d) Thereafter, appropriate calculations were done to evaluate the grading of the various sand samples.

A.2 Compressive strength

Compressive strength tests were done to characterise the mortar mixes. These tests were done in accordance to SANS 5863:2006a. Care was taken to ensure that each specimen was tested immediately after its removal from the curing tank. A summary of the test procedure presented below.

- a) The surface water, grit and projecting fins on the cured $100 \times 100 \times 100$ mm cube specimens was removed.
- b) The mass of each cube was measured (to an accuracy of 1%) using an electronic balance.
- c) The loading surfaces on the loading platens of the compression testing were wiped clean.
- d) The test cube was positioned in the machine in such a manner that the load was applied on any of the smooth surfaces that is perpendicular to the direction of casting.

- e) The compression load was applied without shock continuously at a uniform rate that ranged between $0.3 \text{ MPa/s} \pm 0.1 \text{ MPa/s}$ until the specimen failed.
- f) The maximum load that was applied was recorded. Also, the appearance of the specimen at failure, any unusual features in the specimen during failure - if any - and the type of failure was recorded.

A.3 Elastic modulus

The static modulus of elasticity in compression was determined according to BS 1881: Part 121:1983. This procedure is hereby described.

- a) Three $100 \times 100 \times 100$ mm cubes were cast in conjunction with the elastic modulus specimens that were subsequently tested for compressive strength. The average compressive strength of these cubes was recorded.
- b) The ends of each cylindrical test specimen were made plane and perpendicular to the plane of the axis using a grinder. Utmost care was taken to ensure that specimens were tested within 1 hour after their removal from a curing tank.
- c) The diameter of each test specimen was measured using callipers to the nearest 0.25 mm by averaging two diameters measured at right angles to each other near the centre of the length of the specimen. The length of each specimen was also measured and recorded to the nearest 2.54 mm.
- d) LVDTs were attached to each specimen. Care was taken to ensure that the effective length of each gauge line is not less than three times the maximum size of the aggregate in the concrete or more than two thirds the height of the specimen.
- e) The specimens, with the strain measuring equipment attached, was placed on the lower platen of the testing machine. The axis of the specimen was carefully aligned with the centre of thrust of the spherically-seated upper bearing block.
- f) The data acquisition system of the stress and strains (via the LVDT readings) was switched on.
- g) A compressive stress of 0.5 MPa was applied to the machine and the load gradually increased at a rate of $0.6 \pm 0.4 \text{ MPa/s}$ until a stress equal to one-third of the average compressive strength of the cubes in (a).

- h) The load in the machine was released.
- i) Steps (d) and (e) were repeated twice and the corresponding stress and strains recorded.
- j) Specimens were thereafter loaded until failure and their compressive strength at failure recorded.
- k) The recorded stresses and their corresponding strains were used to calculate the secant modulus of elasticity of the specimens.

A.4 Drying shrinkage

The drying shrinkage tests were done in accordance with SANS 6085:2006b. A summary of the procedure is described below.

- a) The freshly-cast $100 \times 100 \times 200$ mm prism specimens in the mould were covered with an impervious plastic sheet and stored for 20 - 24 hours in a place that was free from vibration and in an atmosphere whose temperature varied between 22°C and 25°C and a relative humidity of at least 90%.
- b) The specimens were demoulded after 24 hours.
- c) The specimens were water cured for 28 days, after demoulding, in potable water maintained at a temperature that varied between 22°C to 25°C .
- d) The specimens were removed from the water bath after 28 days \pm 2 hours after demoulding. Excess water was wiped off.
- e) Strain targets at a gauge length of 100 mm were affixed to two opposite faces in the longitudinal direction.
- f) The distance between the strain targets was measured immediately to the nearest 2 μm . The specimens were also marked such that one end was always oriented in the same direction in relation to the strain gun.
- g) The specimens were transferred to an environmental room whose temperature and relative humidity were maintained at $23 \pm 2^{\circ}\text{C}$ and $50 \pm 4\%$ respectively. These environmental conditions corresponded to the one for ring tests.

- h) The distance between the strain targets within any one face of a specimen was measured using the strain gun every two days. The measurement for shrinkage was monitored daily over a duration of 60 days.

A.5 Restrained shrinkage

The restrained shrinkage cracking was done according to ASTM-C1581, but with modifications owing to lack of equipment such as strain gauges. The test procedure is summarised as follows:

- a) The freshly cast mortar was placed into a mould in two approximately equal layers. Each layer was rodded 75 times using a 10 mm diameter rod and thereafter vibrated on a vibrating table to consolidate it. Flowable mixes were not vibrated. Three specimens were made from each mix under investigation.
- b) The top of each specimen was levelled after consolidation using a trowel. Finishing was done with minimum manipulation necessary to achieve a flat surface. Any fresh mortar that had spilled inside the steel ring or outside was removed so that the base remained clean. The test specimens were thereafter transferred to the testing environment within 10 minutes after the completion of casting;
- c) The specimens were demoulded after 1 day, and then transferred to an environmental room that was maintained at a temperature of 23 ± 2 °C and relative humidity of $50 \pm 4\%$.
- d) Any loose materials from the top surface of the specimen, if present, was removed gently;
- e) The top surface of the specimen was sealed using paraffin wax using a 38 mm wide brush. Care was taken to ensure that the outer circumference of the specimen is not coated with paraffin wax.
- f) The mortar specimens were monitored three times a day - at six-hour intervals for cracking (i.e., at 09h00, 15h00 and 21h00) - for cracking. The duration of monitoring a specimen began immediately after casting and ended upon its cracking.
- g) The crack width of the cracked specimens was measured using a microscope. The crack measurements from a single specimen were taken 10 mm from its top, at its mid-height and 10 mm from the bottom of each crack.

A.6 Durability indexes

A.6.1 Oxygen Permeability Index (OPI)

The oxygen permeability index is defined as the negative log of the coefficient of permeability. The test was conducted to assess the durability of the repair mortars with regard to the Performance-based durability testing, design and specification in South Africa. The test method consists of measuring the pressure decay of oxygen passed through a 28 to 30 mm thick slice of a (typically) 68 to 70-mm diameter core of concrete placed in a falling head permeameter (Alexander & Beushausen, 2009). Concrete samples were initially preconditioned at 50 °C to ensure uniformly low moisture contents at the start of the test. The disc specimens were cored from 7 and 28 day cured 100 x 100 x 100 mm mortar cubes.

The test evaluates the overall micro and macrostructure of the outer surface of the cast concrete and is predominantly sensitive to macro-voids and cracks which provide short-circuit routes for the permeating gas. It is therefore useful to assess the compaction, presence of bleed voids and channel and the degree of interconnectedness of the pore structure (Salvoldi et al., 2015).

A.6.2 Water Sorptivity Index (WSI)

A linear relationship is observed when the mass of water is plotted against the square root of time, and the sorptivity of the concrete is determined from the slope of the straight line produced. The water sorptivity test has been found to be very sensitive to the nature and extent of early curing of the cover concrete, and can thus be used to assess construction quality (Alexander & Beushausen, 2009).

The same specimens that were used in the oxygen permeability test were used in the water sorptivity test. The circular sides of the core were sealed using a tape to ensure unidirectional absorption from the bottom (usually exposed) face. The concrete samples were exposed to water that was slightly above the bottom edge of the specimen and a maximum of 2m up the side of the specimen with the test surface facing downward. At regular time intervals, the specimens were removed from the water and the mass of water absorbed determined using an electronic balance with an accuracy of 0.01 g. Measurements were stopped after 25 minutes, before saturation was reached and the concrete was then vacuum-saturated in water to determine the porosity.

A.6.3 Chloride Conductivity Index (CCI)

The chloride conductivity was determined by measuring the current flowing through the concrete specimen. Test results are presented as mean values from a total of 4 samples per specimen type and test parameter. Outlying values were identified based on statistical analysis and excluded from determination of mean values. The test apparatus consists of a two-cell conduction rig in which concrete core samples of 70 ± 2 mm diameter with a thickness of 30 ± 2 mm are exposed on either side to a 5M NaCl chloride solution. The core samples are preconditioned before testing to standardise the pore water solution (oven dried at 50°C followed by 24 hours vacuum saturation in a 5M NaCl chloride solution). The movement of chloride ions occurs due to the application of a 10 V potential difference. The chloride conductivity was determined by measuring the current flowing through the concrete specimen. The apparatus allows for rapid testing under controlled laboratory conditions (Alexander & Beushausen, 2009).

A.7 Tensile relaxation

The relaxation coefficient ψ (%) was obtained from the following equation:

$$\psi = 100 \times \left(1 - \frac{\sigma_t}{\sigma_o}\right)$$

Where,

σ_o – Original stress at time of loading (MPa)

σ_t – Remaining stress after 48 hours (MPa)

Appendix B: Detailed test results

The results from the experiments detailed in Chapter 3 are provided herein. The compressive strength, tensile strength, elastic modulus, drying shrinkage, pull off bond test, ring tests, durability (OPI, WSI & CCI) tests, tensile relaxation tests, EDS and grading analysis tests are provided from section B1 to B10 respectively. The following terminology has been used in the tables presented; Comp. = compressive strength; Avg. = average; Std. Dev. = standard deviation.

B.1 Compressive strength

The compressive strength results for 3, 7 and 28 days conducted on 100 x 100 x 100 mm cubes as stated in section 3.6.1 are provided herein.

Table B.1: 3-day compressive strength results

Mix ID	Cube	Mass (kg)	Density (kg/m ³)	Load (kN)	Comp. strength (MPa)	Avg. comp. (MPa)	Sdv. Dev
PS	1	1.830	1774	251	25.1	25.5	0.4
	2	1.840	1784	255	25.5		
	3	1.790	1769	259	25.9		
PFS	1	2.075	2064	315	31.5	31.7	0.3
	2	2.070	2046	320	32.0		
	3	2.100	2074	316	31.6		
SA	1	2.325	2326	627	61.7	62.5	1.6
	2	2.340	2300	620	61.5		
	3	2.350	2369	645	64.4		
S1	1	2.035	1891	289	28.1	29.9	2.3
	2	1.995	1936	294	29.0		
	3	2.080	1975	328	32.5		
S2	1	2.285	2160	347	34.3	35.1	1.1
	2	2.215	2082	350	34.5		
	3	2.185	2115	369	36.4		
G1	1	2.120	2086	418	41.1	41.2	2.7
	2	2.135	2051	454	44.0		
	3	2.175	2073	404	38.6		
PF1	1	2.110	2023	298	28.8	28.8	1.7
	2	2.115	2039	280	27.1		
	3	2.050	2023	308	30.5		
G2	1	2.150	2123	366	36.4	36.0	1.0
	2	2.250	2155	360	34.8		
	3	2.235	2180	375	36.7		
P1	1	1.825	1727	258	24.8	24.8	0.5
	2	1.870	1788	262	25.2		
	3	1.820	1761	250	24.3		
PF2	1	2.125	2067	348	34.4	34.2	1.9
	2	2.220	2096	374	36.0		
	3	2.100	2078	324	32.2		
P2	1	1.860	1830	104	10.3	9.9	0.4
	2	1.845	1816	102	10.1		
	3	1.900	1791	100	9.5		
A	1	2.290	2222	260	25.3	25.6	1.8
	2	2.310	2224	284	27.5		
	3	2.290	2212	246	23.9		

Table B.2: 7-day compressive strength test results

Mix ID	Cube	Mass (kg)	Density (kg/m ³)	Load (kN)	Comp. strength (MPa)	Avg. comp. (MPa)	Sdv. Dev
PS	1	1.750	1730	316	31.6	30.5	1.9
	2	1.770	1744	283	28.3		
	3	1.795	1754	315	31.5		
PFS	1	2.105	2041	362	36.2	36.7	0.6
	2	2.135	2001	374	37.4		
	3	2.120	2008	366	36.6		
SA	1	2.370	2343	720	71.4	72.4	1.2
	2	2.355	2356	722	72.0		
	3	2.395	2305	742	73.7		
S1	1	2.085	2018	324	32.2	32.6	1.3
	2	2.030	1959	317	31.6		
	3	2.020	1948	345	34.1		
S2	1	2.170	2178	365	36.7	38.0	2.2
	2	2.140	2195	395	40.6		
	3	2.235	2155	380	36.8		
G1	1	2.110	2085	536	53.4	50.2	2.8
	2	2.150	2034	508	48.9		
	3	2.235	2086	510	48.2		
PF1	1	2.130	2020	368	35.0	35.5	0.4
	2	2.130	2012	374	35.8		
	3	2.080	2008	364	35.6		
G2	1	2.230	2197	464	46.2	45.7	1.7
	2	2.215	2191	468	47.1		
	3	2.220	2148	448	43.7		
P1	1	1.865	1736	260	24.2	26.4	1.9
	2	1.845	1775	280	27.0		
	3	1.820	1752	290	27.9		
PF2	1	2.210	2076	586	56.3	56.4	2.2
	2	2.145	2076	596	58.5		
	3	2.195	2135	558	54.2		
P2	1	1.875	1772	152	14.5	14.0	0.5
	2	1.895	1792	140	13.5		
	3	1.855	1827	142	14.1		
A	1	2.195	2154	390	38.4	37.3	1.3
	2	2.190	2132	384	37.5		
	3	2.420	2283	376	35.9		

Table B.3: 28-day compressive strength test results

Mix ID	Cube	Mass (kg)	Density (kg/m ³)	Load (kN)	Comp. strength (MPa)	Avg. comp. (MPa)	Sdv. Dev
PS	1	1.865	1780	374	35.9	34.5	1.2
	2	1.875	1695	374	34.2		
	3	1.845	1708	362	33.6		
PFS	1	2.120	2079	452	44.5	42.6	1.9
	2	2.105	2079	432	42.7		
	3	2.085	2070	410	40.7		
SA	1	2.420	2305	895	86.0	88.4	2.1
	2	2.335	2353	880	89.3		
	3	2.360	2317	910	89.8		
S1	1	2.100	2098	384	38.4	36.6	2.1
	2	2.085	1999	355	34.3		
	3	2.080	2000	382	37.0		
S2	1	2.210	2195	486	48.6	49.5	2.0
	2	2.195	2187	516	51.8		
	3	2.125	2167	470	48.0		
G1	1	2.145	2054	554	53.8	54.4	2.2
	2	2.150	2097	576	56.8		
	3	2.120	2042	542	52.7		
PF1	1	2.115	2061	530	52.0	52.6	1.3
	2	2.145	2067	534	51.7		
	3	2.175	2076	562	54.0		
G2	1	2.270	2170	598	57.9	55.9	1.9
	2	2.250	2190	568	55.8		
	3	2.235	2181	550	54.1		
P1	1	1.785	1734	363	35.3	34.8	1.0
	2	1.860	1779	368	35.4		
	3	1.870	1763	354	33.7		
PF2	1	2.270	2147	670	63.7	64.9	1.1
	2	2.150	2067	680	65.7		
	3	2.125	2087	664	65.2		
P2	1	1.880	1844	200	19.6	20.2	0.9
	2	1.910	1872	200	19.7		
	3	2.000	1926	219	21.2		
A	1	2.305	2228	584	56.9	55.3	1.4
	2	2.380	2295	564	54.5		
	3	2.245	2187	554	54.3		

B.2 Tensile strength

The direct tensile strength results for 7 and 28 days conducted on dog bone specimens as stated in section 3.6.2 are provided herein.

Table B.4: 7-day direct tensile strength test results

Mix ID	Dog Bone	Load (N)	Tensile strength (MPa)	Avg. tensile strength (MPa)	Sdv. Dev
PS	1	2283	1.4	2.1	0.4
	2	2111	1.3		
	3	3099	1.9		
PFS	1	4139	2.6	3.4	0.3
	2	3708	2.3		
	3	4533	2.8		
SA	1	5854	3.7	5.1	0.7
	2	7070	4.4		
	3	5463	3.4		
S1	1	3186	2.0	2.4	0.2
	2	2765	1.7		
	3	2869	1.8		
S2	1	1145	0.7	1.3	0.3
	2	1653	1.0		
	3	1732	1.1		
G1	1	3445	2.2	3.0	0.1
	2	3669	2.3		
	3	3672	2.3		
PF1	1	3014	1.9	2.6	0.1
	2	3189	2.0		
	3	3189	2.0		
G2	1	3723	2.3	3.1	0.3
	2	4157	2.6		
	3	3395	2.1		
P1	1	3089	1.9	2.3	0.2
	2	2780	1.7		
	3	2534	1.6		
PF2	1	5166	3.2	4.2	0.5
	2	5554	3.5		
	3	4338	2.7		
P2	1	1906	1.2	1.7	0.1
	2	2190	1.4		
	3	2050	1.3		
A	1	3559	2.2	2.9	0.1
	2	3617	2.3		
	3	3350	2.1		

Table B.5: 28-day direct tensile strength test results

Mix ID	Dog Bone	Load (N)	Tensile strength (MPa)	Avg. tensile strength (MPa)	Sdv. Dev
PS	1	3553	2.2	3.1	0.5
	2	4390	2.7		
	3	3352	2.1		
PFS	1	4518	2.8	4.1	0.3
	2	5241	3.3		
	3	5096	3.2		
SA	1	5492	3.4	4.7	0.1
	2	5647	3.5		
	3	5846	3.7		
S1	1	2850	1.8	2.1	0.3
	2	2401	1.5		
	3	2278	1.4		
S2	1	2463	1.5	1.7	0.5
	2	1431	0.9		
	3	2306	1.4		
G1	1	4930	3.1	3.8	0.3
	2	4314	2.7		
	3	4411	2.8		
PF1	1	4198	2.6	4.1	0.5
	2	5354	3.3		
	3	5299	3.3		
G2	1	5056	3.2	3.8	0.3
	2	4244	2.7		
	3	4512	2.8		
P1	1	4300	2.7	3.0	0.5
	2	3052	1.9		
	3	3338	2.1		
PF2	1	4762	3.0	4.1	0.1
	2	4879	3.0		
	3	5093	3.2		
P2	1	2260	1.4	1.8	0.1
	2	1925	1.2		
	3	2121	1.3		
A	1	4863	3.0	3.6	0.4
	2	3808	2.4		
	3	4196	2.6		

B.3 Elastic modulus

The elastic modulus test results for 7 and 28 days as stated in Section 3.6.4 are provided herein.

Table B.6: 7-day elastic modulus test results

Mix ID	Specimen	Elastic Modulus (GPa)	Avg. Elastic Modulus (GPa)	Sdv. Dev.
PS	1	17.65	17.70	0.5
	2	18.18		
	3	17.27		
PFS	1	21.33	20.83	1.2
	2	19.43		
	3	21.74		
SA	1	37.08	36.43	1.5
	2	37.45		
	3	34.75		
S1	1	25.21	24.63	0.9
	2	23.54		
	3	25.13		
S2	1	30.51	29.86	0.7
	2	29.99		
	3	29.07		
G1	1	25.66	25.74	1.1
	2	24.64		
	3	26.93		
PF1	1	21.85	20.85	0.9
	2	20.48		
	3	20.22		
G2	1	25.25	24.00	1.1
	2	23.12		
	3	23.62		
P1	1	17.97	18.06	0.1
	2	18.01		
	3	18.19		
PF2	1	28.66	27.35	1.7
	2	25.49		
	3	27.91		
P2	1	9.74	9.62	0.3
	2	9.26		
	3	9.86		
A	1	31.22	31.64	0.4
	2	32.09		
	3	31.60		

Table B.7: 28-day elastic modulus test results

Mix ID	Specimen	Elastic Modulus (GPa)	Avg. Elastic Modulus (GPa)	Sdv. Dev.
PS	1	19.81	19.65	0.2
	2	19.73		
	3	19.40		
PFS	1	25.76	25.23	1.0
	2	25.87		
	3	24.06		
SA	1	35.85	37.16	1.2
	2	38.12		
	3	37.51		
S1	1	25.58	25.54	0.9
	2	24.64		
	3	26.39		
S2	1	29.66	30.80	1.0
	2	31.52		
	3	31.23		
G1	1	26.21	27.68	1.3
	2	28.79		
	3	28.05		
PF1	1	25.11	25.12	0.1
	2	25.25		
	3	25.00		
G2	1	28.67	29.41	0.7
	2	29.67		
	3	29.89		
P1	1	17.54	17.83	0.4
	2	17.64		
	3	18.32		
PF2	1	35.18	35.93	1.6
	2	37.72		
	3	34.90		
P2	1	9.83	9.74	0.1
	2	9.58		
	3	9.80		
A	1	34.17	33.21	1.7
	2	34.24		
	3	31.22		

B.4 Drying shrinkage

The drying shrinkage results obtained from the drying shrinkage tests as stated in Section 3.6.5 are provided herein.

Table B.8: Drying shrinkage test results

Age (days)	Drying shrinkage (micro-strains)											
	PS	PFS	SA	S1	S2	G1	PF1	G2	P1	PF2	P2	A
0	0	0	0	0	0	0	0	0	0	0	0	0
1	7	27	13	95	138	75	13	45	40	0	47	20
2	90	58	25	148	252	137	22	108	113	0	90	87
3	142	78	112	288	260	207	107	148	203	10	120	103
4	200	120	158	333	320	200	140	187	198	27	160	103
5	207	130	155	340	340	207	185	195	242	18	192	132
6	212	160	195	373	340	295	187	222	280	37	235	152
7	230	195	216	395	348	340	200	228	355	60	282	172
8	248	198	210	405	372	365	210	230	382	65	338	185
9	347	213	211	433	370	398	215	250	385	68	390	198
10	382	260	265	480	402	430	225	260	420	75	420	198
11	398	308	275	483	410	493	232	263	477	85	450	198
12	435	310	286	512	410	502	263	263	483	103	476	203
13	475	338	296	510	420	522	270	263	490	112	545	213
14	537	320	288	512	428	503	265	263	498	118	593	213
15	527	330	288	510	433	518	277	263	512	118	653	213
16	540	373	280	523	440	543	285	267	523	125	685	223
17	577	400	288	537	437	575	295	260	522	125	788	233
18	595	405	298	545	437	600	298	253	552	125	831	255
19	620	398	300	552	440	608	298	265	552	135	871	255
20	640	405	293	568	455	633	300	265	588	135	945	260
21	655	412	285	581	450	632	290	265	627	138	1035	267
22	668	428	291	583	460	655	290	278	627	163	1098	277
23	727	443	281	586	470	645	300	278	627	172	1148	287
24	727	460	300	573	477	655	320	278	650	172	1205	297
25	723	485	316	586	477	645	332	278	675	172	1283	297
26	763	477	320	586	478	665	347	295	695	175	1324	297
27	760	470	320	580	478	678	353	295	680	173	1356	297

Age (days)	Drying shrinkage (micro-strains)											
	PS	PFS	SA	S1	S2	G1	PF1	G2	P1	PF2	P2	A
28	767	498	328	581	478	685	362	295	688	173	1426	293
29	767	500	316	590	478	705	372	307	692	173	1499	300
30	785	473	326	615	485	761	388	312	705	160	1558	308
31	793	480	316	635	475	755	388	307	718	167	1624	305
32	817	485	316	638	478	758	392	303	760	173	1676	327
33	802	485	316	640	478	761	402	315	790	185	1716	322
34	778	495	331	645	475	771	395	315	810	187	1794	327
35	787	508	346	655	478	791	405	318	810	190	1843	327
36	805	535	345	648	477	783	420	318	803	190	1901	330
37	795	543	345	648	475	783	430	330	810	187	1919	330
38	810	535	350	645	478	811	428	355	831	187	1936	330
39	832	543	351	653	475	803	432	355	830	192	1949	330
40	840	545	351	661	478	821	430	350	853	192	1996	330
41	807	550	351	680	478	841	425	352	876	192	2028	330
42	807	552	350	683	475	841	430	365	870	192	2098	330
43	822	517	350	688	478	868	435	365	863	192	2129	330
44	850	512	350	700	475	886	442	367	883	192	2159	330
45	850	513	350	713	478	886	443	363	891	192	2191	330
46	828	520	350	705	478	878	443	367	900	192	2237	330
47	855	520	350	708	478	891	465	362	923	192	2282	330
48	855	522	350	701	475	901	450	362	923	192	2319	330
49	850	522	350	703	478	905	450	363	923	192	2359	330
50	858	530	350	726	478	905	458	377	930	192	2409	330
51	887	543	350	745	475	896	475	377	923	192	2441	330
52	880	557	350	756	483	930	485	377	923	192	2471	330
53	877	563	350	753	478	950	485	377	923	192	2502	332
54	882	553	350	741	475	936	485	382	923	192	2531	332
55	877	552	350	750	480	940	488	377	923	192	2561	332
56	877	568	350	758	483	955	492	377	923	192	2591	332
57	892	572	350	758	483	946	492	377	923	192	2617	332
58	892	572	343	780	483	946	492	377	923	192	2644	340
59	903	587	350	780	487	946	502	377	923	192	2684	340
60	905	590	350	785	495	946	502	377	923	192	2697	340

B.5 Bond strength test

The pull off bond strength test results obtained from the drying shrinkage tests as stated in Section 3.6.7 are provided herein.

Table B.9: 7 day pull off bond strength test results

Mix ID	Specimen	Load (KN)	Tensile Bond (MPa)	Failure Location	Avg. Tensile Bond (MPa)	Sdv. Dev.
PS	1	1.77	0.77	Substrate	1.00	0.2
	2	2.29	1.00	Substrate		
	3	2.81	1.23	Substrate		
PFS	1	1.38	1.38	Interface	1.57	0.5
	2	2.74	1.20	Interface		
	3	4.91	2.14	Interface		
SA	1	3.31	1.69	Substrate	1.88	0.2
	2	3.65	1.86	Substrate		
	3	4.13	2.10	Substrate		
S1	1	3.39	1.48	Substrate	2.00	0.5
	2	5.04	2.20	Substrate		
	3	5.32	2.32	Substrate		
S2	1	3.75	1.64	Substrate	1.72	0.1
	2	4.21	1.84	Interface		
	3	3.88	1.69	Substrate		
G1	1	3.19	1.62	Substrate	1.87	0.2
	2	3.77	1.92	Substrate		
	3	4.05	2.06	Substrate		
PF1	1	0.87	0.38	Interface	0.44	0.1
	2	1.28	0.56	Interface		
	3	0.87	0.38	Interface		
G2	1	4.49	1.96	Substrate	1.87	0.7
	2	5.72	2.50	Substrate		
	3	2.61	1.14	Substrate		
P1	1	3.36	1.71	Interface	1.47	0.2
	2	2.84	1.45	Interface		
	3	2.45	1.25	Interface		
PF2	1	3.94	1.72	Interface	1.71	0.7
	2	2.30	1.00	Substrate		
	3	2.42	2.42	Substrate		
P2	1	3.08	1.34	Interface	1.24	0.2
	2	3.08	1.34	Interface		
	3	2.39	1.04	Interface		
A	1	4.02	2.05	Overlay	2.23	0.2
	2	4.25	2.16	Overlay		
	3	4.87	2.48	Overlay		

Table B.10: 28- day pull off bond strength test results

Mix ID	Specimen	Load (KN)	Tensile Bond (MPa)	Failure Location	Avg. Tensile Bond (MPa)	Sdv. Dev.
PS	1	2.61	1.14	Interface	1.52	0.3
	2	3.69	1.61	Interface		
	3	4.12	1.80	Substrate		
PFS	1	5.16	2.25	Interface	2.33	0.1
	2	5.18	2.26	Substrate		
	3	5.69	2.48	Substrate		
SA	1	3.64	1.95	Substrate	2.36	0.8
	2	3.49	1.90	Substrate		
	3	6.34	3.23	Substrate		
S1	1	3.95	1.72	Interface	1.81	0.2
	2	3.82	1.67	Interface		
	3	4.70	2.05	Substrate		
S2	1	3.95	1.72	Interface	1.52	0.2
	2	3.63	1.58	Substrate		
	3	2.85	1.24	Substrate		
G1	1	3.23	1.64	Substrate	1.83	0.4
	2	4.43	2.26	Substrate		
	3	3.11	1.58	Substrate		
PF1	1	1.47	0.64	Interface	0.61	0.1
	2	1.23	0.54	Interface		
	3	1.46	0.64	Interface		
G2	1	4.38	1.91	Substrate	2.04	0.1
	2	4.79	2.09	Substrate		
	3	4.86	2.12	Substrate		
P1	1	3.17	1.61	Interface	2.11	0.4
	2	4.83	2.46	Interface		
	3	4.44	2.26	Interface		
PF2	1	3.90	1.70	Interface	2.21	0.5
	2	6.33	2.76	Substrate		
	3	4.99	2.18	Interface		
P2	1	3.11	1.36	Interface	1.72	0.3
	2	1.86	1.86	Interface		
	3	1.95	1.95	Interface		
A	1	5.27	2.68	Substrate	2.88	0.2
	2	5.57	2.84	Substrate		
	3	6.16	3.14	Substrate		

B.6 Restrained shrinkage

The results from the restrained shrinkage cracking tests as stated in Section 3.6.6 are provided herein.

Table B.11: Age at cracking for the restrained shrinkage test results

Mix ID	Ring	Age at Cracking (Days)		
		Measured	Mean	Std. Dev.
PS	1	6.00	7	1.2
	2	6.00		
	3	8.00		
PFS	1	7.00	7	0.6
	2	7.00		
	3	8.00		
SA	1	6.00	6	0.6
	2	6.00		
	3	7.00		
S1	1	3.00	3	0.0
	2	3.00		
	3	3.00		
S2	1	1.00	1	0.0
	2	1.00		
	3	1.00		
G1	1	2.00	2	0.6
	2	2.00		
	3	3.00		
PF1	1	5.00	5	0.6
	2	5.00		
	3	6.00		
G2	1	11.00	12	2.3
	2	11.00		
	3	15.00		
P1	1	8.00	8	0.6
	2	8.00		
	3	9.00		
PF2	1	4.00	5	0.6
	2	5.00		
	3	5.00		
P2	1	12.00	13	1.2
	2	12.00		
	3	14.00		
A	1	12.00	12	0.0
	2	12.00		
	3	12.00		

Table B.12: 14-day crack widths and crack area for the ring specimens

Mix ID	Ring	Crack Width (mm)			Crack Length (mm)		Crack Area (mm ²)
		Measured	Mean	Std. Dev.	Measured	Mean	
PS	1	1.80			158.0		171.46
	2	0.65	1.08	0.6	165.5	159.50	
	3	0.78			155.0		
PFS	1	0.94			166.5		130.68
	2	0.79	0.81	0.1	157.5	161.67	
	3	0.70			161.0		
SA	1	0.39			154.5		118.30
	2	1.40	0.78	0.5	151.0	151.83	
	3	0.55			150.0		
S1	1	0.57			164.7		118.05
	2	1.20	0.73	0.4	159.5	162.83	
	3	0.41			164.3		
S2	1	1.58			158.0		188.02
	2	1.19	1.19	0.4	154.0	158.33	
	3	0.80			163.0		
G1	1	0.70			160.5		363.02
	2	2.20	2.30	1.7	158.0	157.83	
	3	4.00			155.0		
PF1	1	0.39			168.0		105.89
	2	0.75	0.63	0.2	163.5	166.83	
	3	0.76			169.0		
G2	1	0.25			163.5		41.08
	2	0.30	0.25	0.1	163.5	164.33	
	3	0.20			166.0		
P1	1	0.83			170.0		201.38
	2	2.20	1.23	0.8	156.0	163.83	
	3	0.66			165.5		
PF2	1	1.10			149.0		146.83
	2	0.43	0.99	0.5	130.8	147.75	
	3	1.45			163.5		
P2	1	0.45			155.5		273.70
	2	0.35	0.41	0.1	160.0	158.67	
	3	0.40			160.5		
A	1	0.48			164.5		55.29
	2	0.20	0.34	0.1	162.0	161.83	
	3	0.35			159.0		

B.7 Durability tests

The results from the durability index (DI) tests as stated in Section 3.6.8 are summarised as below.

B.7.1 Oxygen Permeability Index (OPI)

Table B.13: 7-day OPI test results

Mix ID	Specimen	OPI (-log k m/s)			
		Measured	Mean	Quality	Std. Dev.
PS	1	11.05	10.67	Excellent	0.3
	2	10.55			
	3	10.54			
	4	10.55			
PFS	1	9.61	9.87	Good	0.3
	2	9.63			
	3	10.17			
	4	10.05			
SA	1	12.14	12.24	Excellent	0.1
	2	12.25			
	3	12.28			
	4	12.29			
S1	1	11.80	11.78	Excellent	0.0
	2	11.74			
	3	11.80			
	4	11.79			
S2	1	10.58	10.54	Excellent	0.1
	2	10.59			
	3	10.63			
	4	10.35			
G1	1	10.29	10.18	Excellent	0.1
	2	10.16			
	3	10.01			
	4	10.26			
PF1	1	10.19	10.26	Excellent	0.1
	2	10.45			
	3	10.22			
	4	10.19			
G2	1	10.14	10.17	Excellent	0.1
	2	10.13			
	3	10.15			
	4	10.28			
P1	1	9.97	10.08	Excellent	0.1
	2	10.12			
	3	10.07			
	4	10.17			
PF2	1	9.62	9.62	Good	0.0
	2	9.62			
	3	9.63			
	4	9.63			
P2	1	10.26	10.06	Excellent	0.3
	2	9.55			
	3	10.17			
	4	10.27			
A	1	10.14	9.78	Good	0.6
	2	8.83			
	3	10.02			
	4	10.14			

Table B.14: 28-day OPI test results

Mix ID	Specimen	OPI (-log k m/s)			
		Measured	Mean	Quality	Std. Dev.
PS	1	10.64	10.55	Excellent	0.1
	2	10.42			
	3	10.52			
	4	10.62			
PFS	1	10.06	9.98	Good	0.2
	2	9.74			
	3	9.97			
	4	10.17			
SA	1	10.90	10.82	Excellent	0.1
	2	10.78			
	3	10.80			
	4	10.82			
S1	1	10.72	10.83	Excellent	0.1
	2	10.95			
	3	10.83			
	4	10.82			
S2	1	10.56	10.72	Excellent	0.2
	2	10.74			
	3	10.95			
	4	10.62			
G1	1	10.19	10.27	Excellent	0.1
	2	10.38			
	3	10.28			
	4	10.22			
PF1	1	10.11	10.21	Excellent	0.1
	2	10.22			
	3	10.26			
	4	10.24			
G2	1	10.26	10.06	Excellent	0.3
	2	9.55			
	3	10.17			
	4	10.27			
P1	1	10.15	10.11	Excellent	0.1
	2	10.01			
	3	10.13			
	4	10.16			
PF2	1	10.83	10.75	Excellent	0.1
	2	10.78			
	3	10.76			
	4	10.63			
P2	1	10.03	10.02	Excellent	0.0
	2	10.04			
	3	10.02			
	4	9.98			
A	1	9.45	9.69	Good	0.4
	2	9.45			
	3	10.19			
	4	9.67			

B.7.2 Water Sorptivity Index

Table B.15: 7-day WSI test results

Mix ID	Specimen	WSI					Porosity	Mean
		Measured	Mean	Quality	Std. Dev.			
PS	1	3.6				14.9		
	2	4.3				12.4		
	3	3.8	3.8	Excellent	0.4	14.2	14.1	
	4	3.4				15.0		
PFS	1	3.9				18.7		
	2	2.9				18.3		
	3	3.5	3.3	Excellent	0.4	17.6	18.2	
	4	3.0				18.0		
SA	1	8.0				21.9		
	2	7.4				22.8		
	3	7.5	7.3	Good	0.7	22.9	22.3	
	4	6.4				21.5		
S1	1	7.4				7.7		
	2	6.7				9.4		
	3	6.3	6.2	Good	1.3	8.7	8.4	
	4	4.5				7.7		
S2	1	3.6				10.9		
	2	5.4				10.4		
	3	3.6	4.5	Excellent	1.1	11.1	10.8	
	4	5.6				10.9		
G1	1	5.7				15.9		
	2	5.6				16.4		
	3	6.2	5.8	Excellent	0.2	17.0	16.7	
	4	5.7				17.6		
PF1	1	5.1				19.6		
	2	5.3				17.5		
	3	4.6	5.2	Excellent	0.5	19.6	19.3	
	4	5.8				20.5		
G2	1	4.8				14.6		
	2	5.8				13.7		
	3	5.0	5.4	Excellent	0.6	14.3	13.8	
	4	6.0				12.4		
P1	1	4.8				21.9		
	2	4.9				22.3		
	3	4.3	4.6	Excellent	0.3	22.6	22.1	
	4	4.4				21.7		
PF2	1	6.6				7.9		
	2	6.3				7.6		
	3	5.9	6.1	Good	0.5	8.3	7.9	
	4	5.6				8.0		
P2	1	4.7				14.3		
	2	5.8				13.9		
	3	4.9	5.1	Excellent	0.5	15.1	14.5	
	4	4.9				14.7		
A	1	10.0				23.4		
	2	9.4				24.1		
	3	9.3	9.7	Good	0.4	23.7	23.6	
	4	10.1				23.2		

Table B.16: 28-day WSI test results

Mix ID	Specimen	WSI					
		Measured	Mean	Quality	Std. Dev.	Porosity	Mean
PS	1	3.9				13.8	
	2	4.2				13.9	
	3	4.0	4.3	Excellent	0.6	15.6	14.3
	4	5.2				13.8	
PFS	1	2.9				14.1	
	2	3.1				15.0	
	3	2.9	3.0	Excellent	1.5	15.2	14.8
	4	Invalid				Invalid	
SA	1	10.4				23.4	
	2	10.3				21.2	
	3	11.9	10.8	Poor	0.8	22.8	22.7
	4	10.7				23.5	
S1	1	7.7				10.4	
	2	6.4				9.1	
	3	6.8	6.8	Good	0.7	9.3	9.4
	4	6.1				8.7	
S2	1	4.9				8.8	
	2	5.9				8.2	
	3	5.7	5.2	Excellent	0.7	8.5	8.6
	4	4.3				8.8	
G1	1	5.7				14.4	
	2	6.5				13.5	
	3	5.8	5.8	Excellent	0.5	14.2	14.1
	4	5.2				14.2	
PF1	1	4.0				15.4	
	2	4.4				16.1	
	3	5.0	4.3	Excellent	0.5	15.7	15.7
	4	3.8				15.6	
G2	1	4.7				14.3	
	2	5.8				13.9	
	3	4.9	5.1	Excellent	0.5	15.1	14.5
	4	4.9				14.7	
P1	1	4.2				10.9	
	2	4.4				10.4	
	3	4.1	4.1	Excellent	0.3	11.1	10.8
	4	3.7				10.9	
PF2	1	6.6				7.9	
	2	6.3				7.6	
	3	5.9	6.1	Good	0.5	8.3	7.9
	4	5.6				8.0	
P2	1	4.1				14.3	
	2	4.5				13.9	
	3	4.5	4.3	Excellent	0.2	15.1	14.5
	4	4.2				14.7	
A	1	9.4				24.6	
	2	9.9				25.3	
	3	10.4	9.6	Good	0.7	25.8	25.4
	4	8.9				25.9	

B.7.3 Chloride Conductivity Index

Table B.17: 7-day CCI test results

Mix ID	Specimen	CCI			
		Measured	Mean	Quality	Std. Dev.
PS	1	0.79	1.2	Good	0.4
	2	1.17			
	3	1.19			
	4	1.75			
PFS	1	1.38	1.4	Good	0.1
	2	1.43			
	3	1.59			
	4	1.36			
SA	1	0.71	0.8	Good	0.0
	2	0.79			
	3	0.72			
	4	0.80			
S1	1	0.43	0.5	Excellent	0.1
	2	0.61			
	3	0.43			
	4	0.47			
S2	1	1.36	1.4	Good	0.2
	2	1.57			
	3	1.57			
	4	1.16			
G1	1	1.24	1.1	Good	0.1
	2	0.96			
	3	0.98			
	4	1.09			
PF1	1	0.63	0.7	Excellent	0.1
	2	0.76			
	3	0.89			
	4	0.65			
G2	1	0.98	0.8	Good	0.1
	2	0.91			
	3	0.76			
	4	0.66			
P1	1	2.22	2.1	Poor	0.2
	2	1.90			
	3	1.98			
	4	2.26			
PF2	1	0.34	0.3	Excellent	0.0
	2	0.29			
	3	0.30			
	4	0.29			
P2	1	6.25	6.2	Very Poor	0.1
	2	6.12			
	3	6.05			
	4	6.27			
A	1	1.11	1.1	Good	0.1
	2	1.00			
	3	1.20			
	4	1.01			

Table B.18: 28-day CCI test results

Mix ID	Specimen	CCI			
		Measured	Mean	Quality	Std. Dev.
PS	1	0.85	0.9	Good	0.1
	2	0.96			
	3	0.84			
	4	0.83			
PFS	1	0.77	0.8	Good	0.1
	2	0.73			
	3	0.86			
	4	0.85			
SA	1	0.30	0.3	Excellent	0.0
	2	0.34			
	3	0.32			
	4	0.32			
S1	1	0.50	0.6	Excellent	0.2
	2	0.46			
	3	0.60			
	4	0.85			
S2	1	0.83	0.7	Excellent	0.1
	2	0.75			
	3	0.73			
	4	0.65			
G1	1	1.26	1.1	Good	0.2
	2	0.95			
	3	1.29			
	4	0.97			
PF1	1	0.47	0.5	Excellent	0.0
	2	0.55			
	3	0.57			
	4	0.51			
G2	1	1.41	1.2	Good	0.3
	2	0.88			
	3	1.43			
	4	1.14			
P1	1	1.95	2.0	Poor	0.4
	2	2.52			
	3	1.59			
	4	1.93			
PF2	1	0.32	0.3	Excellent	0.0
	2	0.33			
	3	0.28			
	4	0.26			
P2	1	5.18	5.3	Very Poor	0.4
	2	5.70			
	3	5.34			
	4	4.81			
A	1	0.62	0.6	Good	0.0
	2	0.63			
	3	0.66			
	4	0.64			

B.8 Tensile relaxation

Table B.19: 7-day Tensile Relaxation

Mix ID	Specimen	Tensile Relaxation (%)	Avg. Tensile Relaxation (%)	Sdv. Dev.
PS	1	45.30	44.95	0.5
	2	44.60		
PFA	1	25.20	25.80	0.8
	2	26.40		
SA	1	14.90	15.10	0.3
	2	15.30		
S1	1	46.80	46.65	0.2
	2	46.50		
S2	1	53.10	53.40	0.4
	2	53.70		
G1	1	42.20	42.85	0.9
	2	43.50		
PF1	1	37.10	37.95	1.2
	2	38.80		
G2	1	48.90	49.30	0.6
	2	49.70		
P1	1	37.30	37.95	0.9
	2	38.60		
PF2	1	37.70	38.65	1.3
	2	39.60		
P2	1	47.80	48.20	0.6
	2	48.60		
A	1	34.10	35.10	1.4
	2	36.10		

Table B.20: 28-day Tensile Relaxation

Mix ID	Specimen	Tensile Relaxation (%)	Avg. Tensile Relaxation (%)	Sdv. Dev.
PS	1	42.30	40.95	1.9
	2	39.60		
PFA	1	23.10	23.20	0.1
	2	23.30		
SA	1	12.30	12.75	0.6
	2	13.20		
S1	1	38.65	38.49	0.2
	2	38.33		
S2	1	46.20	46.85	0.9
	2	47.50		
G1	1	29.30	30.25	1.3
	2	31.20		
PF1	1	30.20	28.85	1.9
	2	27.50		
G2	1	44.30	44.25	0.1
	2	44.20		
P1	1	36.60	35.85	1.1
	2	35.10		
PF2	1	22.30	23.45	1.6
	2	24.60		
P2	1	37.80	36.80	1.4
	2	35.80		
A	1	30.20	29.15	1.5
	2	28.10		

B.9 Sieve analysis.

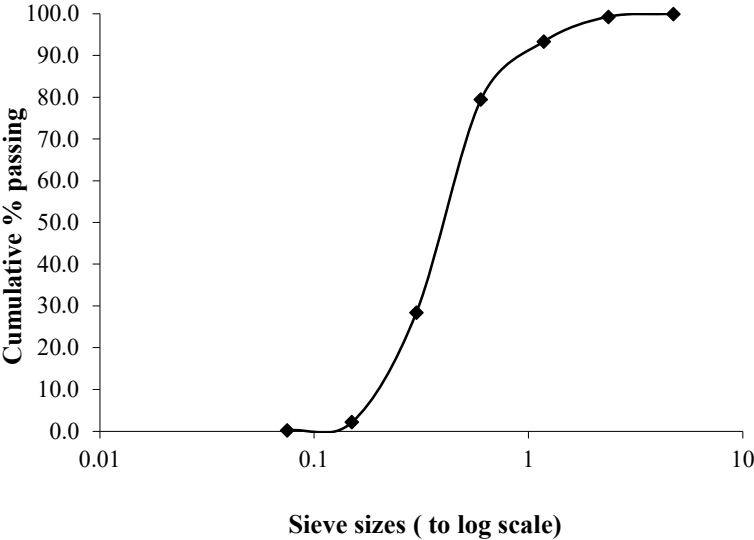


Figure B.1: Mix PS sieve analysis.

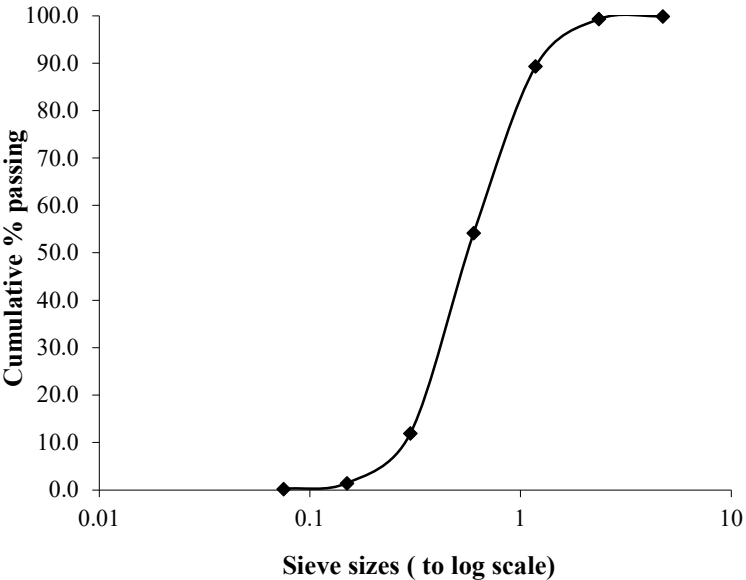


Figure B.2: Mix PFS sieve analysis.

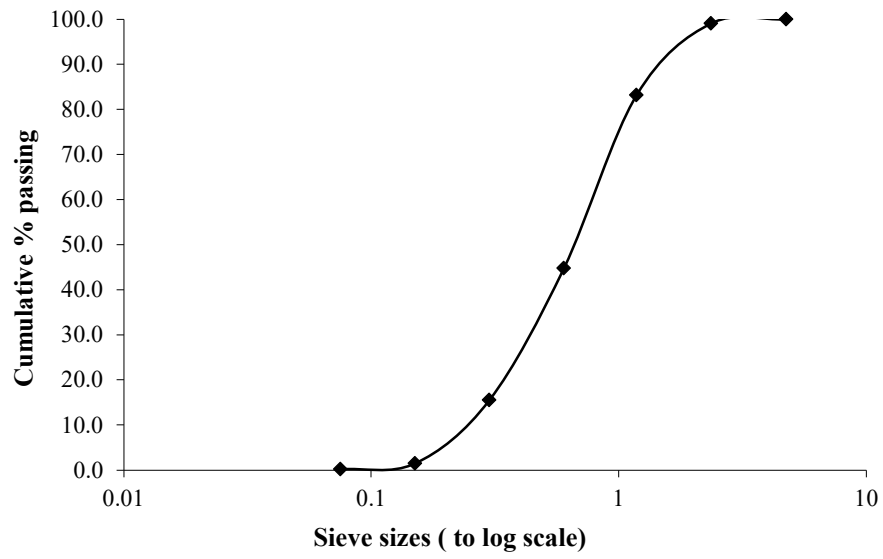


Figure B.3: Mix SA sieve analysis.

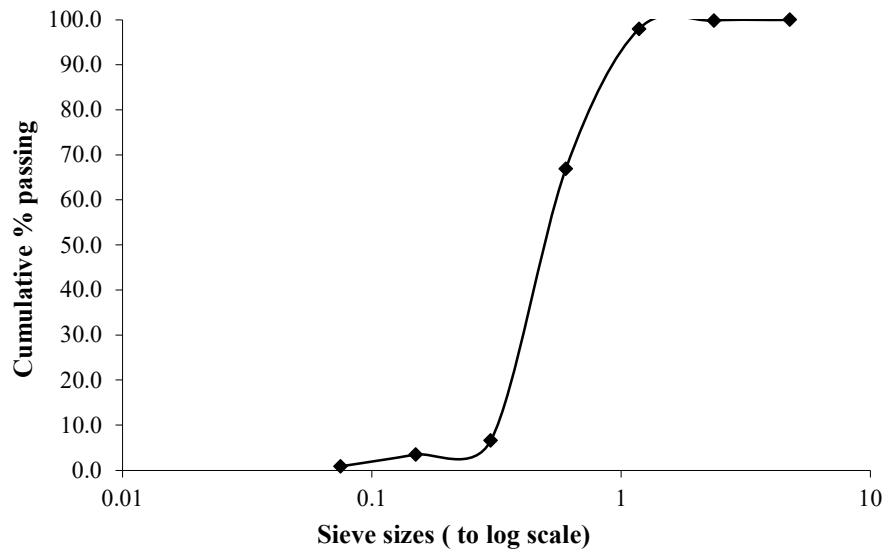


Figure B.4: Mix S1 sieve analysis.

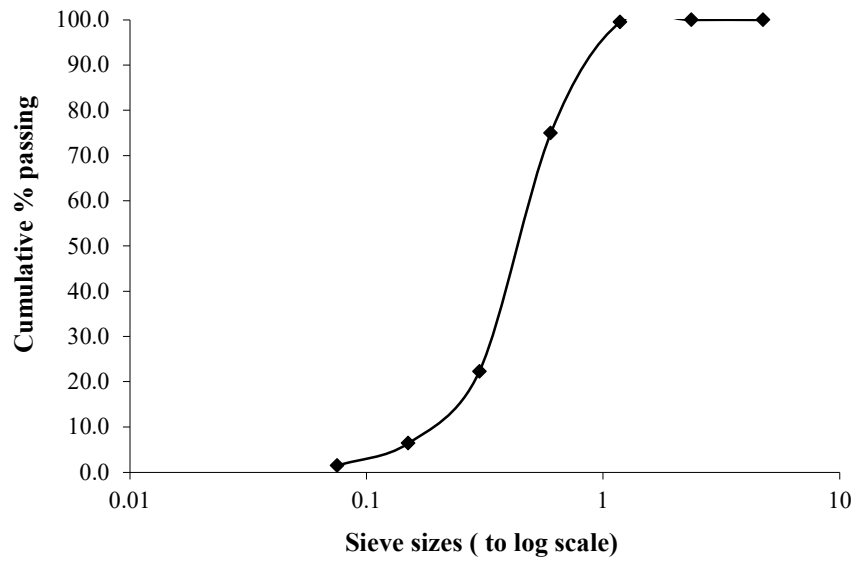


Figure B.5: Mix S2 sieve analysis.

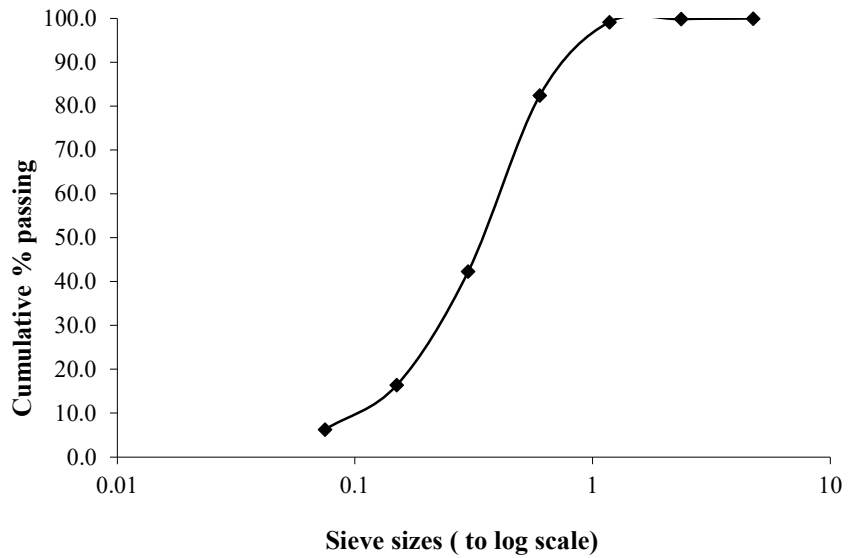


Figure B.6: Mix G1 sieve analysis.

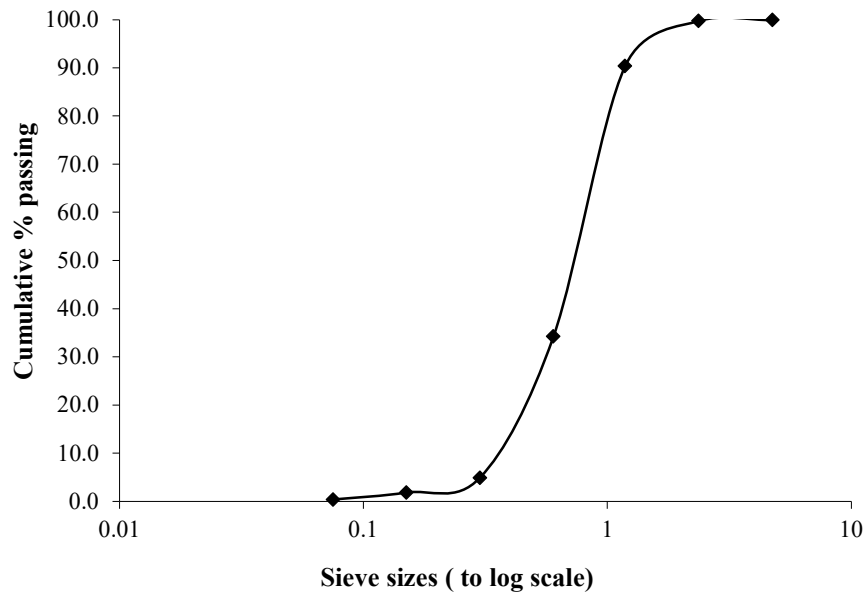


Figure B.7: Mix PF1 sieve analysis.

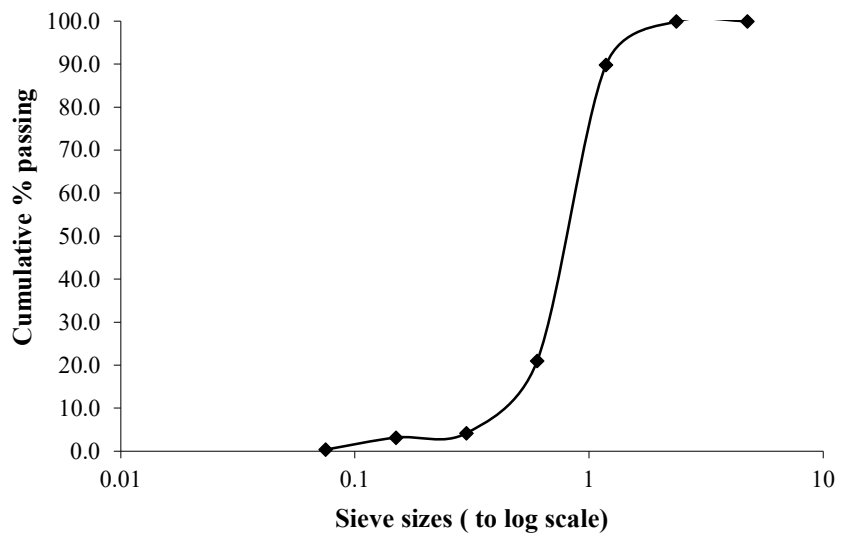


Figure B.8: Mix G2 sieve analysis.

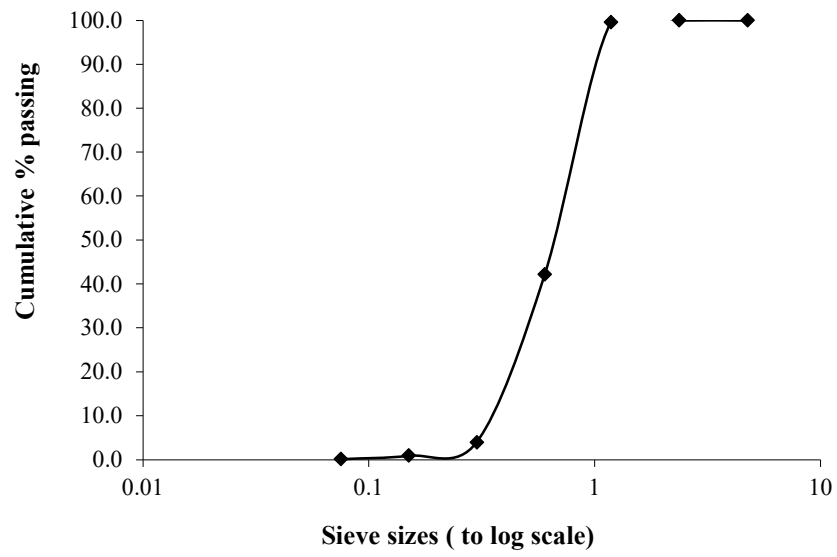


Figure B.9: Mix P1 sieve analysis.

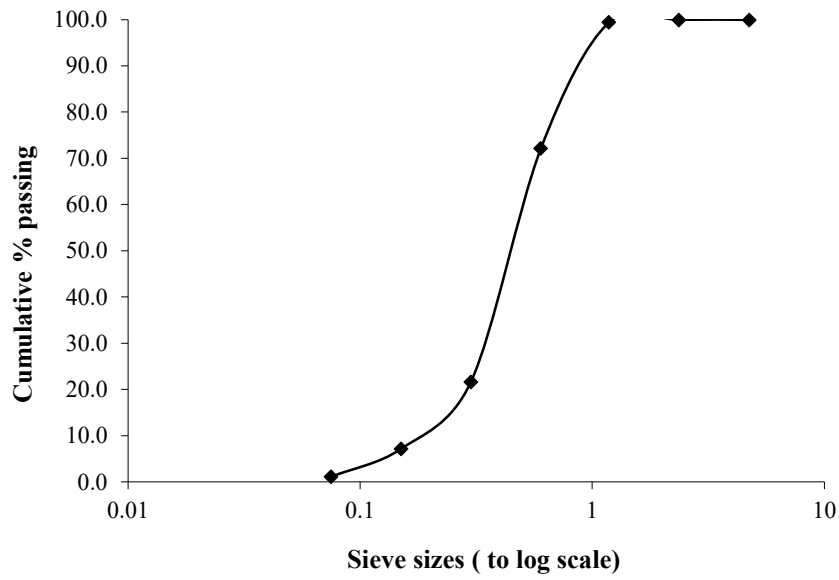


Figure B.10: Mix PF2 sieve analysis.

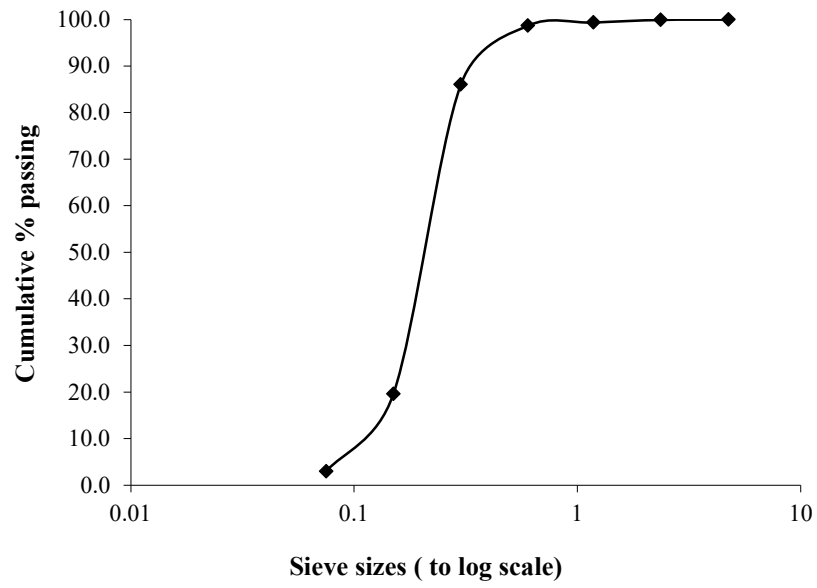


Figure B.11: Mix P2 sieve analysis.

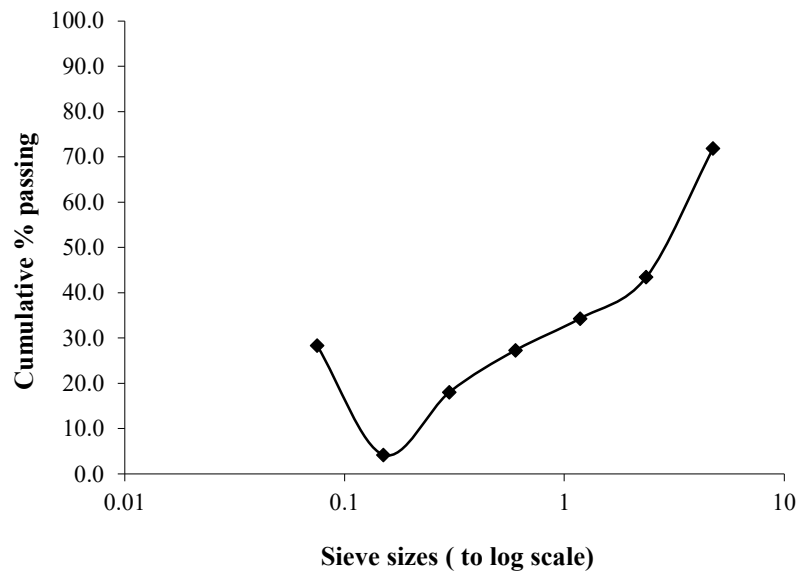


Figure B.12: Mix A sieve analysis.

B.10 Energy Dispersive Spectrometry Tests (EDS)

Table B.21: Analysed spectrum showing the element composition of the repair mortars

Mix ID	All results in weight%									
	O	Mg	Al	Si	S	K	Ca	Ti	Fe	Total
PS	41.05	0.47	2.21	6.01	0.74	0.19	17.87	0.18	0.81	100
PFS	39.04	0.47	1.01	6.62	0.87	0.23	19.92	0	0.8	100
SA	44.24	0.41	0.85	9.83	0.88	0.13	17.0	0	0.82	100
S1	35.67	0.21	5.88	1.39	1.68	0	13.47	0.32	3.78	100
S2	45.45	0	5.02	7.86	1.19	0	8.65	0.3	3.19	100
G1	28.65	0.25	0.78	3.57	0.41	0.1	9.26	0	0.91	100
PF1	30.9	0.14	0.65	4.12	0.34	0	5.19	0.43	0.35	100
G2	29.85	0.19	0.94	4.34	0.58	0	8.75	0	0.42	100
P1	26.09	0.21	0.41	2.08	0.43	0	7.32	0	0.4	100
PF2	30.82	0.15	0.48	5.84	0.76	0.12	4.49	0	0.38	100
P2	38.38	0.23	0.53	10.52	0.53	0	10.78	0	0.6	100
A	37.13	0.55	0.9	4.96	1.07	0.14	17.53	0	0.95	100